THE STRENGTHENING OF CERTAIN STAINLESS STEELS BY THE REVERSE MARTENSITE TRANSFORMATION

A Thesis submitted for the degree

of

DOCTOR OF PHILOSOPHY

in the

University of London

by

HOWARD SMITH

September, 1968.

Department of Metallurgy,

Royal School of Mines,

Imperial College of Science and Technology,

London, S.W.7.

ABSTRACT

The reverse martensite transformation in two stainless steel alloys has been investigated; one is a pure ternary alloy (Fe - 16% Cr - 12% Ni) and the other also contains molybdenum and carbon (Fe - 15% Cr - 8½% Ni - 2% Mo - 0.1% C). Both alloys are fully austenitic at room temperature after solution-treatment but undergo partial transformation to martensite when quenched to -196°C or deformed at room temperature.

The transformation has been studied by room temperature measurements of specific saturation magnetic intensity, by hardness measurements and by transmission electron microscopy after heating the partially martensitic specimens for short times (1 or 2 minutes) in molten salt baths. Reversion during slower rates of heating has also been studied by a differential dilatometry technique and by elevated temperature measurements of dynamic Young's modulus. The results suggest that the reverse martensite transformation in these alloys occurs mainly by a diffusionless (shear) mechanism but that diffusion-controlled reversion and, possibly, stabilisation effects are also present when slower heating rates are employed.

The 'reversed austenite' contains a high density of tangled dislocations together with stacking faults and reversal twins and suggestions have been made regarding the formation of these structural imperfections in the austenite. Strengthening and stabilisation effects produced by repeated transformation cycling, $\gamma \rightarrow \alpha' \rightarrow \gamma$, have also been studied.

The process of 'annealing-out' of the reversed austenite structure in the ternary alloy has been studied and it is suggested that this occurs by a continuous recovery mechanism rather than by the movement of high angle boundaries through the deformed austenite.

The ageing behaviour of the carbon-containing alloy has been studied in the solution-treated condition and in the structures produced by reversion of the martensite produced by either quenching or deformation. The precipitating phase has been identified as $M_{23}C_6$.

The rather moderate increase in the strength of the austenite which can be produced by reversion is attributed to the small amount of martensite which can be produced in these alloys and the failure of the direct and reverse martensite transformation to produce appreciable deformation in the retained austenite.

CONTENTS

		Page No.
CHAPTER 1.	INTRODUCTION	1
CHAPTER 2.	REVIEW OF LITERATURE	5
2.1.	General.	5
2.2.	The Formation of Martensite in Stainless Steels.	5
2.2.1.	The effect of deformation.	9
2.2.2.	Isothermal aspects.	11
2.3.	Reversion in Stainless Steels.	11
2.4.	Reversion in Fe - Ni and Fe - Ni - C Alloys.	13
2.4.1.	Structure of reversed austenite.	15
2.4.2.	Increased strength of reversed austenite.	17
2.5.	Reversion in Some Other Systems.	18
2.6.	The Effect of Prior Deformation on Reversion.	20
2.7.	Precipitation During Reversion.	21
2.8.	Austenite Stabilisation Effects of Reversion.	22
CHAPTER 3.	EXPERIMENTAL PROCEDURE	25
3.1.	Alloy Preparation.	25
3.2.	Fabrication and Heat Treatments.	25
3.2.1.	Homogenising.	25
3.2.2.	Rolling and intermediate heat treatments.	25
3.2.3.	Sub-zero treatments.	27
3.2.4.	Reversion, annealing and ageing treatments	27
3.3.	Magnetic Measurements.	27
3.4.	Dynamic Young's Modulus Measurements.	29
3.5.	Measurement of M_s Temperature.	30
3.6.	Measurement of A_s and A_f Temperatures.	30
3.7.	Hardness Measurements and Light Microscopy.	30
3.8.	Mechanical Property Measurements.	31
3.9.	Dilatometry Measurements.	31
3.10.	Electron Microscopy.	32
3.10.1.	Specimen preparation.	32
CHAPTER 4.	RESULTS	34
4.1.	Formation of Martensite on Cooling.	34
	Alloy A.	34
	Alloy B.	34

4.2. Reversion of Martensite to Austenite. 39
Alloy A. 39
4.2.1. Determination of A_s and A_f on rapid heating. 39
4.2.2. Structural changes. 42
4.2.3. Prolonged heating at the reversion temperature. 45
4.2.4. Young's modulus measurements. 45
4.2.5. Dilatometry. 47
Alloy B. 50
4.2.6. Determination of A_s and A_f on rapid heating. 50
4.2.7. Structural changes. 52
4.2.8. Dilatometry. 52
4.3. Effect of Cold Work on Reversion. 56
Alloy A. 56
4.3.1. Transformation to martensite by deformation. 56
4.3.2. Determination of A_s and A_f on rapid heating. 59
4.3.3. Structural changes. 59
4.3.4. Dilatometry. 59
Alloy B. 60
4.3.5. Transformation to martensite by deformation. 60
4.3.6. Determination of A_s and A_f on rapid heating. 60
4.3.7. Structural changes. 63
4.3.8. Dilatometry. 63
4.4. Annealing of Reversed Austenite; Alloy A. 66
4.4.1. Reversed austenite obtained from martensite produced by quenching. 66
(i) hardness changes. 66
(ii) structural changes. 73
(iii) comparison with deformed austenite. 75
4.4.2. Reversed austenite obtained from martensite produced by deformation. 78
(i) hardness changes. 78
(ii) structural changes. 78
4.5. Ageing Behaviour; Alloy B. 78
4.5.1. Solution treated. 80
4.5.2. Quenched and reversed. 85
4.5.3. Cold-worked and reversed. 88
4.6. Transformation Cycling. 90
4.6.1. Alloy A. 90
4.6.2. Alloy B. 94

CHAPTER 5. DISCUSSION OF RESULTS 96

5.1. The Direct Transformation. 96
5.1.1. General. 96
5.1.2. Isothermal aspects. 97
5.1.3. Effect of cold work. 98

5.2. Interpretation of Dilatometry Results. 99
5.2.1. General 99
5.2.2. Quenched specimens. 99
5.2.3. Cold worked specimens. 103
5.3. The Reverse Transformation. 107
5.3.1. Reversion of specimens transformed to martensite at -196°C. 107
(i) the reversion mechanism. 107
(ii) fine structure of reversed austenite. 109
5.3.2. Reversion of specimens transformed to martensite by deformation. 112
(i) transformation temperatures. 112
(ii) structural changes. 115
5.4. Annealing Behaviour. 117
5.4.1. Annealing mechanism. 117
5.4.2. Activation energies. 120
5.5. Ageing Behaviour. 121
5.5.1. Structure and morphology of precipitates. 121
5.5.2. Increase in ferromagnetic response. 123
5.5.3. Influence of initial sub-structure. 126
5.6. Strengthening. 129
5.6.1. Solution-treated specimens. 129
5.6.2. Martensitic specimens. 130
5.6.3. Reversion treatments. 131
5.6.4. Annealing of reversed austenite. 134
5.6.5. Ageing treatments. 135
5.7. Transformation Cycling. 137
5.7.1. Stabilisation. 137
5.7.2. Strengthening. 140

CHAPTER 6: CONCLUSIONS 144

SUGGESTIONS FOR FUTURE WORK 150

ACKNOWLEDGEMENTS 152

REFERENCES 153

APPENDIX A: Estimation of Martensite Content Using a Magnetic Ring Balance. 158

APPENDIX B: Elevated Temperature Measurement of Young's Modulus. 170

APPENDIX C: Dilatometry. 174

CHAPTER 1

INTRODUCTION

The direct transformation of austenite to martensite, $\gamma \longrightarrow \alpha'$, in stainless steels has received considerable attention in the past, but comparatively little work has been carried out on the reverse martensite transformation, $\alpha' \longrightarrow \gamma$, in these steels. This is shown quite clearly by the review of the published literature on these transformations in the next section. However, it has been shown [1, 2] that the product of the reverse transformation, known as 'reversed austenite', has superior strength properties compared to the original austenite.

Considerably more attention has been paid to the reverse martensite transformation in iron - nickel alloys and, again evidence exists to show that the reversed austenite is stronger than the original austenite [2 - 5].

Although many similarities might be expected between the reversed austenite in stainless steels and iron - nickel alloys, differences might arise because of the different morphologies of the martensites in the two systems, lath and internally-twinned martensites respectively. Furthermore, the annealing behaviour of the reversed austenite in these systems would be expected to differ because of their different stacking fault energies (SFE) [6, 7] and the known dependence on SFE of the ability of dislocations to climb and cross-slip. It might be expected, then, that the reversed austenite in stainless steels of low SFE would be more stable at elevated temperatures than that in the iron - nickel alloys already investigated.

Reversed austenite in stainless steels has been shown to have a substructure containing a high density of complex dislocation tangles [8, 9] and, as precipitation of carbides can occur preferentially at dislocation

sites, the combined effects of reversion and precipitation in stainless steel might lead to considerable strengthening. Reversion carried out in a structure already containing a fine dispersion of carbides, or the subsequent formation of such carbides in the reversed austenite might provide a strengthening mechanism for martensitic steels analogous to that of ausforming. Furthermore, reversion strengthening might provide a useful method of improving the properties of a steel without requiring any external shape change as in deformation strengthening.

Thus, it would appear useful to extend the present knowledge on basic features of the reverse martensite transformation in stainless steel and the properties of the resulting 'reversed austenite'. This is, essentially, the aim of the present project in which two alloys have been examined.

One was a pure iron - chromium - nickel ternary alloy, Alloy A, in which the reverse martensite transformation could be studied without the possible complication of decomposition of the martensite by carbide precipitation during heating. The other, Alloy B, also contained molybdenum and carbon to develop precipitation behaviour which could then be studied in association with the reversion. In order that the austenitic structures could be examined at room temperature, it was necessary for both alloys to have an M_s temperature below this, yet sufficiently close to room temperature to produce partial transformation to martensite on quenching to -196°C.

The choice of composition for Alloy A was relatively straightforward, in that a steel containing 16 wt % chromium and 12 wt % nickel is completely austenitic at about 1000°C, retains this structure on rapid cooling to room temperature, and has a suitable sub-zero M_s temperature. In the case of Alloy B there is a danger of forming δ - ferrite which would add unnecessary complications to the investigations, particularly to magnetic measurements.

Both chromium and molybdenum promote the formation of ferrite whereas nickel and carbon tend to prevent it. The information provided by Irvine et al [10] and Truman [11] in their studies of 'controlled-transformation stainless steels' was used to balance the δ-ferrite promoting tendency of the alloying elements with their influence on the M_s temperature, to deduce a composition which was both ferrite-free and had a suitable M_s. A very low M_s would reduce the amount of transformation to martensite at -196°C while one too close to room temperature would produce problems during even short precipitation treatments where depletion of carbon and alloying elements from the matrix might raise the M_s to above room temperature and produce some transformation to martensite on subsequent cooling to this temperature. A steel containing 15.0% chromium, 8.5% nickel, 2.0% molybdenum and 0.09% carbon by weight was estimated to be free from δ-ferrite and have an M_s of about -40°C. This was therefore chosen for Alloy B.

The equilibrium constitution of the two alloys at their reversion temperatures is of interest; it can be seen from Fig. 1.1. that Alloy A is fully austenitic at such temperatures. It is not possible to plot the exact composition of Alloy B on this diagram because it contains Mo and C; the former is a ferrite promoter while the latter strongly stabilises austenite. On balance the alloy is likely to tend towards a fully austenitic structure more strongly than is suggested by point B on the ternary diagram in Fig. 1.1.

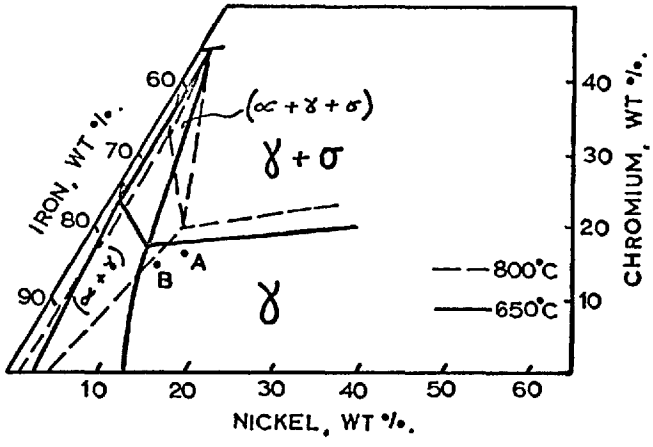

A : 16% Cr, 12% Ni

B : 15% Cr, 9% Ni

Fig. 1.1. Fe-Cr-Ni Isothermal Sections (12)

Transmission electron microscopy, magnetic analysis, dilatometry and elevated temperature measurements of dynamic Young's modulus are among the techniques used in this investigation.

CHAPTER 2

REVIEW OF LITERATURE

2.1. GENERAL:

A wealth of literature exists on the direct transformation of austenite (γ) to martensite (α') in stainless steels, both during cooling below the M_s [13 - 25] and during deformation [19 - 34]. However, no comprehensive review of such literature has been published and so it was considered worthwhile to summarise points of interest from these papers before reviewing previous work on the reverse martensite transformation ($\alpha' \rightarrow \gamma$).

By comparison with the direct transformation, relatively little work has been carried out on reversion in stainless steels [1, 2, 8, 9, 14, 21, 22, 23, 35]. This is in contrast to the considerable attention paid to the reverse martensite transformation in Fe - Ni alloys [2 - 5, 20, 36 - 51] where studies have been made of the fine structure of the reversed austenite [5, 37, 39, 40, 42, 46], its increased strength [2 - 5] and the recovery and recrystallisation of the reversed austenite structure during subsequent annealing [2 - 5, 39].

2.2. THE FORMATION OF MARTENSITE IN STAINLESS STEELS:

Stainless steels having about 18% Cr and 8% Ni transform martensitically from austenite (γ) to a b.c.c. structure (α') and a h.c.p. structure (ε) when they are either cooled below M_s or deformed below their M_d temperatures. Numerous investigations have found that the temperature at which γ begins to transform into martensite on cooling, M_s, is critically dependent on chemical composition [52, 53]. The product is described as having a lath-morphology.

No significant differences have been reported in the nature of the martensitic transformation in the alloy under investigation (16/12) and those of the 18/8 type. The amount of martensite formed during the initial quench to -196°C is small compared to that in other Fe - base alloys of similar M_s temperature [24]. The M_s of a 16/12 alloy is known [23] to be very dependent on grain size (increasing as the grain size increases) and the amount of transformation at a given temperature is correspondingly dependent on the structure.

Kelly and Nutting [15] describe the α' as needles oriented in $\langle \bar{1}10 \rangle$ directions within $\{111\}_\gamma$ sheets. The longest direction of these needles was $\langle 11\bar{1} \rangle_M$ which is parallel to $\langle 1\bar{1}0 \rangle_\gamma$ and the α' grains in a sheet are always twin related to each other with the same direction in each twin normal to the sheet. The needles were not, however, internally twinned. Breedis [13] also found that the α' in a 16/12 alloy appeared as needles but Reed [17] and Venables [25] showed that α' formed as plates with $\{111\}_\gamma$ habit planes, as did Imai et al [54]. A $\{259\}_\gamma$ habit plane has been reported by Lagneborg [19] and Thomas and Krauss [9]. The latter authors showed that the crystallographic relationship followed Kurdjumov-Sachs, namely $\{111\}_\gamma$ // $\{101\}_\alpha$, $\langle 110 \rangle_\gamma$ // $\langle 111 \rangle_\alpha$. The α' grains have been described as needles in the deformed material and as plates after cooling [19]. The lattice parameters of the phases have been determined by several workers [6, 14, 21, 23, 24].

An h.c.p. phase, ε, also appears in other ferrous alloy systems; Fe - Mn [27, 55 - 58], Fe - Cr - Mn [27, 59], Fe - Ir [60], Fe - Mn - Ni [27], Fe - Mn - Co [27], Fe - Mn - C [27] and Fe - Mn - Cr - Ni [16]. Experimental evidence suggests that in Fe - Cr - Ni stainless steels, ε is unlikely to form in alloys which have a (Cr + Ni) content of less than about 26%; apparently depending on a low SFE in the alloy.

The occurrence of the h. c. p. phase, ε , in Fe - Cr - Ni alloys has been widely reported [6, 7, 13, 14, 16, 17, 19 - 21, 23, 25, 26, 27, 29, 33, 54, 61, 62] and several authors [14, 15, 20, 21, 23, 25] have suggested that the ε is a transitional phase in the transformation of $\gamma \rightarrow \alpha'$; the suggested sequence is commonly $\gamma \rightarrow SF_s \rightarrow \varepsilon \rightarrow \alpha'$. This view is not, however, supported by other writers [13, 17, 61] and their results suggest that the ε forms in these steels of low SFE [6, 7, 13] as a consequence of the large strains in the austenite accompanying the martensitic transformation to α' .

To produce ε , every other $\{111\}$ plane in the γ must fault. If this regularity is only partially maintained then faulted ε is produced. If the faulting plane periodicity is random then stacking fault clusters are formed. Breedis [13] and Venables [25] have shown that a true h. c. p. structure does exist, and that it is not merely random faulting of the austenite. The ε phase is, however, always heavily faulted [16, 17, 25] but relatively dislocation free [17].

Kelly and Nutting [15] failed to detect any ε in their 18/8 steel but Lagneborg [19] suggests that as their material contained large amounts of α' this is not surprising because it has been shown [13, 21, 23, 26, 29, 36,] that the ε content decreases while the martensite transformation proceeds.

Cina [21] found that the % ε and the % α' increased as the transformation temp. decreased, suggesting that the mode of transformation was martensitic. He also found that the hcp phase can be eliminated and transformed to α' by deformation, and so concluded that it is an intermediate structure in the formation of some or all of the α' . The first investigation of the ε phase in stainless steel by electron microscopy was carried out by Venables [25]. The formation of ε was attributed to the movement of $\frac{a}{6}\langle 11\bar{2}\rangle$ partial dislocations on every other $\{111\}_\gamma$ plane. The α' phase was observed in contact

with ε, especially at the intersection of two $\{111\}_\gamma$ planes and it was concluded that ε was an intermediate structure in the $\gamma \rightarrow \alpha'$ transformation. Venables suggested that the α' nucleates from ε and grows by the motion of a parallel grid of screw dislocations. ε sheets were found [14] to form on cooling before any α' was detected and were seen to be nucleation sites for the formation of α'. Lagneborg [19] found that ε formed during holding immediately above the M_s temperature. This is in agreement with the findings of Reed [14]. Breedis and Robertson [20] also supported the view that ε is an intermediate structure but acknowledge that this model would require two separate M_s temperatures which have not yet been identified. In fact, Goldman et al [61] failed to detect two M_s temperatures using three sensitive techniques and concluded that the reaction is $\gamma \rightarrow \varepsilon + \alpha'$. In another paper [13] Breedis studied a series of Fe - Cr - Ni alloys in some of which the h. c. p. phase formed. He found that the morphology of the martensite in these alloys was not influenced by the presence of ε or SF_s (this does not mean that α' may not nucleate at such regions) and concluded that the h. c. p. phase was therefore not a transitional structure. The same view is held by Dash and Otte [17] but for different reasons. Firstly, the α' crystals appeared to determine the features of ε rather than vice versa; secondly, the ε can be suppressed and even eliminated, whereas this is not possible with α' and if suppression of ε does not cause suppression of α' then it is unlikely to be an intermediate step in the transformation. The orientation relationship between ε and γ is found [25] to be $(111)_\gamma \;//\; (0001)_\varepsilon$ and $[1\bar{1}0]_\gamma \;//\; [\bar{1}2\bar{1}0]_\varepsilon$, i.e. close-packed planes and rows in the two structures are parallel.

The structure of the b. c. c. transformation product, α', has been investigated. It has been shown [9, 13, 16, 30] to have a high internal dislocation density but no regular dislocation substructure.

Dash and Otte [17] found that α' was not internally faulted whereas Goldman and Wagner [7] observed SF_s on $\{112\}$ in α'. Koepke et al [18] have shown that the α'/γ interface is composed of an array of dislocations and suggest a mechanism of formation of the dislocations and SF_s observed in the γ in the vicinity of α' needles. Breedis [8] has stated that a characteristic feature of lath martensite formation is the absence of substantial deformation of the γ outside the deformation band. Nevertheless immediately ahead of the interface, dislocations, most commonly as tangles, can be seen [17]. The dislocation density falls off sharply with distance into the γ grain over a distance of the order of magnitude of the width of the particular α' feature observed [9]. The dislocations in the γ are much simpler than in the α' and more readily resolved. Extensive stacking faults have also been observed around the transformation product [9].

2.2.1. The Effect of Deformation:

Deformation can affect the martensitic transformation in several ways depending on the temperature at which it is performed. That below the M_d temperature induces the formation of martensite whereas deformation above the M_d can enhance subsequent transformation or, at higher strains, can cause mechanical stabilisation.

During deformation below the M_d, martensite forms along active slip planes [23] and, although the morphology changes, the crystallographic aspects of the transformation remain unchanged. Some γ grains contain large amounts of α' and others almost none. It has been suggested [19] that α' forms in those grains having $\langle 111 \rangle_\gamma$ almost parallel to the tensile axis whereas the relatively untransformed γ grains have a $\langle 100 \rangle_\gamma$ direction almost coincident with the tensile direction of the specimen.

Many observers, including Fielder et al [24], have found that the amount of α' formed by deforming at various temperatures increased as the % deformation was raised and the temperature lowered. However, it has been reported [21, 29, 62] that although α' forms more easily during deformation at sub-zero temperatures, than at room temperature, the transformation to α' becomes more difficult at very low temperatures (e.g. 20°K). The formation and subsequent suppression of ε formation with increasing strain has been widely reported [19, 21, 23, 26, 27, 29, 62].

Venables [25] observed the formation of single and overlapping SF_s at very low strains. Further deformation produced more overlapping SF_s and finally platelets of h.c.p. ε up to 1000 Å thick formed. Lagneborg [19] reported similar findings and said that the α' then occurs as needle-shaped crystals in contact with ε discs. The first lamellae are built up by ε - sheets containing α' needles.

Deformation above the M_d of Fe - Cr - Ni alloys has been shown [30] to produce a dislocation cell structure, with a decrease in the cell size as the temperature of deformation is lowered. The regularity of the substructure in such alloys increases as the SFE increases.

Small prior strains are known to enhance subsequent transformation to α' in such alloys [14, 15, 19, 24, 30] forming α' in more grains and in broader regions comprised of several parallel laths, implying an increase in the number of nucleating sites after such treatment. Breedis [30] suggests that such stimulation occurs when dislocations are restricted to their slip planes, as with low SFE materials. The formation of cell structures does not produce stimulation of the transformation, and mechanical stabilisation of the γ is associated with high dislocation densities. Similar views are expressed by Kelly and Nutting [15] who propose a martensitic transformation mechanism consistent with such facts.

2.2.2. Isothermal Aspects:

The martensitic transformation has been shown to occur isothermally in stainless steels, usually on holding at low temperatures in the presence of athermal transformation products which have formed as a result of prior quenching to low temperatures [13, 20, 21, 24, 34] although, in general isothermal transformation will not proceed above the M_s unless products of a previous transformation at a lower temperature are present, such a phenomenon has been reported by Fielder et al [24], Imai et al [54] and Kulin and Speich [63].

The isothermal transformation is characterised by an initially very rapid rate of transformation followed by progressively slower rates. As a consequence of isothermal transformation, it has been shown [63] that more martensite can be obtained in a 14/9 alloy by holding at $-30^{\circ}C$ than by quenching directly to $-196^{\circ}C$.

The part of the martensitic transformation occurring isothermally can be described in terms of a TTT diagram [19, 54, 63]. Lagneborg [19] found a 'nose' at $-150^{\circ}C$ for an 18/8 type steel whereas Imai et al [54], investigating a 17/8 alloy, found that the TTT diagram had two 'noses' at $-100^{\circ}C$ and $-135^{\circ}C$. At the upper nose ε formed, followed by α' if held for sufficiently long periods, whereas only α' formed at the lower nose. The α' formed at the upper nose had a $\{111\}_{\gamma}$ habit plane whereas that formed isothermally at the lower nose and that formed athermally had $\{225\}_{\gamma}$ habit planes.

The isothermal transformation has been shown [24] to be influenced by prior deformation in the same way as the athermal transformation, namely enhanced by small strains and hindered by larger strains.

2.3. REVERSION IN STAINLESS STEEL:

Early work by Uhlig [64] on an 18/8 type steel, later confirmed by Cina [21, 22], established that the $\alpha' \rightarrow \gamma$ transformation occurred

over a range of temperature (approximately 500°C to 700°C) rather than at one fixed temperature. Further measurements of the temperatures at which the $\alpha' \rightarrow \gamma$ transformation starts and finishes (A_s and A_f) in various stainless steels have been made by both X-ray techniques [14, 23] and by the measurement of magnetic properties [1, 2, 8, 9, 14].

The reversion of ε occurs at much lower temperatures [14, 23], beginning at ~ 140°C and reaching completion on holding for short times below 400°C.

The martensitic nature of the reverse transformation is indicated by the dependence of the amount of reversion with temperature, rather than time at temperature [8], and by the surface relief effects which accompany the transformation [23].

Of the two main studies so far reported, one by Thomas and Krauss [9] deals with a commercial steel while the other by Breedis [8] relates to a pure 16/12 alloy. Breedis observed that after a short anneal at 500°C, the densities of dislocations, deformation faults and twins between martensite crystals comprising a lath are diminished as compared with the as-quenched condition (partially α'). Even after reversion was complete the volumes previously occupied by the α' could be recognised because of the fine structure noticed in such regions of 'reversed austenite'. Although the orientation of the parent γ grain was mainly reproduced from the α' crystals during reversion, small twins in the f.c.c. structure and deformation faults on $(111)_\gamma$ were identified. Breedis concluded that the reversion appears to mostly retrace the transformation path as opposed to a recrystallisation process to randomly oriented grains. Certain stabilisation effects as a result of the reverse transformation were noted.

Thomas and Krauss [9] again found that the reversed austenite regions were identifiable in what was previously a retained austenite background even using optical metallography. Such regions have been termed 'ghost' areas. The fine structure of reversed austenite was shown to consist of a high and varied density of complex tangled dislocations (as did the α' from which it had formed). On a larger scale the structure remained one of islands or zones of dense dislocation arrangements within a matrix relatively free of dislocations. Both studies have shown that structures other than f. c. c. are not present in reversed austenite.

Several investigations [1, 9, 22, 35] of reversion in stainless steels have also been concerned with precipitation during reversion and this aspect will be dealt with in a later section.

2.4. REVERSION IN Fe - Ni AND Fe - Ni - C ALLOYS:

Considerably more attention has been paid to reversion in Fe - Ni and similar alloys than in stainless steels. The transformation of $\alpha \rightarrow \gamma$ in alloys containing approximately 30% Ni has been shown to occur athermally, and martensitically with high heating rates [42, 46, 65]. Kessler and Pitsch [42] found that with slow rates of heating ($0.3^{\circ}C$/min), although the transformation begins martensitically in an Fe - 32.5 Ni alloy it then ceases and later continues by a diffusion controlled process. Jana and Wayman [46] also found that reversion can occur via both mechanisms in an Fe - 33.95 Ni alloy during slow heating ($1^{\circ}C$/min) but that it begins by a diffusion process and later changes to a martensitic process as the temperature is raised, rather than vice versa.

Gorbach and Malyshev [65] found that at low heating rates the transformation may be diffusion-controlled and that the critical rate which determines the diffusionless nature of the $\alpha \rightarrow \gamma$ transformation

in carbon containing alloys depends on their tempering resistance and the values of A_s and A_f. Seldovich et al [48] heated Fe - Ni specimens at 2°C/min. and reported that the transformation is dictated by diffusion processes in alloys with a low nickel content (below about 20%), while at higher nickel concentrations it is of a martensitic nature. Surface upheavals are associated with the diffusionless reverse transformation [36, 43, 45, 46, 66] as well as with the direct $\gamma \longrightarrow \alpha$ transformation. Several early Russian papers indicate that a mirror reproduction (surface relief) has been found to arise in the reverse martensitic transformation, but other references [36, 43, 45, 67] show that the relief accompanying reversion is more complicated than a simple mirror reflection of the relief of the direct transformation, suggesting that a large number of γ fragments arise during reversion at a place occupied by one martensite crystal. This aspect of the reversion mechanism will be dealt with later.

The austenite formed during reversion has a different appearance to the original austenite producing 'ghost' regions in optical micrographs.[3, 4, 36, 43] This is generally attributed to the inheritance by the reversed austenite of defects produced during both the direct and reverse transformations. These defects produce strengthening of the austenitic structure equivalent to that produced by considerable (e.g. 20%) plastic deformation of the original austenite [2, 3]. The extent of strengthening obtained depends on many factors but most markedly on the amount of martensite which participates in the reverse transformation [2, 65, 68].

The strengthened reversed austenite is capable of primary recrystallisation [2, 3, 37, 39, 69, 70] in an analogous manner to deformed austenite.

A recent paper by Hyatt and Krauss [70] has considered the effects of cyclic $\alpha \longrightarrow \gamma \longrightarrow \alpha$ transformation on the structure and properties of both austenite and martensite in a series of Fe - Ni - C alloys of various carbon contents.

Tempering of the martensite before reversion was reported by these authors as well as by Habrovec et al [71], and Hyatt and Krauss also investigated subsequent recrystallisation effects of the reversed austenite.

2.4.1. The Structure of Reversed Austenite:

Krauss and Cohen [3] observed that reversion begins at the periphery of α plates but that these plates subsequently break up in a piecewise fashion. Gorbach and Butakova [43] investigating a similar alloy found that, at the beginning of the transformation, plates of γ appear in the α crystals, lying across and intersecting the α crystal. These plates were seen to form very rapidly, absorbing a small volume of an α crystal and then ceasing to grow. Further transformation occurs only if the temperature is raised, and involves the formation of new plates of γ. Thus a martensite crystal transforms over quite a wide temperature range. Similar results have been reported by Kessler and Pitsch [42] and Jana and Wayman [46] in that early reversion begins inwardly at the α/γ interface and reversed γ plates later form within the α. The midrib section of the martensite disappears early during reversion [46].

The reverse martensitic transformation, therefore, does not necessarily reproduce the austenite lattice in its original orientation and the original grain of austenite then contains polycrystalline regions [42]. One can consider the presence of the substructure in the martensite crystal, or other features of its fine structure as considerably hindering the growth of an austenite crystal. In the reverse transformation the γ is growing in a medium with a different fine structure to that in which the α grew, causing the γ regions to be smaller than α. Gorbach and Butakova [43] suggest, therefore, that the reverse transformation be regarded not as the reverse process of the development of α crystals, but as a discontinuous process of the transformation of individual sections of an α crystal into fine γ fragments.

Electron microscopy has shown that the reversed austenite crystals contain dense dislocation networks [37, 42, 72] and sometimes a few SF_s along $\{111\}_\gamma$ planes. Krauss [37] found that the complex dislocation tangles were completely different to the straight or smoothly curved dislocations in the retained austenite and that the dislocation density was about ten times higher in the reversed austenite. Izmailov and Gorbach [40] found that the reversed austenite consists of a large number of small fragments generally 0.01 - 0.05 x austenite grain size. The complex dislocation tangles can be considered to have broken up the austenite lattice into a large number of blocks each having a small disorientation from the others in a mosaic type of structure. Many Russian workers [2, 5, 39, 40, 72] have measured these block sizes and disorientations during the direct and reverse transformations. Their results seem to suggest that the reverse austenite inherits the block size, disorientation and dislocation density possessed by the α immediately before transformation [4, 5, 39, 40, 72].

During the disappearance of 'ghost' areas at higher temperatures, Krauss and Cohen [3] noticed the formation of twins in the reversed austenite matrix which were termed reversal twins. Krauss confirmed their presence by electron microscopy [37] and found that they differed from annealing twins in the austenite in so far as they contained a highly imperfect internal structure with a high concentration of tangled dislocations. He suggested that they may represent the initial stage of recovery after reversion. Yakhontov [72] showed that no twins from the α were retained in the reversed γ and Shapiro and Krauss [45] were able to show that twins in the austenite formed during reversion by observing secondary tilts occurring during the surface upheavals associated with the reverse transformation. The same authors found that the macroscopic shear accompanying reversion was appreciably higher than that reported for the direct transformation and suggested a possible relationship between the $\{127\}_{bcc}$ twinning mode and the

nucleation of the reverse martensitic transformation.

The crystallographic aspects of the reverse transformation have received relatively little attention. Kessler and Pitsch [73] found that the crystallographic nature of the direct and reverse transformations in Fe - Ni is the same and they then concluded that the $\alpha \longrightarrow \gamma$ transformation is purely martensitic in such alloys at high heating rates. Further aspects of the crystallography of the reverse transformation in Fe - Ni have been reported by the same authors [49, 50]. Shapiro and Krauss [45] found that the orientation relationship between reversed - γ and α could not be accurately described by any simple parallelism of low index planes. Their results indicated the occurrence of two distinct habit planes for the transformation.

2.4.2. Increased Strength of Reversed Austenite:

The considerable fragmentation and disorientation of the crystal lattice and the high dislocation density lead to a substantial increase in strength relative to the original austenite as these will act as barriers to plastic deformation. Many reports exist of this strengthening effect of reversion in Fe - Ni alloys [2 - 5, 68, 69]. In similar work Malyshev et al [2] and Krauss and Cohen [3] showed that although the first reversion cycle produced a large increase in the yield strength, tensile strength and hardness of Fe - Ni alloys, subsequent cycles resulted in little further increase in strength. Krauss and Cohen found that the work hardening capacity of reversed austenite had been reduced, together with the extent of uniform elongation. The strengthening produced by one reversion cycle was equal to that obtained by deforming the annealed γ about 20% but as the latter had a greater work hardening rate it reached the same true stress at maximum load as the reversed austenite.

Reversion strengthening must be carried out at temperatures only slightly above the A_f as recovery and recrystallisation processes occur at higher temperatures [2 - 5, 39, 68, 69] after which the strength properties become the same as those of the original austenite. Krauss and Cohen [29] found that recrystallisation takes place by the migration of existing grain boundaries rather than the formation of new grains to produce a structure with more annealing twins than the original austenite. Izmailov et al [39] proposed that recrystallisation occurs in two stages. At lower temperatures the reversed - γ recrystallises followed at higher temperatures by recrystallisation of the retained austenite. They found the recrystallised grains were smaller in size by a factor of 2 or 3 and were randomly oriented with respect to retained austenite crystals. Some recrystallisation of the defect structure produced by the reverse transformation was found [48] in an Fe - 22 Ni - 0.6 C alloy after a reversion treatment of two minutes at 740°C.

There is evidence [74] to suggest that increasing the rate of heating during reversion lowers the temperature at which recrystallisation begins and increases the speed of recrystallisation.

2.5. REVERSION IN SOME OTHER SYSTEMS:

The reverse martensite transformation has been studied in ferrous systems in addition to Fe - Cr - Ni and Fe - Ni. These include Fe [75 - 77], Fe - Cr [78], Fe - Mn [48, 79 - 81], Fe - Ni - V [68, 72], Fe - Ni - Ti [68,82], Fe - Ni - C [65, 70, 71, 83], Fe - Ni - Mn [84], Fe - Mn - C [65, 80], Fe - Cr - C [65], Fe - Ni - Cr - C [65], Fe - Ni - Cr - Si - C [65], Fe - Mn - Cr - Ni [2], and maraging steel [85, 86].

An investigation by Zwell et al [75] into the effect of transformation cycling on the dislocation substructure of pure iron showed that a polycrystal developed a rather complex arrangement of dislocations, which became increasingly complex and more dense as the number of

$\alpha \rightarrow \gamma \rightarrow \alpha$ cycles increased. X-ray work showed that the cycling had produced a fine substructure and increased cycling increased the total lattice misorientation of the grains. These are local orientation differences which are generated by intermediate dislocation groupings which are more diffuse than well-defined sub-boundaries and are not recognised as such in electron micrographs. Zerwekh and Wayman [77] showed that the $\alpha \rightarrow \gamma$ transformation in pure iron can occur martensitically.

Investigation of the $\gamma \rightleftharpoons \varepsilon$ transformations in Fe - Mn alloys has been made by Shklyav et al [79], Seldovich et al [48], Lysak and Nikolin [80] and Yershova and Bogachev [81]. The transformation is shown to be a 'diffusionless shearing process' in which one of the octahedral γ planes remains parallel to the basal plane of the h. c. p. phase. The transformation strengthens not only the γ, but also the ε (i. e. second generation ε) and can lead to initial enhancement and later stabilisation effects of the $\gamma \rightarrow \varepsilon$ transformation [81].

The $\alpha \rightarrow \gamma$ transformation in an Fe - Cr alloy has been shown by Lacoude and Goux [78] to occur in two different stages between A_s and A_f. The first stage is very rapid and the authors conclude that it is martensitic in nature. The second stage starts firstly by the growth of existing γ grains and then by the nucleation and growth of new γ grains.

The influence of heating rate on the nature of the $\alpha \rightarrow \gamma$ transformation in an 18% nickel maraging steel has been studied by Goldberg and O'Connor [86] and in greater detail by Goldberg [85]. It was shown that the transformation can be diffusional or martensitic in nature according to the heating rate, and that compositional changes are important in the case of slow heating.

A study of $\beta \rightleftharpoons \alpha$ cycling in cobalt has been made by Yegolayev et al [87].

2.6. THE EFFECT OF PRIOR DEFORMATION ON REVERSION:

The effect of deformation on reversion strengthening in Fe - Ni alloys has been indicated by a number of Russian investigators [4, 5, 41, 48, 51, 68]. Melnikov et al [41] deformed, at various temperatures, a martensitic structure which had formed on quenching to -196°C. They found that deformation at room temperature had a progressive stabilising effect in that it raised the A_s temperature whereas that carried out nearer to the A_s induced transformation to γ and lowered the A_s. This is analogous to the effect of deformation of austenite near to the M_s temperature and well above this temperature, i.e. deformation appears to affect the direct and reverse transformations in a similar manner.

Zatsev and Gorbach [5] showed that deformed martensite transforms at a higher temperature but more rapidly i.e. A_s and A_f are raised but the range $A_s \longrightarrow A_f$ is narrower. The reversed austenite which forms is stronger than the normal reversed austenite but was found to be less stable, as shown by the fact that it recrystallised at lower temperatures. These findings are in agreement with the results of Golovchiner [68] on an Fe - Ni - V alloy. Papers by Seldovich et al [48] and Sokolov et al [51] on various Fe - Ni alloys show that prior deformation lowers the A_s temperature of low Ni alloys and raises that of higher nickel alloys; the distinction appears to coincide with the change from a diffision-controlled to a martensitic reversion process. An increased tendency to recrystallisation by the austenite formed from deformed martensite is also reported [48].

Zatsev and Gorbach [4] showed that the reversed austenite in an Fe - 28 Ni alloy had a structure very similar to that of the deformed martensite from which it had formed even though completely austenitic. This 'deformed' reversed austenite softened rapidly due to the disappearance of the inherited lattice defects by the annihilation of dislocations and the subsequent development of recrystallisation.

Reed [14] has shown that, in an 18/8 type of steel, the A_s temperature is raised and the rate of $\alpha' \rightarrow \gamma$ reversion is more rapid in the case of deformation induced martensite than with that formed by quenching.

2.7. PRECIPITATION DURING REVERSION:

Precipitation processes occurring during reversion have been reported on several occasions [1, 2, 9, 22, 35, 65, 68, 70, 71, 82]. Of the reports concerned with stainless steels [1, 9, 22, 35] only that by Thomas and Krauss [9] provides much useful information. These authors found precipitates, identified as Cr - rich $M_{23}C_6$ in laths or bands in many different orientations in areas of α' after reversion. The α' was present because precipitation had depleted the austenite matrix of alloying elements and thus raised the M_s temperature above room temperature. The precipitation was thought to have occurred in the α' just prior to reversion; and the habit plane was found to be about 5° from $\{2\ 11\ 22\}_\gamma$.

The effect of precipitation on the strengthening of reversed austenite was not measured by Thomas and Krauss but the combined effect of reversion and precipitation strengthening in an Fe - Mn - Cr - Ni - C alloy [2] was found to increase the yield stress by more than 400%. However, after 3 cycles the strength falls off again.

Golovchiner [68] observed that the strength of an Fe - Ni - Ti alloy after reversion was even higher than that of the work hardened martensite from which it had formed. The difference between properties obtained from Fe - Ni - Ti and Fe - Ni - V alloys was attributed to the fact that the Fe - Ni - Ti system possesses a process of precipitation of some Ti - rich disperse phase from the α, which actually altered the nature of the reverse transformation and led to further strengthening.

Gorbach et al [82] also noticed that the strengthening by reversion of Fe - Ni alloys is greatly increased by the presence of small amounts of Ti (1 or 2%). However they showed that the structure of reversed austenite in the Fe - Ni - Ti alloy was no more disperse than under the same conditions in an Fe - Ni alloy. Furthermore, slow heating produces a much harder structure than rapid heating, contrary to expectations. The strengthening could not therefore be attributed solely to the γ - substructure which develops on reversion and they suggested that it was due to a combination of reversion strengthening and dispersion hardening. Gorbach et al attempted to separate the two effects and ascertain whether precipitation occurred in the α or γ phase. They concluded that the important factor in the strengthening by reversion of Fe - Ni - Ti alloys is precipitation in the austenite which has a fine substructure as a result of the $\gamma \rightarrow \alpha \rightarrow \gamma$ transformations.

The formation of carbides in martensite in Fe - Ni - C alloys prior to reversion has been reported by Hyatt and Krauss [70] and Habrovec et al [71]. The former authors suggest that appreciable coalescence and spheroidisation of the carbides occurs during the reversal treatment.

2.8. AUSTENITE STABILISATION EFFECTS OF REVERSION:

Breedis and Robertson [23] found that after reversion of a 16/12 Fe - Cr - Ni alloy transformation occurred at exactly the same sites as before on cooling again, suggesting that no stabilisation of the austenite had occurred as the result of the reverse martensitic transformation. However, in a similar alloy, Breedis [8] found that up to 35% stabilisation occurred but that this effect was less after two hours at the reversion temperature, than after two minutes. Transformation could be enhanced by reversion near to the A_s temperature. Breedis concluded that the defect structure in austenite, and not solute redistribution, is behind the observed stabilisation effects.

Stabilisation in an Fe - 9 Cr - 14 Ni alloy was also found by Malyshev et al [2] who found that the martensite transformation could be almost completely suppressed by two reversion cycles. While accepting that the presence of carbon and nitrogen might influence stabilisation, the main cause was attributed to the non-removal of stresses in the austenite during heating.

Conflicting reports exist on the development of stabilisation by reversion in Fe - Ni alloys [2, 3, 36, 44, 47, 74]. Edmondson & Ko. [36] found that the austenite could be fully stabilised by 15 cycles of the reverse transformation in an Fe - 34 Ni alloy. Malyshev et al [2] found only slight stabilisation in so far as the M_s was lowered but the amount of martensite formed at -196°C was about the same in their study of an Fe - 27.8 Ni alloy.

Jordan and Borland [47] suggest that whether or not the residual stress pattern in the 'reversed' austenite will stimulate or retard subsequent transformation to martensite will depend in part on the relative magnitude of the flow stress of the alloy and the stresses set up by the transformation strains during the course of a cycle. They have attempted to make a quantitative interpretation of their ideas for both slow and rapid cooling.

Golovchiner and Tyapkin [74] found that the reverse martensitic transformation hinders subsequent transformation to martensite in Fe - Ni and Fe - Ni - Ti alloys but that heating in a lead bath produces less stabilisation than heating in air. The importance of the heating rate was also noticed by Krauss and Cohen [44] who explained the absence of stabilisation in their previous investigation [3] and its presence in similar material studied by Edmondson & Ko. [36] in terms of the opportunity for the formation of low - Ni ferrite by diffusion during slow heating. They concluded that 'the lattice imperfections and strengthening produced by the reverse transformation are not

responsible for the marked stabilisation which has been observed by other investigations in these alloys'.

Golovchiner and Tyapkin [74] suggested that the heating rate is most important in the temperature range 300 - 400°C, but rejected the idea of diffusion processes playing an important role in stabilisation. Presumably stabilisation effects produced by lattice imperfections only would be removed by recrystallisation but these authors offer no explanation of the incomplete correlation between the removal of stabilisation and the onset of recrystallisation.

CHAPTER 3

EXPERIMENTAL PROCEDURE

3.1. ALLOY PREPARATION:

The vacuum melted alloys, supplied by International Nickel Ltd., were received as 3/8" thick hot-forged plate. Their compositions, in weight per cent, are as follows:

Alloy A:

Fe	C	Cr	Ni	Mo	Al	Si	Mn	S
bal	0.002 0.003	16.1	11.7	<0.01	0.01	<0.02	<0.05	0.007
P	Cu	Ti	Co	V	Pb	B	Zr	Mg
0.003	<0.05	<0.05	<0.10	<0.02	<0.001	<0.002	<0.01	<0.01

Alloy B:

Fe	C	Cr	Ni	Mo	Al	Si	Mn	S	P
bal	0.090	14.9	8.7	2.05	<0.01	<0.05	<0.05	0.002	<0.002

3.2. FABRICATION AND HEAT TREATMENTS:

3.2.1. Homogenising:

Strips approximately 4" x 1" x 3/8" were cut from the hot-forged plates and surface ground to a minimum depth of 0.05" on each surface. Homogenising was then performed under dynamic vacuum for 24 hours at 1100°C followed by furnace cooling under vacuum.

3.2.2. Rolling and Intermediate Heat Treatments:

Both alloys were then rolled at room temperature to a thickness of 0.2". Further homogenising-annealing treatments were performed for three hours at 1100°C under vacuum followed by furnace cooling. After cleaning the surface the specimen thickness was reduced by 50% by cold rolling,

i.e. to about 0.1".

For further treatments, specimens were sealed in silica tubes under a partial atmosphere of argon and heated in a vertical crucilite rod furnace. Direct quenching from the annealing temperature was obtained by passing an electric current through the fuse-wire from which the specimen was suspended, allowing it to fall. The specimen pierced the aluminium foil seal on the bottom of the furnace before entering a bucket of water placed beneath it. The silica tube was smashed directly on entering the water and a rapid quench was thus obtained by this technique.

The solution treatment time and temperature, following a standard deformation, determine the material grain size and hence also influence mechanical properties and subsequent transformation to martensite. In Alloy A a treatment of 20 minutes at 1050°C was given, 10 minutes being allowed for the specimen to reach the treatment temperature. An average grain diameter of about 40 microns was obtained by this technique. Subsequent rolling-annealing treatments were repeated on this pattern of 50% deformation followed by 20 minutes at 1050°C and water quenching until the required thickness was obtained. After each heat treatment surface layers were removed chemically by immersing in a warm solution containing 50% HCl, 10% HNO_3, 5% H_3FO_4, 35% H_2O.

Alloy B was treated for one hour at 1250°C, also with 10 minutes allowed for heating up. In this case the treatment conditions were chosen by consideration of carbide solution, grain size and the amount of martensite which could be produced by subsequent treatment at -196°C. The specimen surfaces were cleaned in the same way as for Alloy A.

3.2.3. Sub-zero Treatments:

Partial transformation to martensite was obtained by quenching the steels to -196°C for 15 minutes and one hour for alloys A and B respectively. Treatments at other sub-zero temperatures (e.g. for M_s determinations) were performed by immersion in various mixtures of iso-pentane and liquid nitrogen. These mixtures could be kept to $\pm \frac{1}{2}$°C for periods up to about 5 minutes.

3.2.4. Reversion, Annealing and Ageing Treatments:

Reversion treatments were performed with rapid heating rates for short times on the assumption that the reverse martensite transformation is largely athermal in nature under such conditions and isothermal processes would be largely suppressed. These treatments were thus carried out by plunging specimens suspended by wire into a salt bath at the required temperature. Small disc specimens for electron microscopy were contained in a gauze cage. Specimens were water quenched from the reversion temperature.

Annealing and ageing treatments were usually done in a horizontal tube furnace with the specimens sealed in silica under a partial atmosphere of argon. Specimens were either air-cooled or water quenched to room temperature depending on the nature of the treatment. In either case the silica was smashed immediately the specimen was removed from the furnace. Treatments requiring rapid heating to the annealing temperature, or those of less than about one hour in duration, were performed in a salt bath.

3.3. MAGNETIC MEASUREMENTS:

Room temperature measurements of specific magnetic intensity, and hence of martensite content, were made using a Sucksmith Ring Balance built as part of this project. Detailed information on the Balance is given in Appendix A.

Specimens approximately $\frac{1}{4}$" x $\frac{1}{4}$" x 0.025" were cut from cold rolled strip and their centres drilled using a No. 50 drill. They were then annealed in the usual way at 1050°C or 1250°C to remove any deformation produced by the specimen preparation. Subsequent heat treatments were followed by chemical removal of about 0.01" from the surface layers which may have undergone compositional changes.

The specimens were weighed and their displacements measured under the influence of a field gradient produced by an electromagnet as described in Appendix A. By comparison with the displacement of a pure iron specimen of similar weight, it was possible to evaluate the specific magnetic intensity of the specimens and hence their martensite content. The small contributions to the measured specimen deflections arising from the weakly paramagnetic nature of the specimen holder and the influence of the magnetic field on the transducer meter were eliminated from the recorded results by taking a 'zero' reading under the normal operating conditions, using a specimen holder but no specimen.

Specimen to specimen variations were often noticed which exceeded the reproducibility of readings on a given specimen (see Appendix). These variations were attributed to the inherently inhomogeneous nature of the martensite transformation and their importance was minimised by taking readings on several specimens (usually three) in each heat treated condition. An average value was then obtained.

It is known [88] that a strong magnetic field can enhance the transformation of austenite to martensite; an increase in the M_s of 5°C was detected on cooling a low alloy steel in a field of 16 kG. There exists, then, the possibility of specimens undergoing martensitic transformation during magnetic measurements.

In the case of Alloy A the M_s is about 70°C below room temperature and remains at about this level after the various heat treatments. Room temperature measurements on Alloy A are thus unlikely to induce transformation to martensite. The same applies to Alloy B after solution treatment, quenching and short reversion treatments. However, after ageing treatments the M_s temperature of this alloy can be raised to above room temperature and it is possible that some further martensitic transformation could then be induced during magnetic measurements. The amount of transformation, if any, is likely to be very small because of the characteristics of the martensite transformation in these steels (cooling almost 150°C below the M_s produces only about 12% transformation, see Results section) and the value of the magnetic field used, about 12 kG. Furthermore, the results for aged specimens are not presented as percentage of martensite but as displacement per unit mass because of the uncertainty of the composition of the alloy-depleted matrix after ageing. Thus, any slight effects of the magnetic field on these semi-quantitative results are not of great importance.

3.4. DYNAMIC YOUNG'S MODULUS MEASUREMENTS:

Strip specimens approximately 4" x 0.25" x 0.020" were quenched in liquid nitrogen after solution treatment. They were then used to measure dynamic Young's modulus utilizing transverse free-free vibration under vacuum at temperatures up to about 650°C. The apparatus is described in Appendix B and is similar to that of Lytton et al [89]. It permits accurate measurement of the resonant frequency, fr, of the specimen which is related to the square root of the modulus, E.

A heating rate of about 20°C/minute was used.

3.5. MEASUREMENT OF M_s TEMPERATURES:

Solution treated magnetic balance specimens were chemically cleaned and electro-polished (see below) before being held for one minute at various sub-zero temperatures. The specimens were then used for measurements of specific magnetic intensity at room temperature. Near the M_s temperature treatments were performed at 2°C intervals, the temperature being constant to $\pm \frac{1}{2}$°C. The treatment temperature for which martensite was first detected (about 0.1%) was taken to be the M_s temperature.

3.6. MEASUREMENT OF A_s AND A_f TEMPERATURES:

The temperatures representing the start and finish of the reverse martensite transformation were estimated from measurements of hardness and specific magnetic intensity after heating for short times (2 minutes and 1 minute for Alloys A and B respectively) by plunging the specimens into molten salt baths at the required temperature, and requenching to room temperature in water.

The A_s and A_f were also estimated, during slower heating rates, by measurements of dynamic Young's modulus and by dilatometry.

3.7. HARDNESS MEASUREMENTS AND LIGHT MICROSCOPY:

Specimens approximately $\frac{1}{2}$" x $\frac{1}{4}$" x 0.05" were cleaned by chemical thinning to a depth of about 0.01" after heat treatment and polished on silicon carbide papers. Hardness measurements were then made using a diamond indentor and a 5 Kg load except for measurements on cold-worked samples, when a 10 Kg load was used. Average values were obtained from at least two specimens using a minimum of 5 indentations on each specimen and often as many as 10.

Specimens for light microscopy were further polished using diamond paste down to $\frac{1}{4}$ micron. Electro-polishing was performed using parallel stainless steel electrodes and a saturated solution of chromium

trioxide in orthophosphoric acid at 50 volts. Etching was done either electrolytically using a 10% solution of oxalic acid in water at 1.8 volts for 3 - 5 minutes or chemically by swabbing with a fresh solution containing 1 part HNO_3, 3 parts HCl and 2 parts glycerol.

3.8. MECHANICAL PROPERTY MEASUREMENTS:

A small number of tensile tests were carried out on Alloy A using standard strip specimens with a 1" gauge length, 0.188" width, and about 0.020" thickness. An Instron machine was used at a cross-head speed of 0.1 cm/min. The usual machine corrections were made.

The specimens were machined from 0.020" cold-rolled strip before heat treatment. Their surface was then cleaned chemically and their dimensions measured before testing. Values of the 0.2% Proof Stress, Ultimate Tensile Strength and % Elongation were obtained from the results. Steels of this type are known [31] to transform partially to martensite during testing and allowance must be made for this when interpreting the results.

3.9. DILATOMETRY:

Dilatometric measurements were made using a differential technique (see Appendix C) during continuous heating at several different rates. Specimens of Alloys A and B, in which martensite had been produced by quenching in liquid nitrogen and by cold rolling, were investigated. Their changes in length during heating were continuously compared to the thermal expansion of a fully austenitic sample of similar composition in which no phase transformations occurred; viz. the 'control' specimen. A fully annealed specimen of Alloy A was chosen for this purpose.

The heating rates used were approximately linear above 300°C and can be described relatively as 'fast', 'medium' and 'slow', corresponding to average rates of about 165, 16 and 4.5°C/min.

The fast heating rate was obtained by having the furnace controlling at a temperature about 150°C above the A_f temperature for the alloys and then removing it up around the specimens. For the two slower heating rates the furnace was raised while at an initial temperature of about 350°C. As the specimen temperature rose power was applied to the furnace such as to produce the 'medium' and 'slow' heating rates.

Aspects of the accuracy and reproducibility of the technique are discussed in Appendix C.

3.10. ELECTRON MICROSCOPY:

Thin foil specimens were examined in an EM6G electron microscope, operating at 100 kV, using standard techniques. The usual calibrations for image magnification and rotation were made.

3.10.1. Specimen Preparation:

Discs of 3 mm diameter were punched from cold-rolled sheet 0.02" thick. Subsequent heat treatment thus eliminated any deformation introduced by the punching operation. After heat treatment the discs were chemically thinned (using the solution described above) to 0.008" and polished on fine silicon carbide papers to 0.005" to remove any etching/pitting effects of the chemical thinning.

A jet profiling technique was used as the first of the two stages of the thinning process. The specimen was held horizontally in a PTFE holder and a solution of 37% HCl was directed onto the specimen. A potential of 60 volts produced a current of about 0.6 amps and was applied for 6 seconds on each side. Final thinning in a saturated solution of chromium trioxide in orthophosphoric acid, cooled by an ice + water mixture, at 13 volts (about 0.45 amps) produced perforation at the centre of the disc after 1-2 minutes.

In the case of aged specimens of Alloy B, this method was found to lead to preferential attack at the grain boundaries and was thus unsuitable for the preparation of thin foils in such specimens. Instead, a solution containing 133 c. c. glacial acetic acid, 25 gm. chromic oxide and 7 c. c. distilled water was used at 10 - 15°C for the final stage. A potential of 22 volts (about 35 mAmps) produced almost no preferential grain boundary attack and thin areas were obtained after about 10 minutes.

The specimens were washed by directing a jet of distilled water tangentially onto their surface, and dried between sheets of absorbent tissue. If examination was not performed almost immediately after preparation, the specimens were stored in gelatine capsules in a dessicator until required.

CHAPTER 4

RESULTS

4.1. FORMATION OF MARTENSITE ON COOLING:

Alloy A.

In the standard condition, produced by a 50% reduction by rolling at room temperature and annealing for 20 minutes at 1050°C followed by water quenching, the alloy has an M_s temperature of -50°C. Magnetic measurements show that holding for 15 minutes at -196°C produces just over 15% ferromagnetic martensite, α'. Although hexagonal martensite, ε, is also present in small amounts, no attempt has been made to determine the precise quantity.

Light microscopy, FIG. 4.1, shows that transformation to martensite occurs in laths on certain crystallographic planes in the austenite. In this photograph one grain has etched preferentially, the surrounding grains being only mildly attacked. Electron microscopy shows that the laths are bounded by $\{111\}_\gamma$ planes. The well-known morphology of the transformation products is shown in FIG. 4.2.; many individual grains of α' containing a high dislocation density exist within the transformed laths, together with more isolated α' grains joined by regions of ε martensite and/or stacking fault clusters. The remaining areas are retained austenite and are observed to have a characteristically low dislocation density.

Alloy B.

The alloy was found to have a M_s temperature of -40°C after a solution treatment of 1 hour at 1250°C and water quenching. The transformation to martensite at -196°C shows isothermal characteristics, FIG. 4.3.

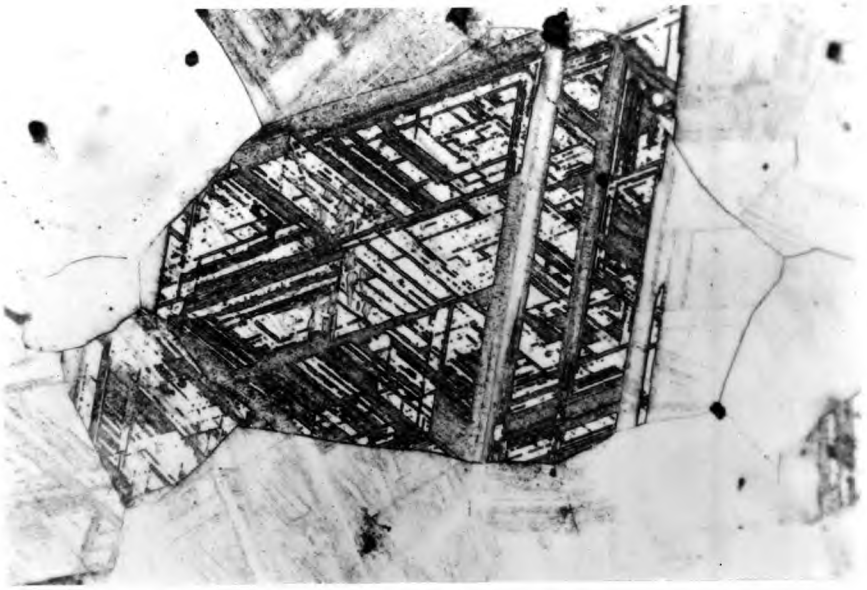

FIG. 4.1. Alloy A. Partial transformation to martensite (dark regions) produced by holding for 15 minutes at -196°C. Light micrograph X 300.

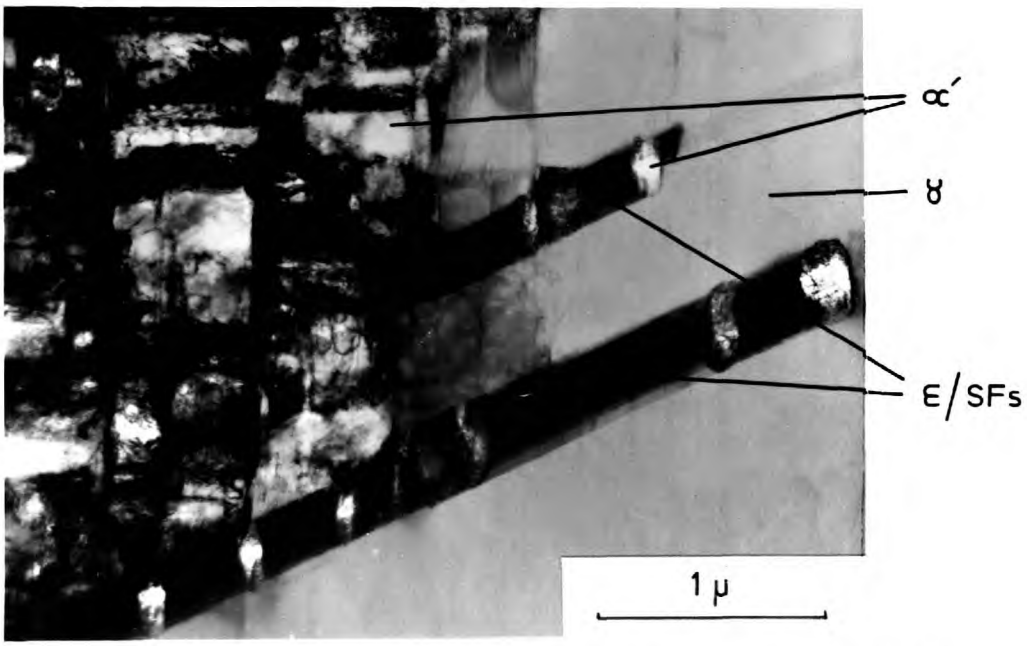

FIG. 4.2. Alloy A. Electron micrograph of the partially martensitic structure.

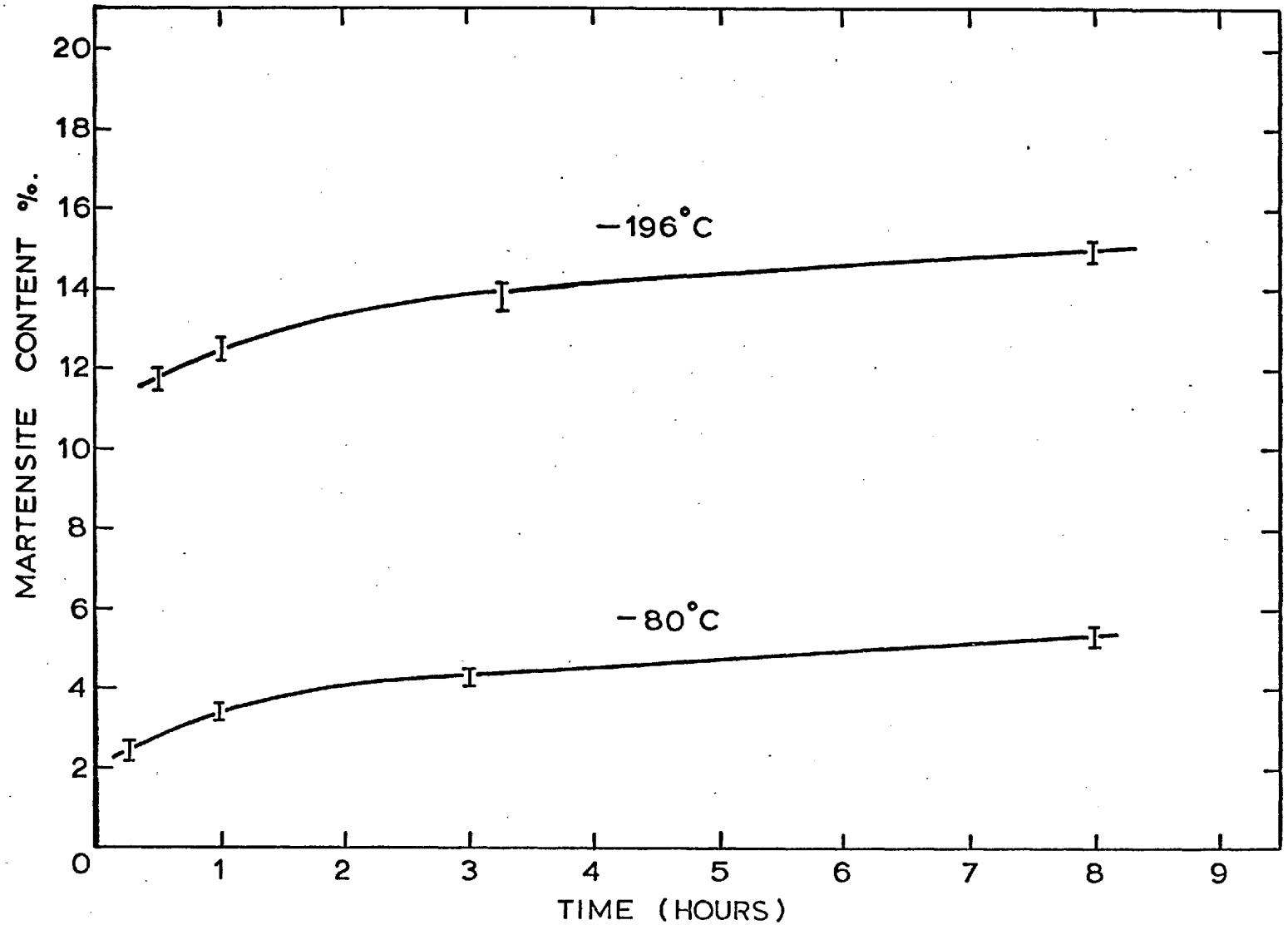

FIG. 4.3. Alloy B: Martensite formation during holding at -80°C and -196°C.

A commercial steel of similar composition, FV 520(S), is known to produce more martensite during holding at -80°C than at -196°C. To investigate whether Alloy B exhibits similar characteristics, specimens were held at -80°C for various times after which measurements of their saturation magnetic intensities were made at room temperature. The results, FIG. 4.3., show that although the transformation proceeds isothermally, the amount of martensite formed is small.

Furthermore, repeated cycles of quenching from room temperature to -196°C for 1 hour produced little additional martensite after the first cycle (Table I) although it has been reported [90] that such a treatment does lead to further transformation. Comparison with FIG. 4.3. shows, in fact, that less martensite is produced by three separate 1 hour quenches (to -196°C) than by holding for 3 hours at that temperature.

TABLE I

Treatment:	1st Quench	2nd Quench	3rd Quench
% α' :	12.5	12.8	12.9

The standard treatment for partial transformation to martensite was chosen as 1 hour at -196°C, producing approximately 12.5% martensite.

The structure of the partially martensitic alloy is shown by light microscopy, FIG. 4.4., to consist of laths of martensite on certain crystallographic planes in the retained austenite, similar to Alloy A. Features of the transformation product are visible within the laths. The electron micrograph of FIG. 4.5. shows two laths close together, containing α' and ε martensites, and retained austenite with a characteristic low dislocation density.

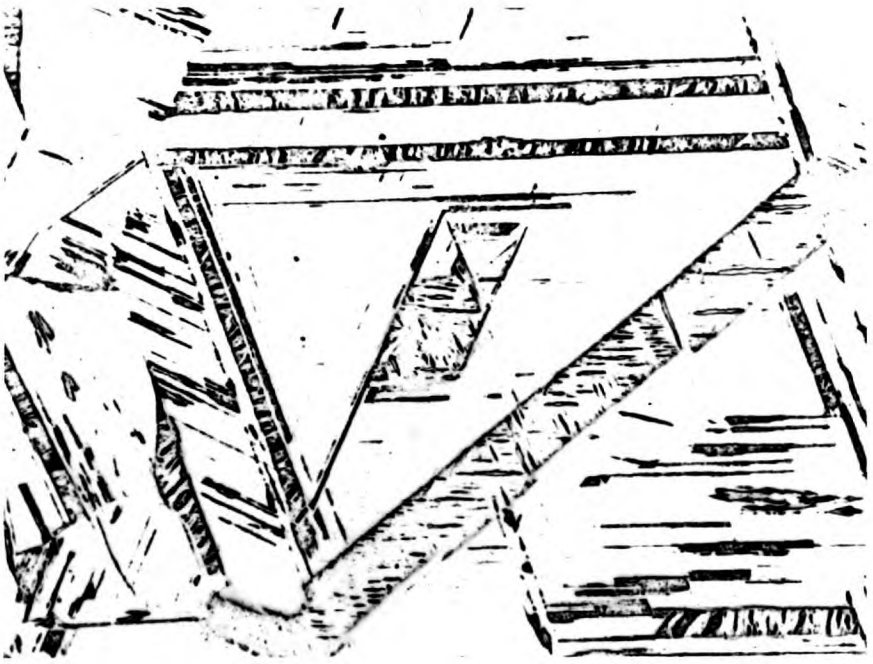

FIG. 4. 4. Alloy B. Partial transformation to martensite produced by holding at -196°C for 1 hour.
Light micrograph X 240.

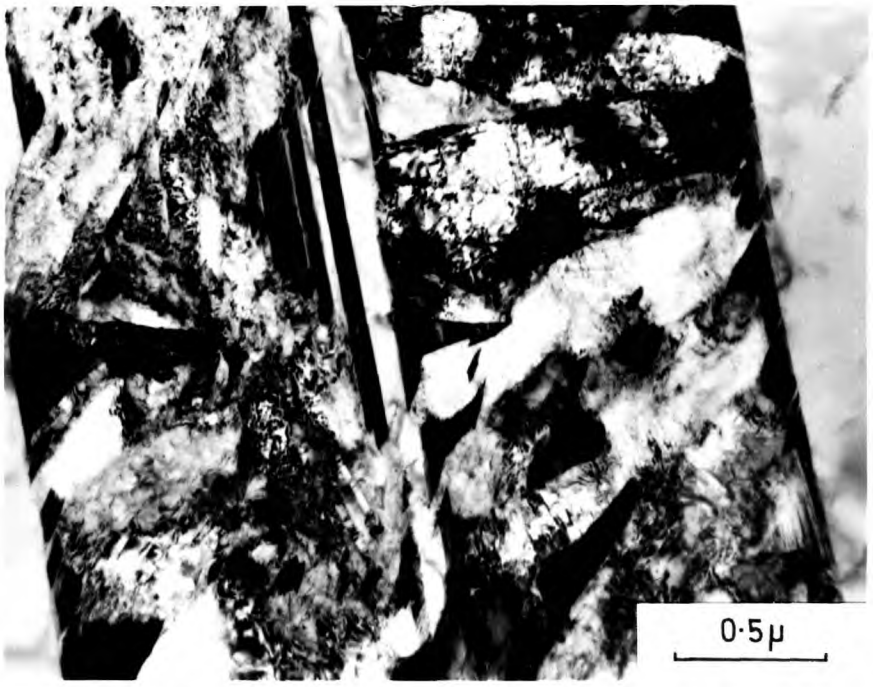

FIG. 4. 5. Alloy B. Electron micrograph of the partially martensitic structure; showing bands of transformation product bounded by retained austenite.

4.2. REVERSION OF MARTENSITE TO AUSTENITE:

Alloy A.

4.2.1. Determination of A_s and A_f on Rapid Heating:

The partially martensitic structure was heated for 2 minutes at various temperatures by plunging specimens into fused salt baths and then quenching them in water. The resulting changes in hardness and martensite content measured at room temperature are shown in FIG. 4.6. The hardness is seen to increase slightly after heating in the range 450 - 500°C; it falls to a 'plateau' between 600 and 700°C and then decreases towards the hardness of the original austenite. There is a small increase in martensite content after heating between 300 and 400°C but the % α' drops rapidly above 500°C and after 2 minutes at 600°C the structure contains no ferromagnetic phase. The temperature at which the reverse transformation ($\alpha' \longrightarrow \gamma$) begins, A_s, is less well defined than that at which the transformation is completed, A_f. From FIG. 4.6., A_s and A_f are estimated as approximately 450°C and 600°C respectively.

The hardness results in FIG. 4.6. have been supplemented by an investigation of tensile properties, FIG. 4.7. These curves are not directly comparable as the tensile properties refer to material with a larger grain size, having been annealed for 1 hour at 1050°C; their general form is, however, very similar. Because of the transformation of austenite to martensite during plastic deformation, it is the proof stress values which are the most representative of the different structures. It is noticed that the proof stress after reversion ($\sim 14\frac{1}{2}$ t. s. i.) is almost double that of the annealed austenite ($\sim 7\frac{1}{2}$ t. s. i.) even though only about 15% of the alloy participates in the direct and reverse transformations, i.e. $\gamma \longrightarrow \alpha' \longrightarrow \gamma$.

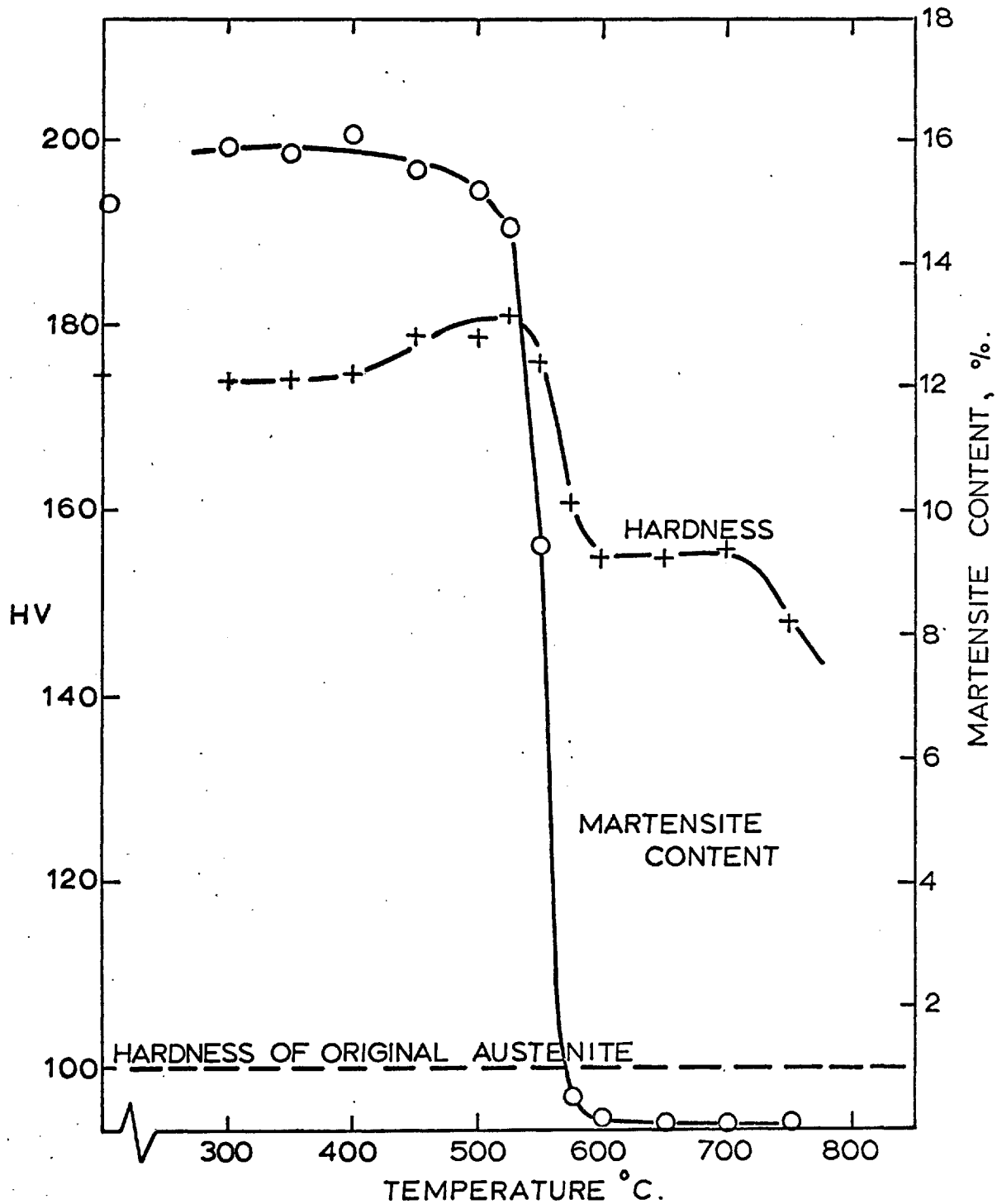

FIG. 4.6. Alloy A: Changes in hardness and martensite content after heating the partially martensitic structure for 2 minutes to the temperatures shown and water quenching to room temperature.

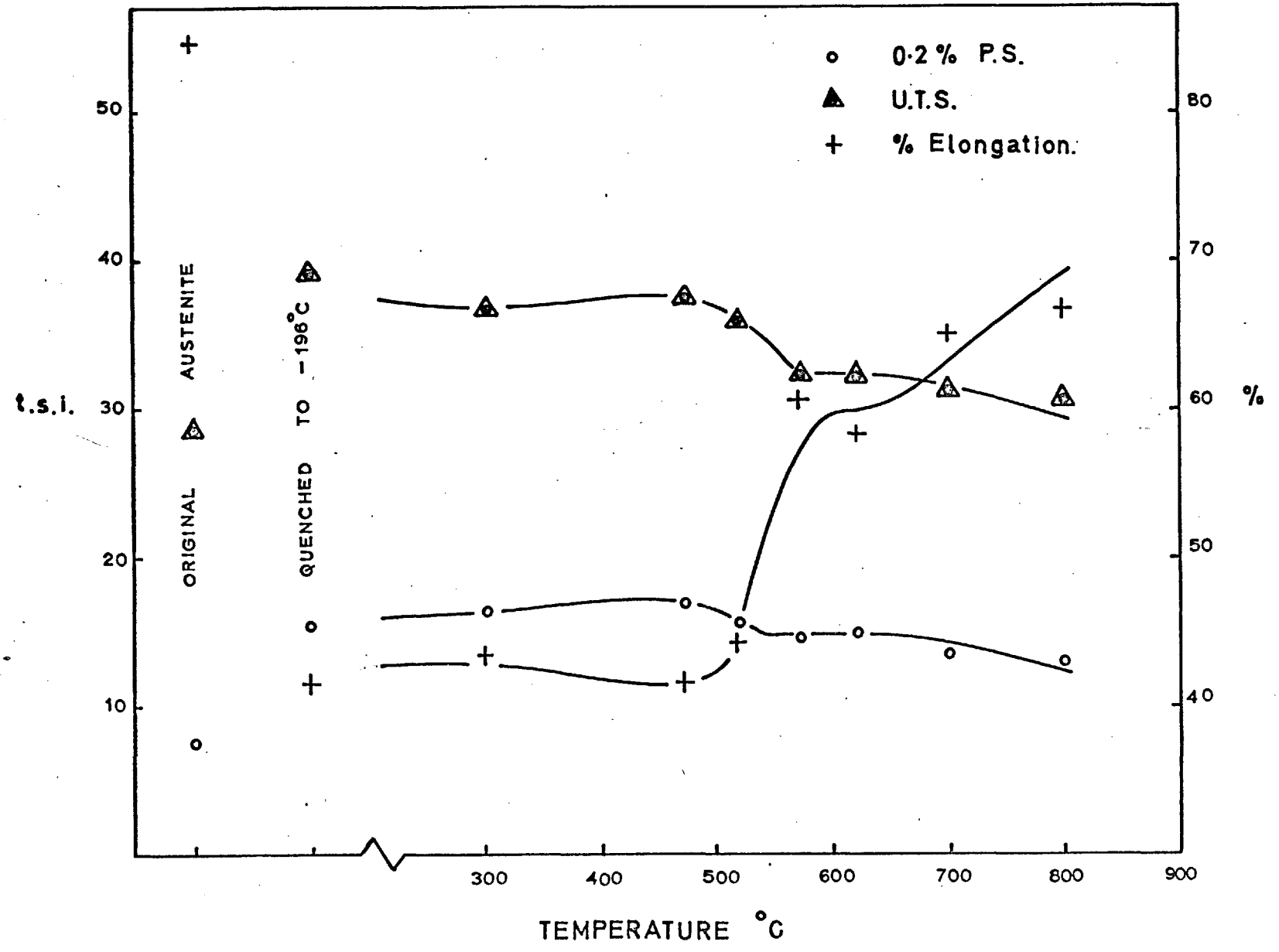

FIG. 4.7. Alloy A: Tensile properties after treating as for FIG. 4.6.

4.2.2. Structural Changes:

After heating for 2 minutes at 600°C, when the alloy is again fully austenitic, light microscopy reveals the presence of 'ghost areas' which etch preferentially to the retained austenite, FIG. 4.8., and have a similar morphology to the original martensitic regions (FIG. 4.1.). The fine structure of these areas of 'reversed austenite' is shown in FIG. 4.9. and is seen to contain a very high density of tangled dislocations as compared to that of the retained austenite shown at the top and bottom of the figure. Many small twins lying parallel to the boundaries of the lath are visible.

It is of interest to know how this structure of reversed austenite develops from that of the martensite already described. Thus, samples were heated for 2 minutes at temperatures between the A_s and A_f, after quenching for 15 minutes at -196°C, and then examined in the electron microscope. The structure shown in FIG. 4.10. was observed after heating for 2 minutes at 525°C; the large number of twins and/or stacking faults between the α' grains comprising the lath is a typical feature of the structure after such a treatment. FIG. 4.11. shows twins and stacking faults within a lath after heating for 2 minutes at 550°C.

In many cases the transformation of $\alpha' \longrightarrow \gamma$ produces austenite which has essentially the same crystallographic orientation as the retained austenite. An example of this is shown in FIG. 4.12. Grains A and B have an f.c.c. structure and exhibit almost the same orientation as the retained austenite; all three areas have a [100] zone axis. Furthermore the [002]directions in grain A and in the retained austenite show no measurable misorientation although a different reflection is found to operate in each case, namely (020) and (002) respectively, indicating that some small misorientation does exist. The [002] direction in grain B is found to be about 4° from the same direction in grain A and the retained austenite.

FIG. 4.8. Alloy A. 'Ghost areas' after reversion at 600°C for 2 minutes. Light micrograph X 185.

FIG. 4.9. Alloy A. Reversed austenite bounded by retained austenite; treated as in FIG. 4.8.

FIG. 4.10. Alloy A. Heated for 2 minutes at 525°C after quenching to -196°C for 15 minutes.

FIG. 4.11. Alloy A. Heated for 2 minutes at 550°C after quenching to -196°C for 15 minutes.

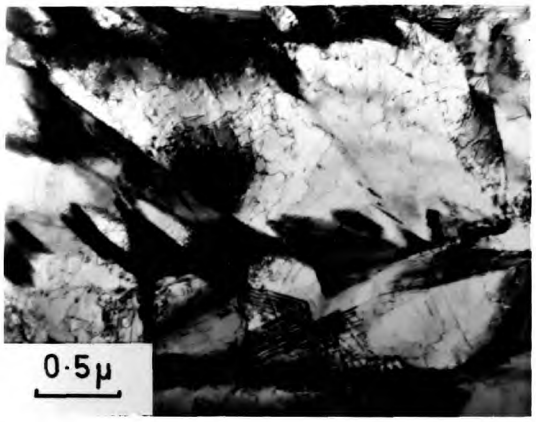

FIG. 4.12. (a). Alloy A. Heated for 2 minutes at 555°C after quenching to -196°C for 15 minutes.

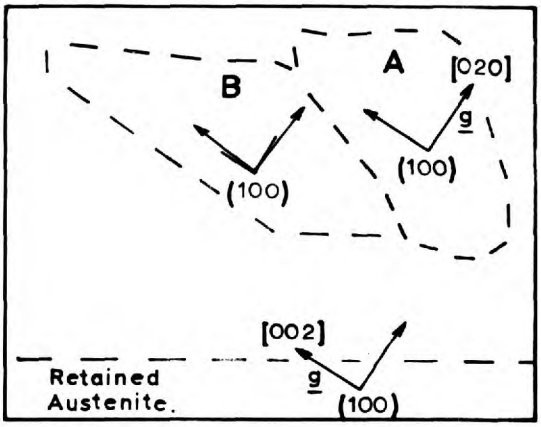

FIG. 4.12. (b). Diffraction pattern data shows that regions A and B have effectively returned to the orientation of the retained austenite.

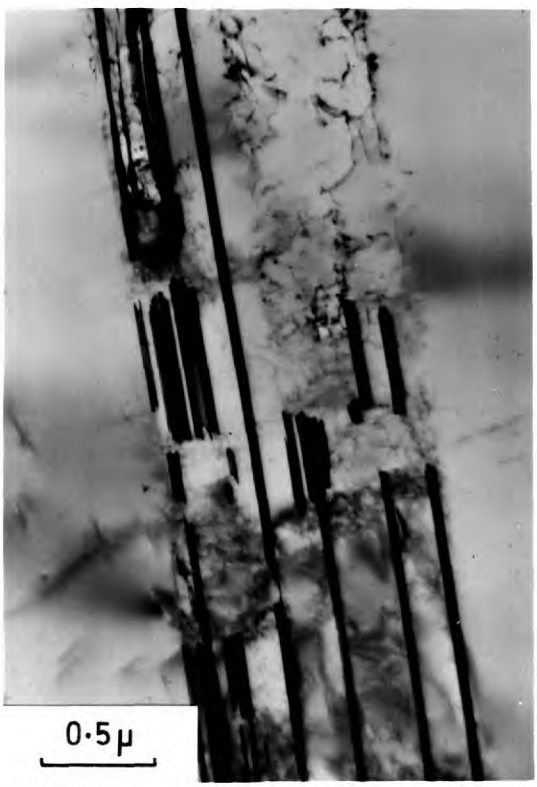

FIG. 4.13. Alloy A. Heated for 2 minutes at 575°C after quenching to -196°C for 15 minutes.

FIG. 4.14. Treated as for FIG. 4.13. showing clearly twins in what was originally a martensitic region.

After heating to 575°C for 2 minutes large areas of martensite have completely retransformed to austenite and a typical area is shown in FIG. 4.13. Retained austenite is shown on either side of a lath containing a higher dislocation density and many long twins (dark) lying parallel to the side of the lath. Tilting this area in the microscope relative to the electron beam showed that the lath contained a higher density of lattice defects than is apparent from this micrograph and was, in fact, similar to that already shown in FIG. 4.9. FIG. 4.14., from a different area in the same specimen as FIG. 4.13., shows clearly the absence of the fringe contrast normally associated with stacking faults and confirms the opinion that these regions are twins in the reversed austenite.

4.2.3. Prolonged Holding at the Reversion Temperature:

In order to assess the importance of the holding time at the reversion temperature, 600°C, specimens which had been quenched to liquid nitrogen temperature were heated to 600°C in a salt bath for various times before quenching in water to room temperature. The change in specimen hardness after such treatments is shown in FIG. 4.15. A holding time of 15 seconds has little effect on the hardness and testing with a hand magnet showed that the specimen was still ferromagnetic. Times from 30 seconds to 10 minutes produced a lower but equal hardness, whereas longer times resulted in a progressive, but slight, softening effect.

4.2.4. Young's Modulus Measurements:

Measurements of resonant frequency, f_r, of partially martensitic specimens during heating to approximately 650°C and on subsequent cooling were performed as described in Appendix B. The dynamic Young's modulus, E, is proportional to the square of the resonant frequency, but, as the present investigation is concerned with the

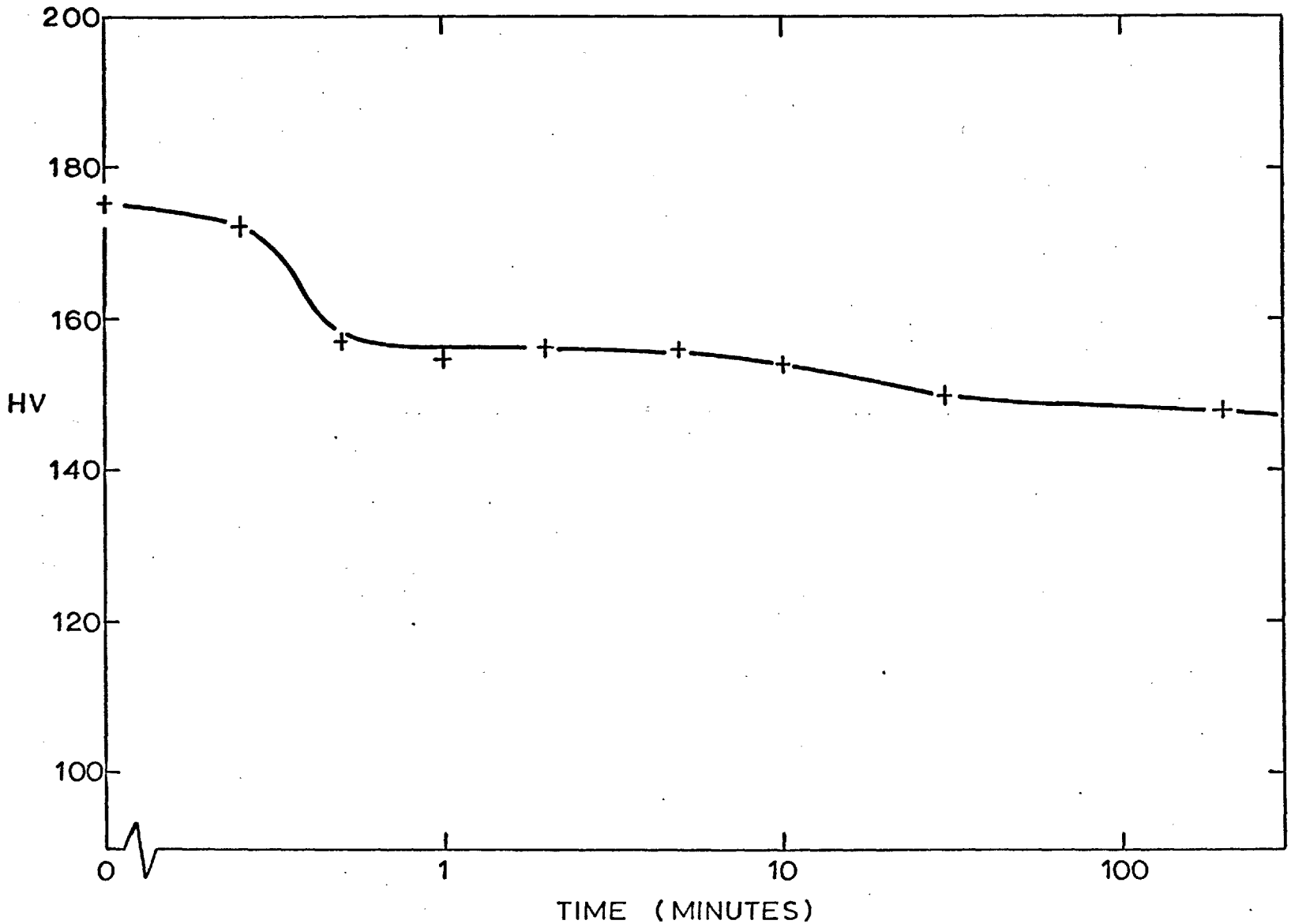

FIG. 4.15. Alloy A: Changes in hardness during holding the partially martensitic structure at 600°C.

temperatures at which rapid changes in E occur rather than the absolute value of such changes, it is sufficient to plot f_r against temperature, as in FIG. 4.16.

The results show a progressive decrease in resonant frequency on heating until, at about 545°C, an abrupt increase occurs; this is considered to represent the start of the reverse transformation. A less well-defined change at about 570°C is followed once more by a continuous decrease in resonant frequency with increasing temperature and is believed to indicate the completion of the reverse transformation. During cooling to room temperature the results show merely the temperature dependence of the resonant frequency and the absence of an abrupt change which would indicate a phase transformation.

4.2.5. Dilatometry:

The differential dilatometry results obtained during the heating of specimens of Alloy A, which had been partially transformed to martensite by holding at -196°C for 15 minutes, are shown in FIG. 4.17. In each case an arbitrary zero value for the specimen contraction has been taken to permit a clearer presentation of the results. The temperatures at which specific changes occurred were obtained directly from the recorder charts.

(i) Slow heating (4.5°C/min.)

A gradual change in the transducer reading was observed at about 450°C; no abrupt change occurred and the relative specimen contraction was completed at about 635°C. At higher temperatures a slight linear expansion with increasing temperature was found. The greatest rate of specimen contraction occurred between 550°C and 580°C.

(ii) Medium heating (16°C/min.)

A gradual change beginning at 520°C was followed by a more

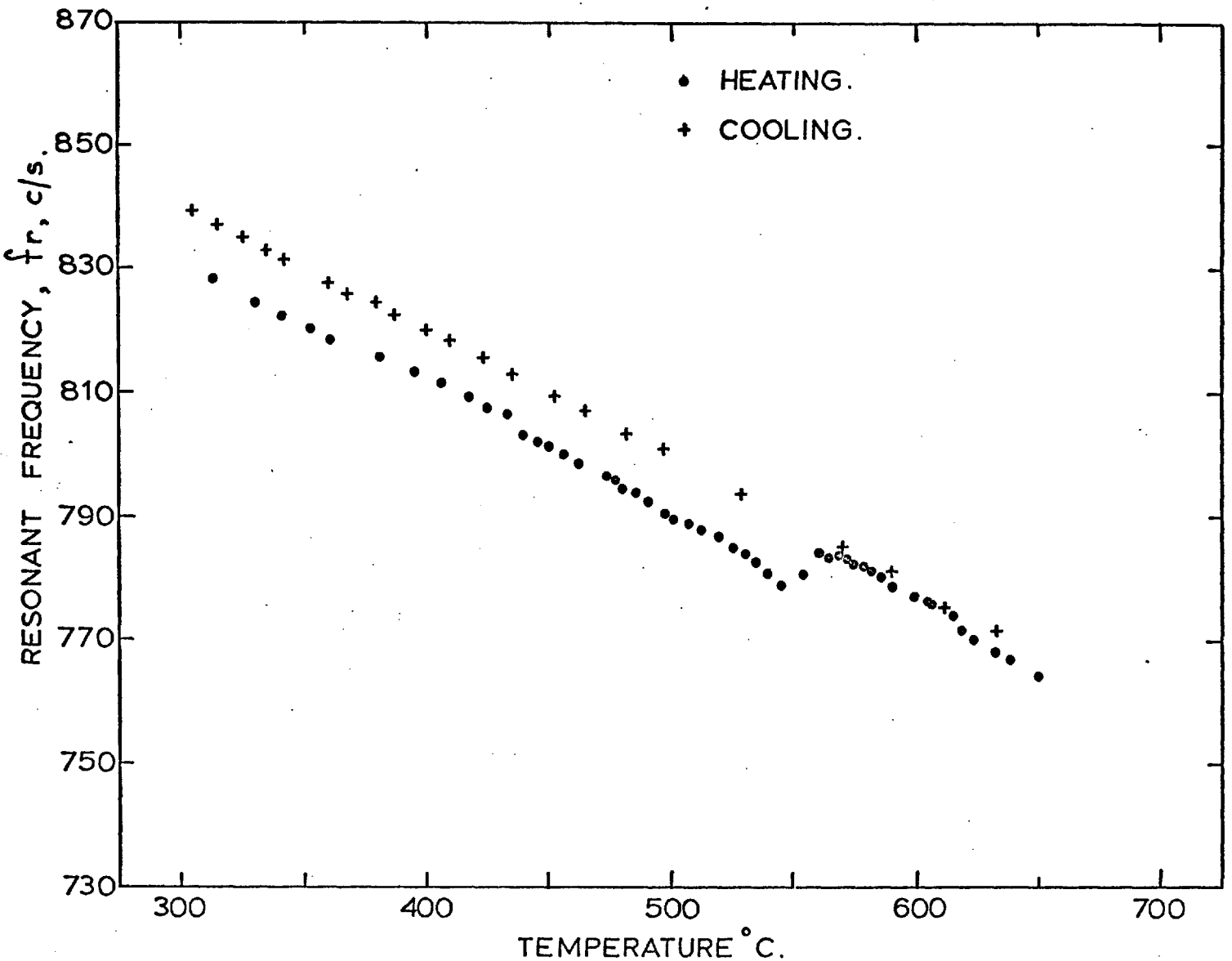

FIG. 4.16. Alloy A: Changes in resonant frequency during the heating of the partially martensitic structure, and on subsequent cooling.

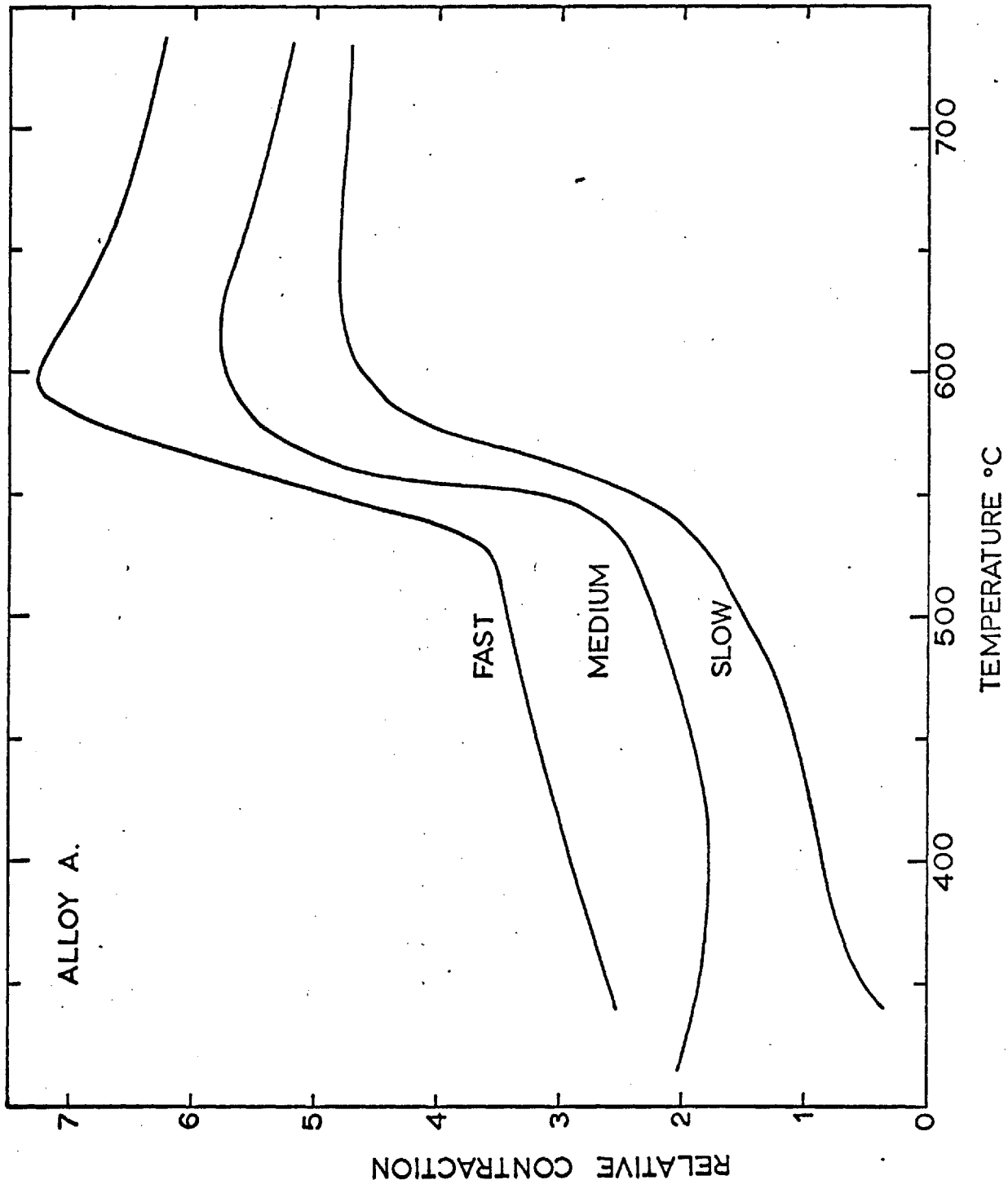

FIG. 4.17. Differential length change during heating partially martensitic specimens at different rates: 1 unit = 10 microns, arbitrary zero in each case.

abrupt specimen contraction at 540°C. The maximum rate of contraction with temperature was between 550°C and 560°C and the contraction reached completion at about 600°C, being followed by a small linear expansion.

(iii) Fast heating (165°C/min.)

No gradual change was observed but an abrupt contraction, beginning at 540°C, continued almost linearly with temperature to a peak at 600°C. An apparent specimen expansion above this temperature became linear with temperature above 650°C.

Alloy B.

4.2.6. Determination of A_s and A_f on Rapid Heating:

In Alloy B there is a possibility of precipitation occurring during heating to the reversion temperature, either in the martensite prior to reversion or in the austenite after retransformation. To minimise this possibility, the standard reversion time at temperature for Alloy B was reduced to 1 minute and the changes in hardness and martensite content of the specimens after heating to various temperatures for this time are shown in FIG. 4.18. The martensite content remains unaltered after heating to temperatures up to 560°C above which the content decreased progressively until it becomes nil after a treatment of 1 minute at 775°C; the most rapid drop in martensite content occurs between 650°C and 700°C. The corresponding change in hardness is seen to be a slight increase after heating to temperatures up to 500°C above which, 1 minute treatments result in a gradual softening to a constant level of HV = 165 between 850°C and 950°C as compared to the annealed austenite, HV = 146.

From FIG. 4.18. the values of A_s and A_f for Alloy B during rapid heating are estimated as 560°C and 775°C respectively. A standard reversion treatment of 1 minute at 775°C was chosen.

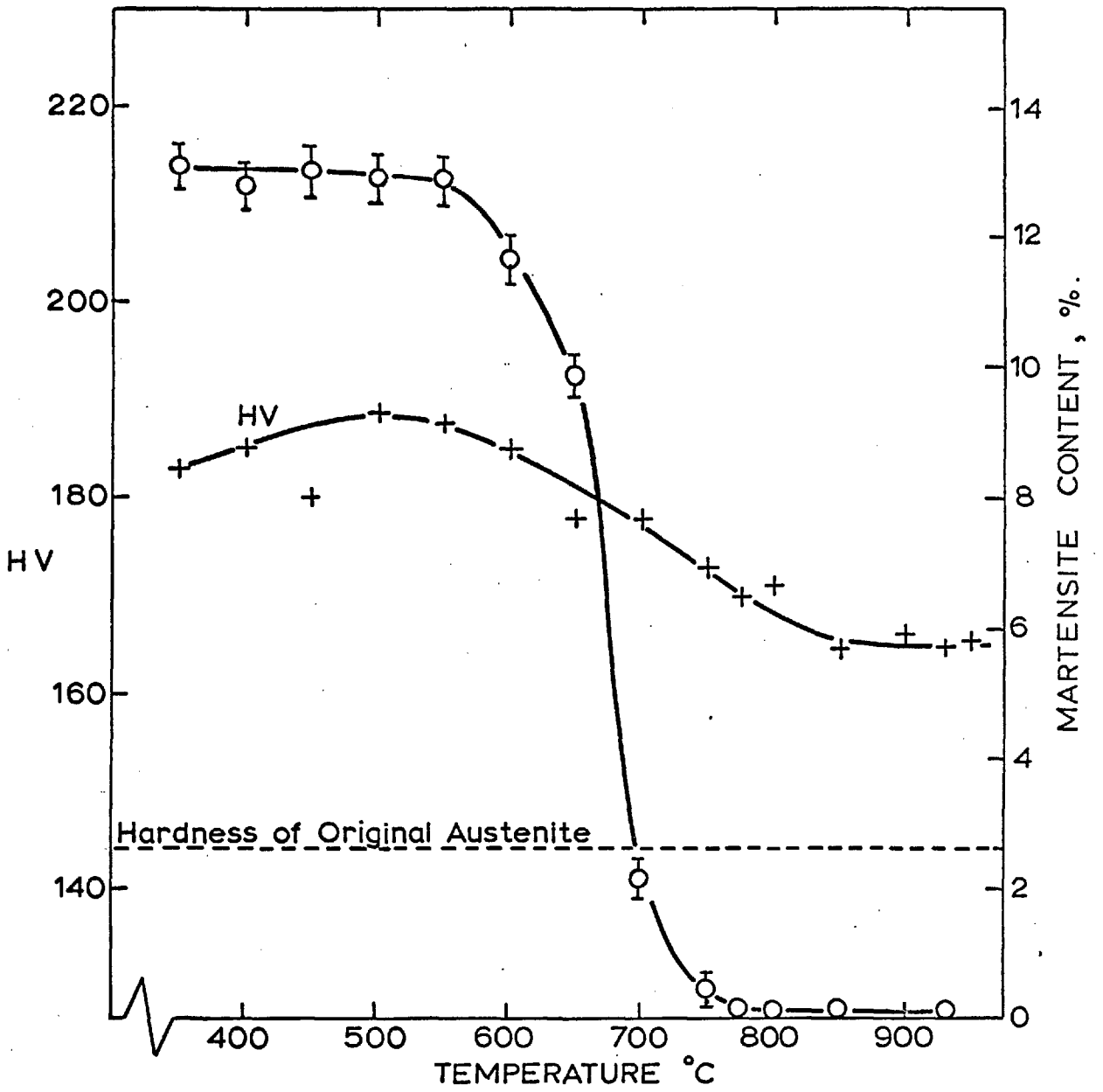

FIG. 4.18. Alloy B: Changes in hardness and martensite content after heating the partially martensitic structure for 1 minute to the temperatures shown and water quenching to room temperature.

4.2.7. Structural Changes:

'Ghost areas' of reversed austenite in retained austenite were again revealed by light microscopy, FIG. 4.19., after reversion at 775°C. The fine structure of the reversed austenite regions, shown in FIG. 4.20., contains a high dislocation density and many small twins and stacking faults. No evidence for carbide precipitation during this short reversion treatment was obtained; any fine precipitation which may have occurred on dislocations was not observable in the complex sub-structure of the reversed austenite regions and it was not possible to identify precipitate spots in the complicated diffraction patterns obtained from such areas.

An early stage in the reversion of $\alpha' \rightarrow \gamma$ in Alloy B is shown in FIG. 4.21. after a treatment of 1 minute at 600°C. The martensite grains appear to have broken up and the lath, as a whole, gives poorer contrast than the original martensite structure; this deterioration in contrast during reversion was commonly observed in Alloy B. Other laths in the same specimen had remained apparently unaffected by heating to 600°C; an example appears in FIG. 4.22. and suggests that different laths revert at different temperatures between A_s and A_f. A typical structure after heating higher in the retransformation temperature range, namely at 700°C for 1 minute, is shown in FIG. 4.23. A lath close to an austenite grain boundary exhibits a diffuse structure containing many small twins (dark) which are again observed tc lie with their longest dimension parallel to the sides of the lath.

4.2.8. Dilatometry:

The results are shown in FIG. 4.24.

(i) Slow heating (4.5°C/min.)

A relative specimen contraction began gradually at about 500°C, followed by a more pronounced contraction between 590°C and

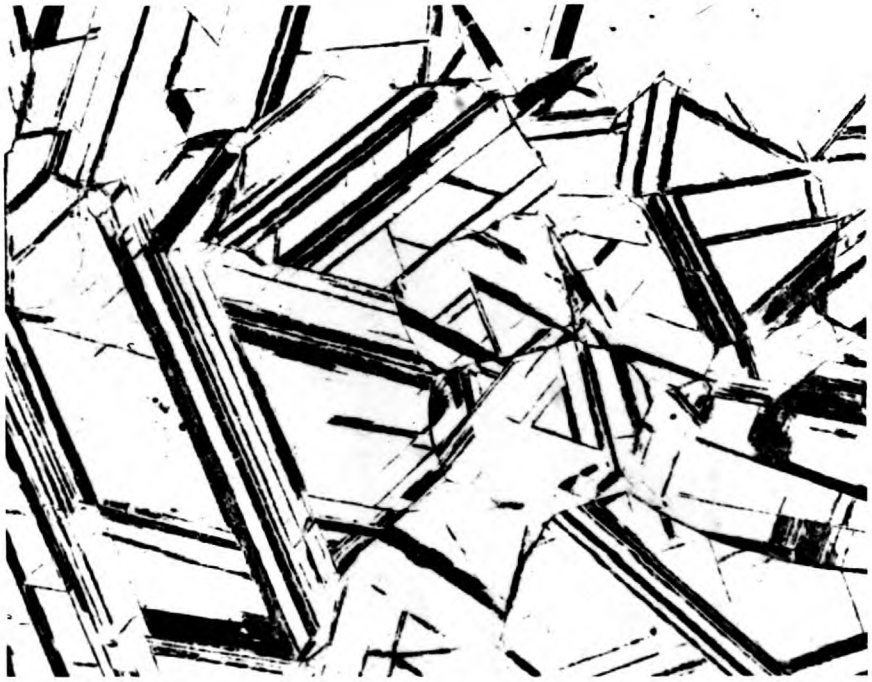

FIG. 4.19. Alloy B. 'Ghost areas' of reversed austenite in retained austenite after heating the partially martensitic structure for 1 minute at 775°C. Light micrograph X 240.

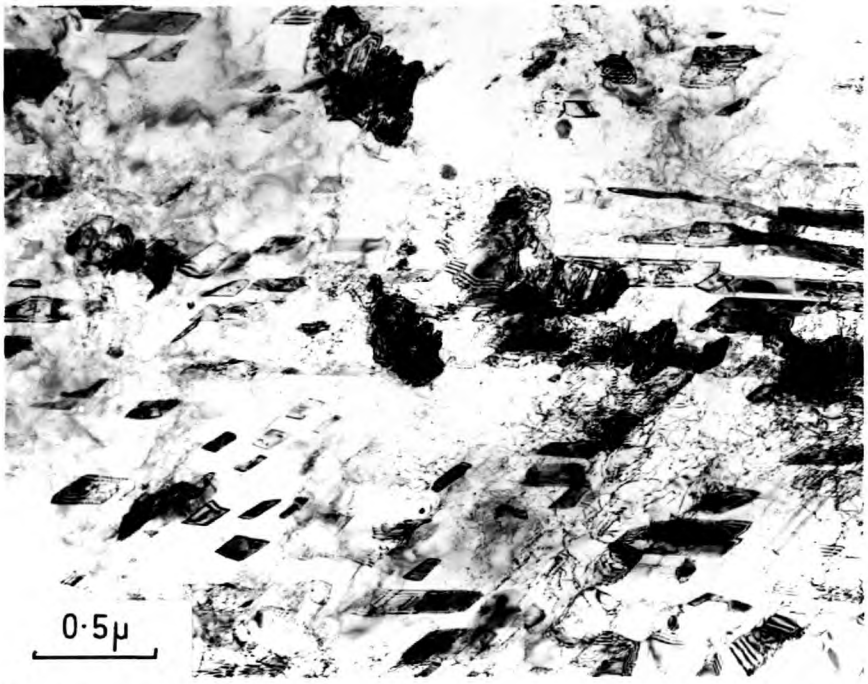

FIG. 4.20. Alloy B. Fine structure of reversed austenite. Electron micrograph.

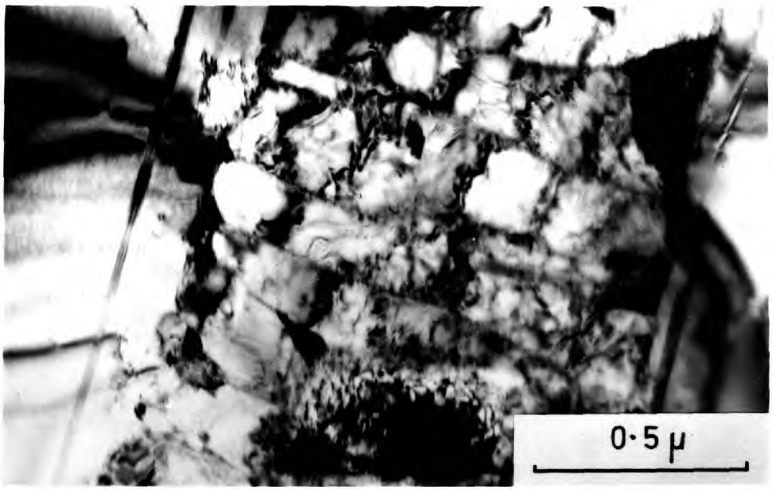

FIG. 4.21.

Alloy B. Heated for 1 minute at 600°C after quenching to -196°C for 1 hour; beginning of retransformation.

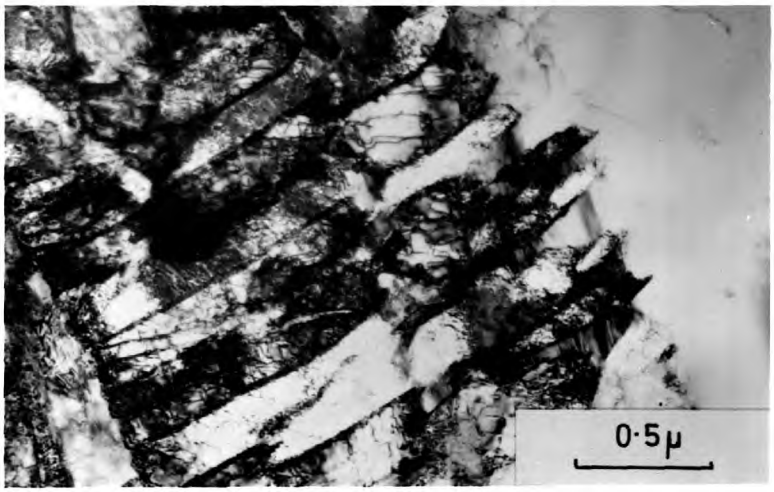

FIG. 4.22.

Alloy B. Treated as for FIG. 4.21. showing an area which has not begun to retransform.

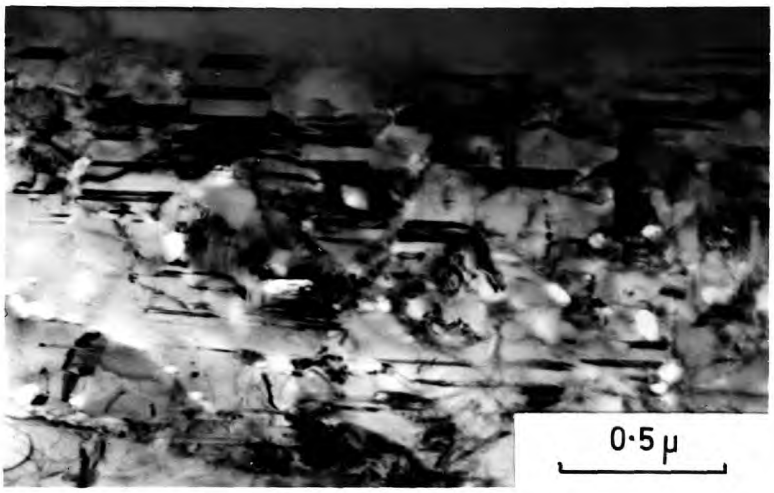

FIG. 4.23.

Alloy B. Heated for 1 minute at 700°C after quenching to -196°C for 1 hour.

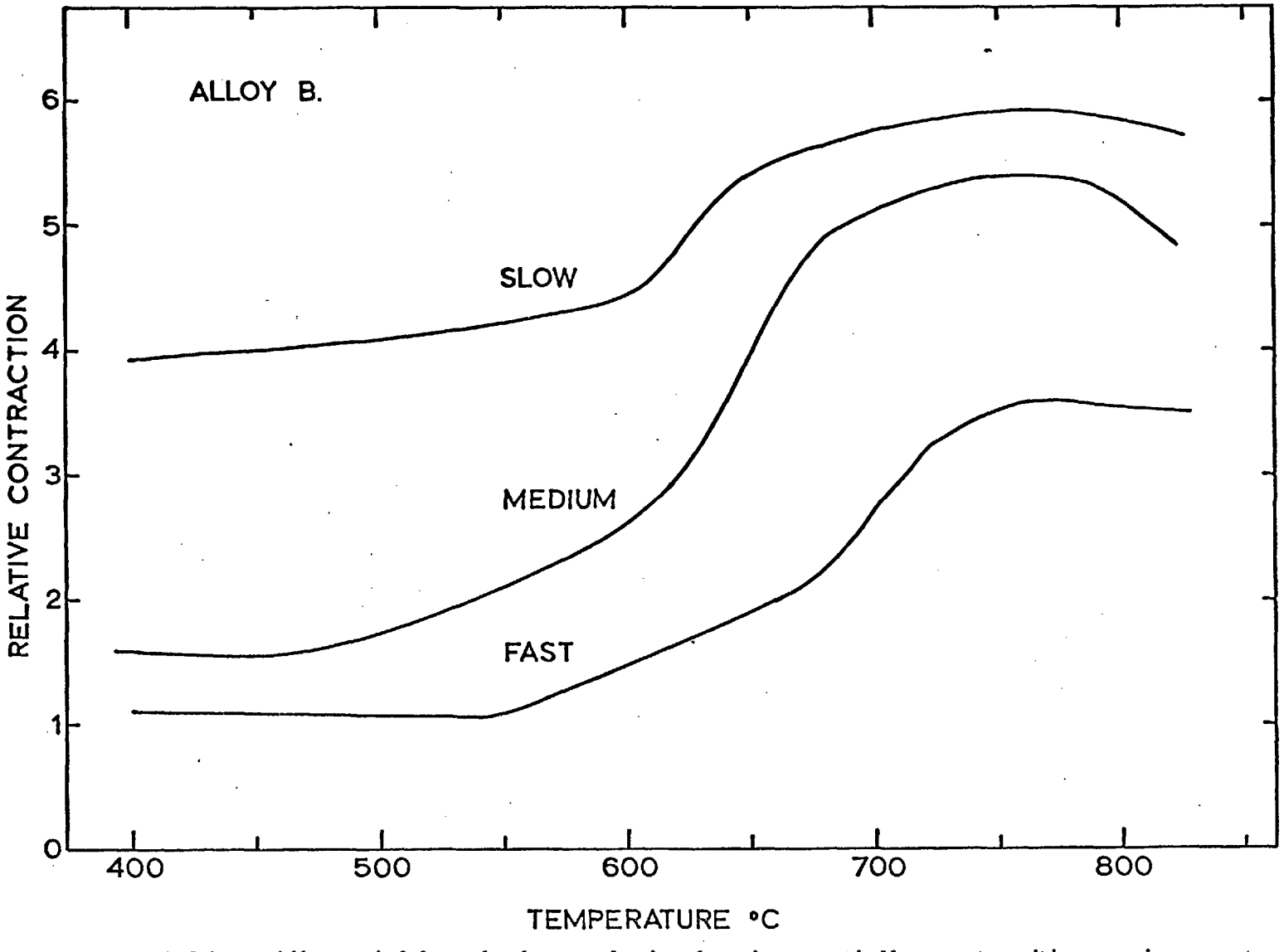

FIG. 4.24. Differential length change during heating partially martensitic specimens at different rates: 1 unit = 10 microns, arbitrary zero in each case.

640°C. Above 640°C the contraction is again more gradual and reaches completion at about 760°C when the change becomes linear with temperature.

(ii) Medium heating (16°C/min.)

A well pronounced specimen contraction beginning at 600°C was maintained up to about 680°C after which it proceeded less rapidly to completion at about 760°C.

(iii) Fast heating (165°C/min.)

A relative length change began at about 550°C and continued as the temperature rose to about 680°C. The rate of contraction then increased before more gradually approaching the completion of contraction, once more at a temperature of 760°C and above which the usual small linear expansion was observed.

4.3. EFFECT OF COLD WORK ON REVERSION:

Alloy A.

4.3.1. Transformation to Martensite by Deformation:

Magnetic balance measurements show that a reduction of 50% by rolling at room temperature produces a martensite content of just over 10% in Alloy A. A typical structure of the deformed austenite is shown in FIG. 4.26. where the foil orientation is $(110)_{\gamma}$. The crystallography of the banded structure is consistent with bands representing the intersection of $(111)_{\gamma}$ slip planes with the foil surface. Only face centered cubic diffraction spots were obtained from this area and it was not found possible to identify the martensitic areas in the electron microscope.

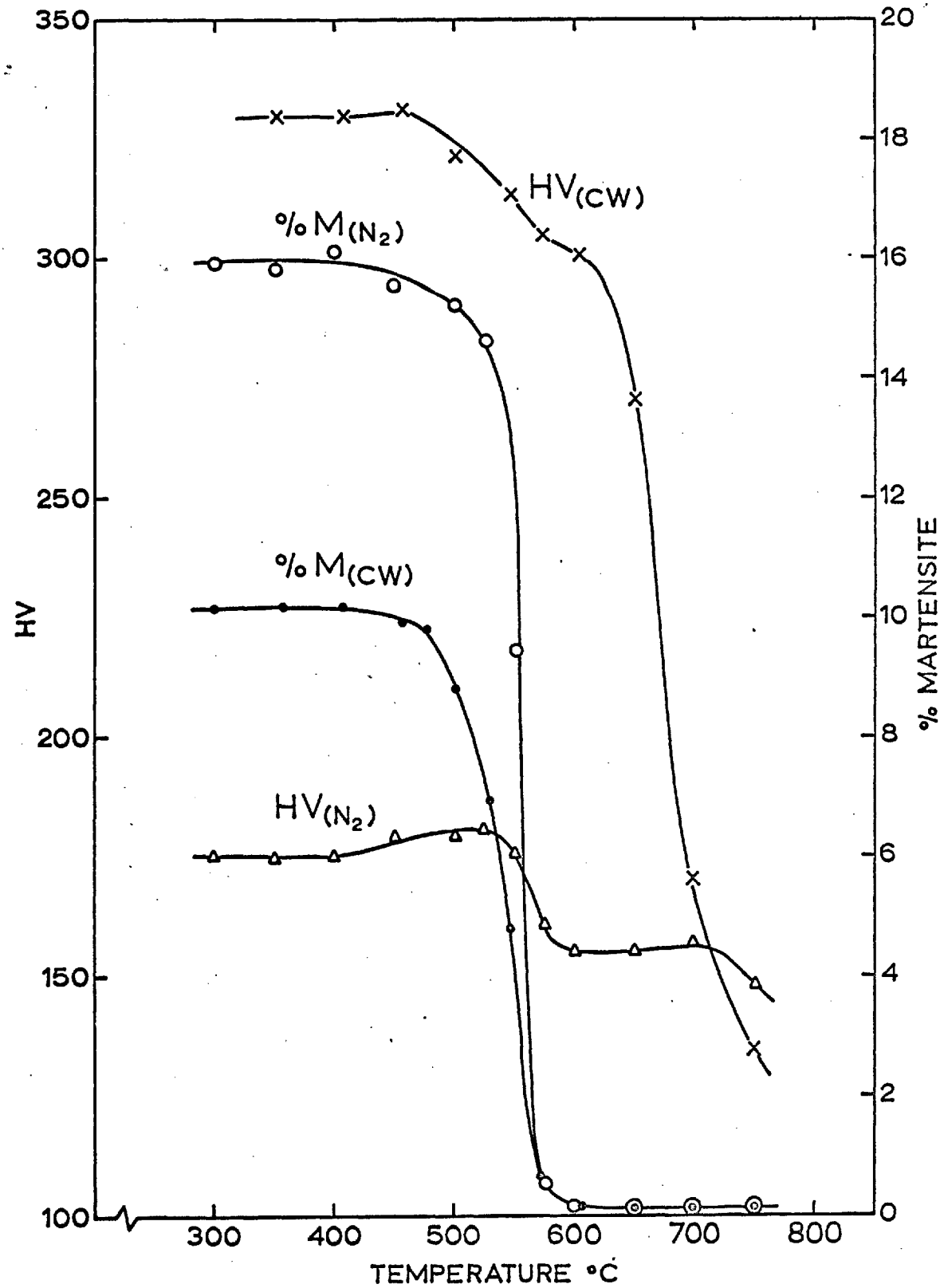

FIG. 4.25. Alloy A: Reversion of martensite formed by deformation compared to that formed by quenching to -196°C (cf. FIG. 4.6.)

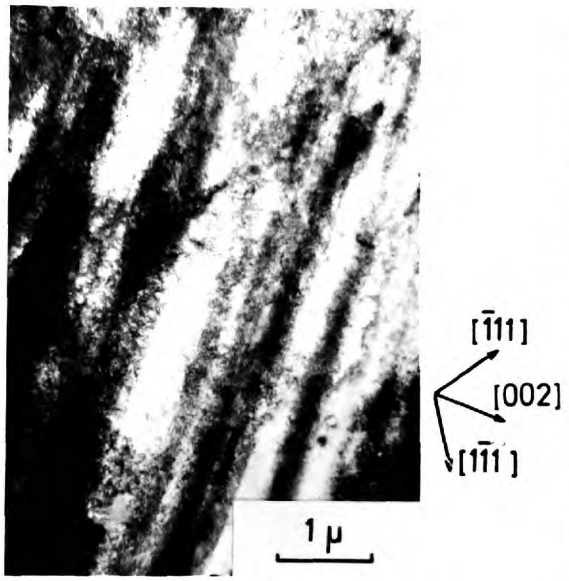

FIG. 4.26. Alloy A. Rolled 50% at room temperature, showing banded structure of deformed austenite.

FIG. 4.27. Alloy A. Cold worked structure heated for 2 minutes at 600°C, showing twins in austenite.

FIG. 4.28. Alloy A. Cold worked structure heated for 2 minutes at 525°C.

FIG. 4.29. Alloy A. Cold worked structure heated for 2 minutes at 555°C; recrystallised grains.

4.3.2. Determination of A_s and A_f on Rapid Heating:

The partially martensitic structure produced by cold working was heated for 2 minutes at various temperatures in the same way as for the quenched specimens (Section 4.2.1.). The resulting changes in hardness and martensite content, after quenching to room temperature, are shown in FIG. 4.25. Both the hardness and martensite content remain constant after heating to temperatures up to about 450°C; both then begin to decrease. The martensite content falls progressively until, after 2 minutes at 600°C, the specimen contains no ferromagnetic phase. The hardness fall shows a decrease in rate between about 575°C and 625°C but becomes more rapid on heating to higher temperatures.

The equivalent curves for the reversion of the quenched specimens of Alloy A are also shown in FIG. 4.25. to facilitate comparison of the two. No obvious change in the values of A_s and A_f is observed in the cold-worked material; again, these temperatures are estimated at 450°C and 600°C respectively.

4.3.3. Structural Changes:

After reversion at 600°C several regions in the fully austenitic specimens were found to contain small twins as shown in FIG. 4.27. Such regions had not been observed in the cold-worked condition but were in evidence after heating for 2 minutes at 525°C (FIG. 4.28.).

Small areas of recrystallised grains were found after a treatment of 2 minutes at 555°C, FIG. 4.29., as well as after complete reversion at 600°C.

4.3.4. Dilatometry:

The results are shown in FIG. 4.30.

(i) Medium heating.

On heating specimens at approximately 16°C/min. a relative specimen contraction occurred as the temperature rose to about 425°C. An apparent specimen expansion was then recorded up to 555°C when the gradient flattened to indicate almost no relative length changes between this temperature and 600°C. Above 600°C the apparent specimen expansion continues almost linearly with increasing temperature.

(ii) Fast heating.

The specimen exhibits a relative contraction up to a peak in the curve at 505°C which is followed, at higher temperatures, by a specimen expansion. A small increase in the rate of expansion was observed to begin at about 600°C.

Alloy B.

4.3.5. Transformation to Martensite by Deformation:

A reduction of 50% by cold rolling solution treated specimens of Alloy B at room temperature was found, by magnetic balance measurements, to produce transformation to about 41% ferromagnetic martensite. The highly deformed nature of the specimen after cold working is indicated by FIG. 4.32; the micrograph shows the different directions of banding in two adjacent grains.

Once more, it was not found possible to identify martensitic regions in the highly deformed austenitic matrix. This fact is dealt with in the discussion.

4.3.6. Determination of A_s and A_f on Rapid Heating:

The cold-worked structure was heated for 1 minute at various temperatures in the usual way and FIG. 4.31 shows the effects of these treatments on hardness and martensite content. The latter is not

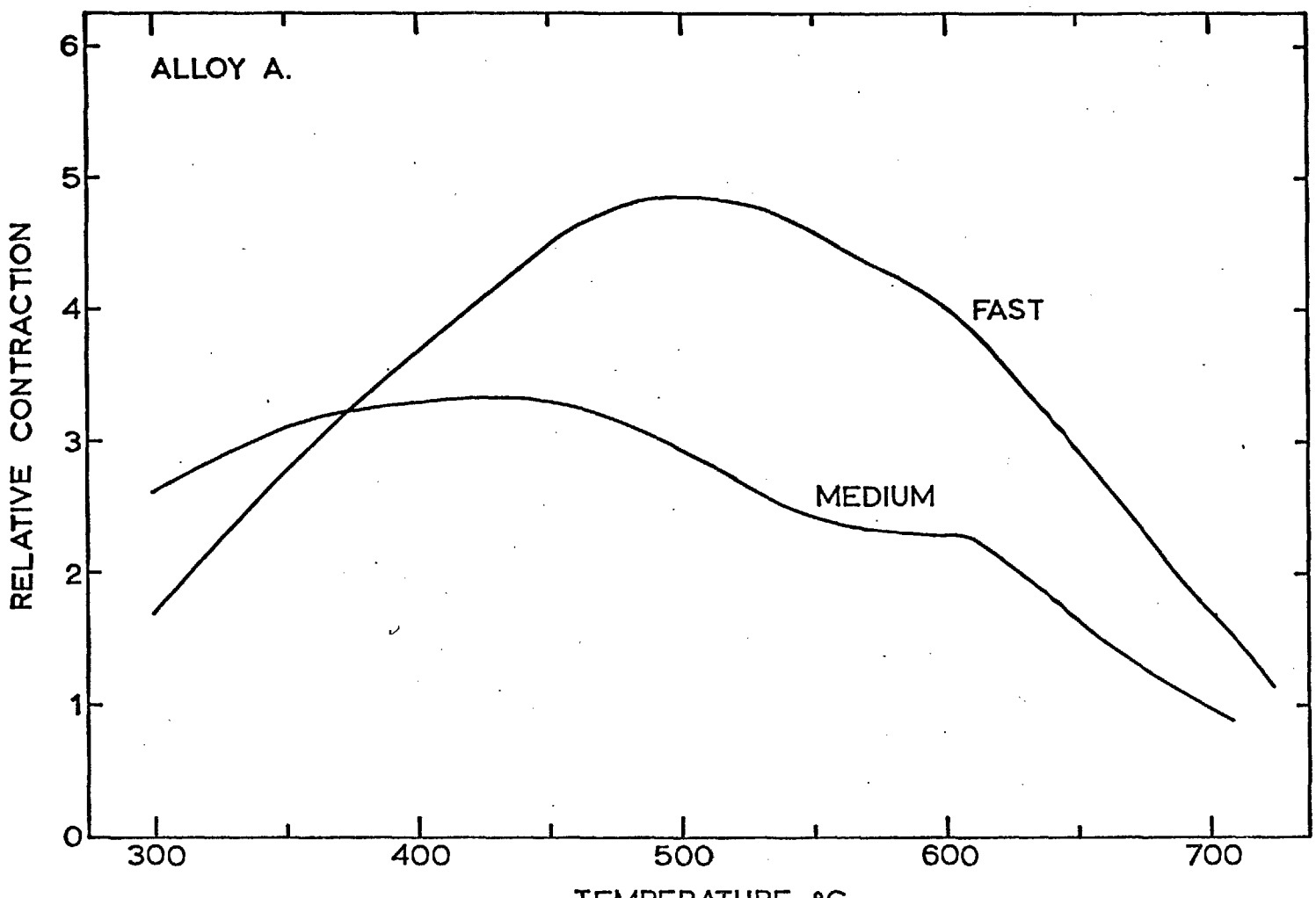

FIG. 4.30. Differential length change during heating specimens which have been rolled 50% at room temperature: 1 unit = 10 microns, arbitrary zero in each case.

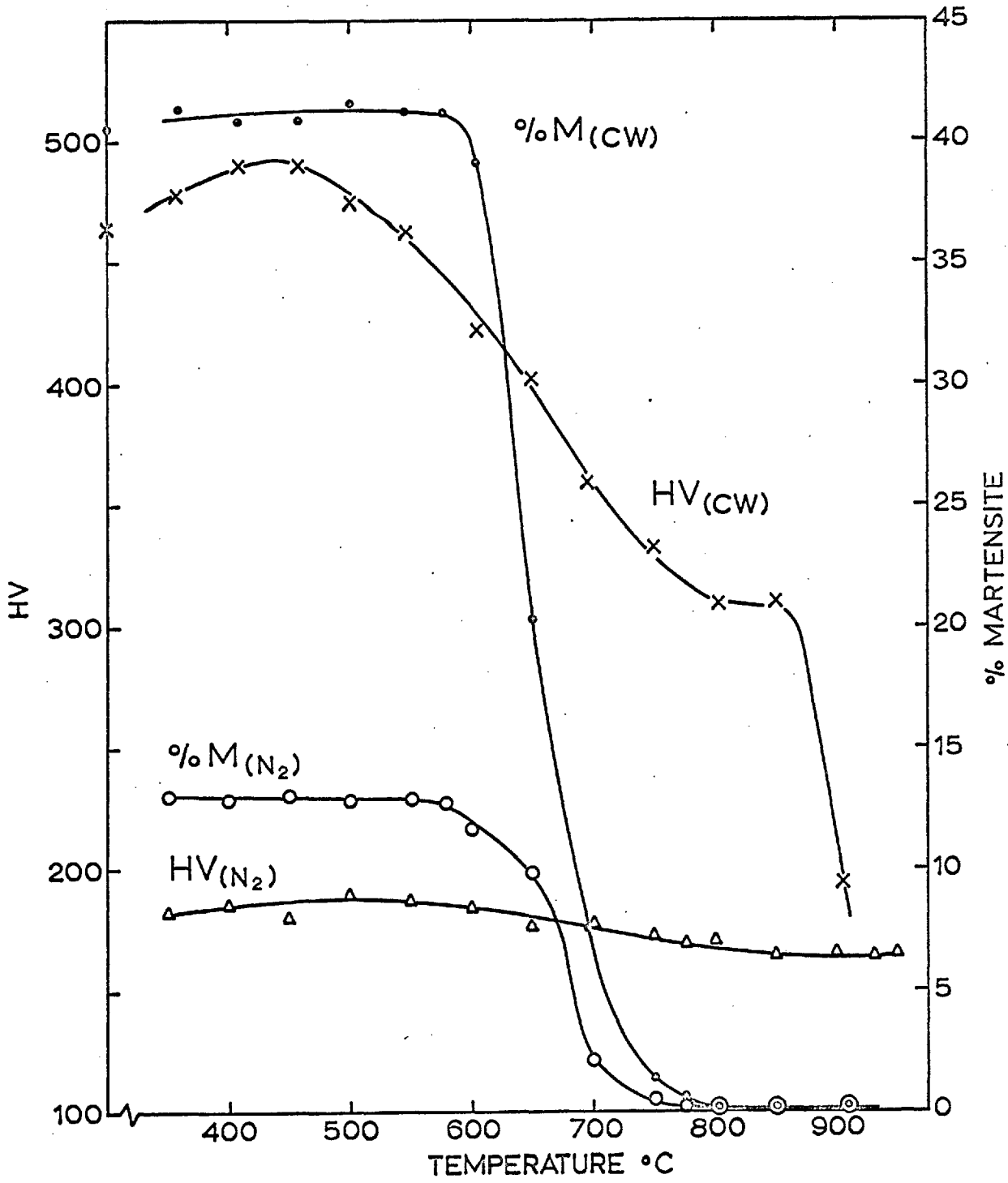

FIG. 4.31. Alloy B: Reversion of martensite formed by deformation compared to that formed by quenching to -196°C (cf. FIG. 4.18).

appreciably affected by heating to temperatures up to 575°C but at higher temperatures it decreases as the treatment temperature is increased until no ferromagnetic phase is detected after heating for 1 minute at 775°C. The specimen hardness shows a slight increase after heating between 350°C and 450°C and a progressive decrease at higher temperatures until a small plateau is reached between 800°C and 850°C. Above 850°C the hardness drops rapidly towards that of the annealed austenite.

From these results the A_s and A_f temperatures were estimated as being 575°C and 775°C respectively. The equivalent curves for the reversion of the quenched specimens of Alloy B are also shown; the similarity between the two sets of results is evident.

4.3.7. Structural Changes:

The deformed matrix of the fully austenitic structure, following a reversion treatment of 1 minute at 775°C, contained occasional small twins; an example of this is seen in FIG. 4.33. The fully reversed structure also contained some areas of small recrystallised grains, as shown in FIG. 4.34.; these regions were first observed after heating for 1 minute at 700°C. Although small twins had not been visible in the cold-worked structure, they were observable after a treatment at only 600°C; FIG. 4.35. Two sets of twins are shown in the micrograph and $\langle 111 \rangle_\gamma$ directions in the matrix were found to be perpendicular to each set. The structure shown in FIG. 4.36. was obtained after heating for 1 minute at 655°C; it is quite different in appearance to the original cold-worked structure and may represent the initial stages of recrystallisation.

4.3.8. Dilatometry:

The results are shown in FIG. 4.37.

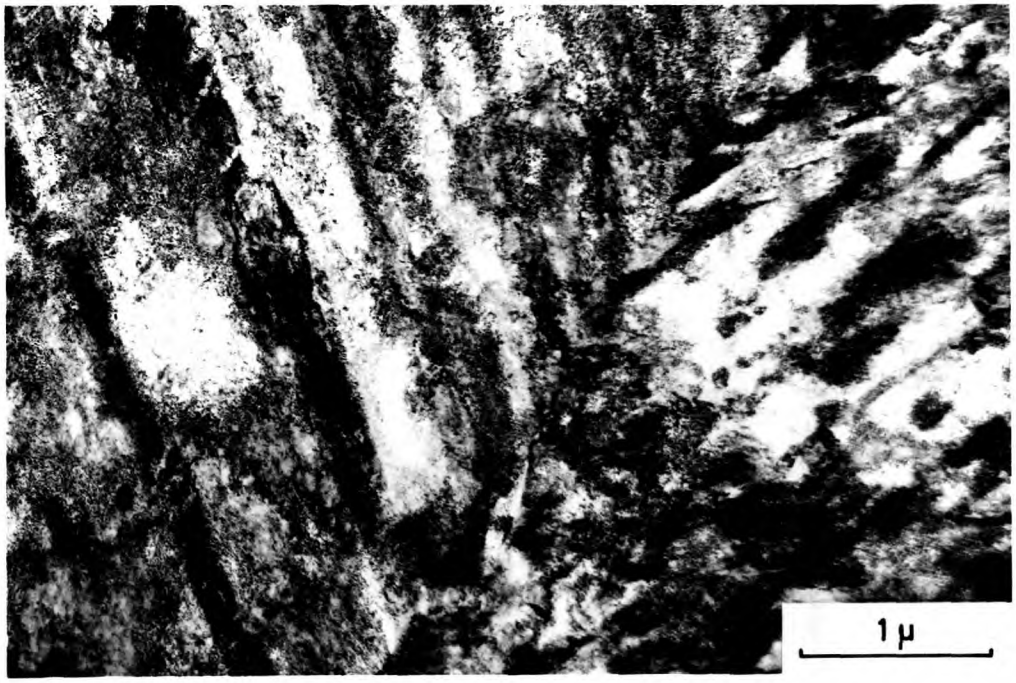

FIG. 4.32. Alloy B. Rolled 50% at room temperature. Electron micrograph.

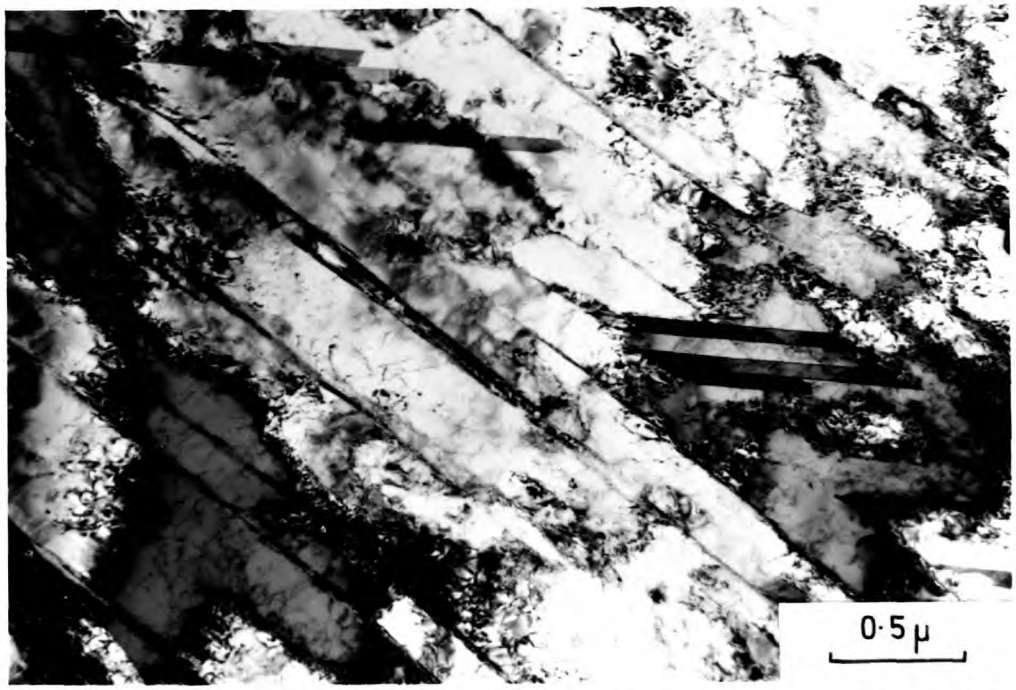

FIG. 4.33. Alloy B. Twins in austenite after heating the cold rolled structure for 1 minute at 775°C.

FIG. 4.34.

Alloy B. Recrystallised grains produced by heating the cold rolled structure for 1 minute at 775°C.

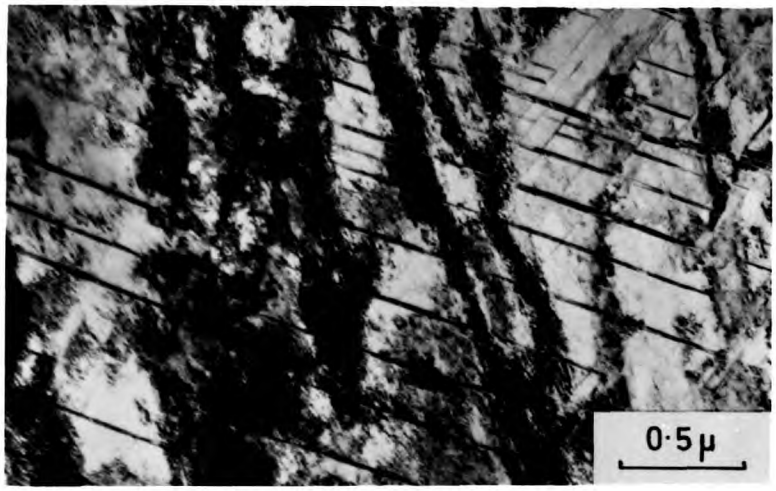

FIG. 4.35.

Alloy B. Cold worked structure heated for 1 minute at 600°C.

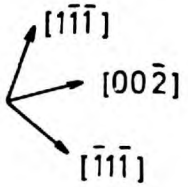

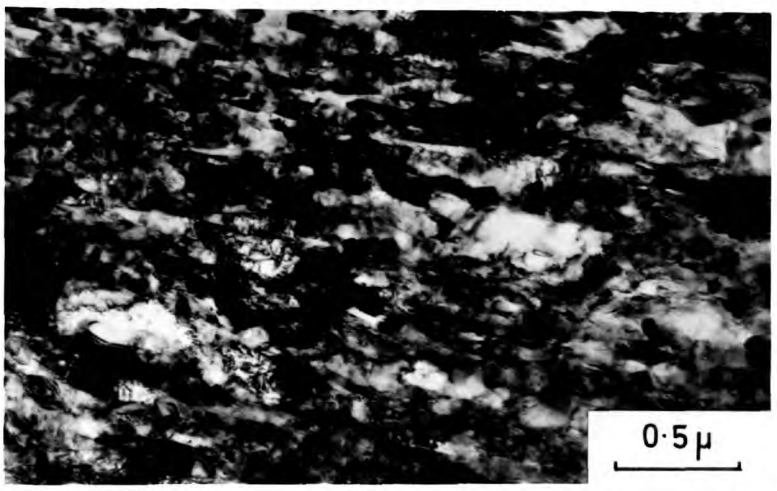

FIG. 4.36.

Alloy B. Cold worked structure heated for 1 minute at 655°C.

(i) Medium heating.

A substantial contraction, which is almost linear with temperature, occurs on heating up to a peak on the graph at 560°C. This is followed by a drop, representing a specimen expansion, which levels out at about 660°C and the length then remains unchanged, relative to the control specimen, until the temperature rises above 790°C. A further specimen expansion was then recorded.

(ii) Fast heating:

The initial contraction is maintained up to 640°C when a change to a relative expansion occurs. The gradient of the curve during this expansion decreases at 680°C and changes to a relative contraction once more at 720°C. The contraction ceases at approximately 780°C and gives way to a steady relative expansion.

4.4. ANNEALING OF REVERSED AUSTENITE:

Alloy A.

Because of the complications introduced by carbide precipitation in Alloy B, studies of the annealing behaviour of reversed austenite were confined to Alloy A. The reversed austenite was produced from martensite which had formed, in one case, by quenching to liquid nitrogen temperature and, in the other, by deformation at room temperature.

4.4.1. Reversed Austenite Obtained from Martensite Produced by Quenching:

(i) Hardness Changes.

Heating the partially martensitic structure directly to the annealing temperature and holding at that temperature for

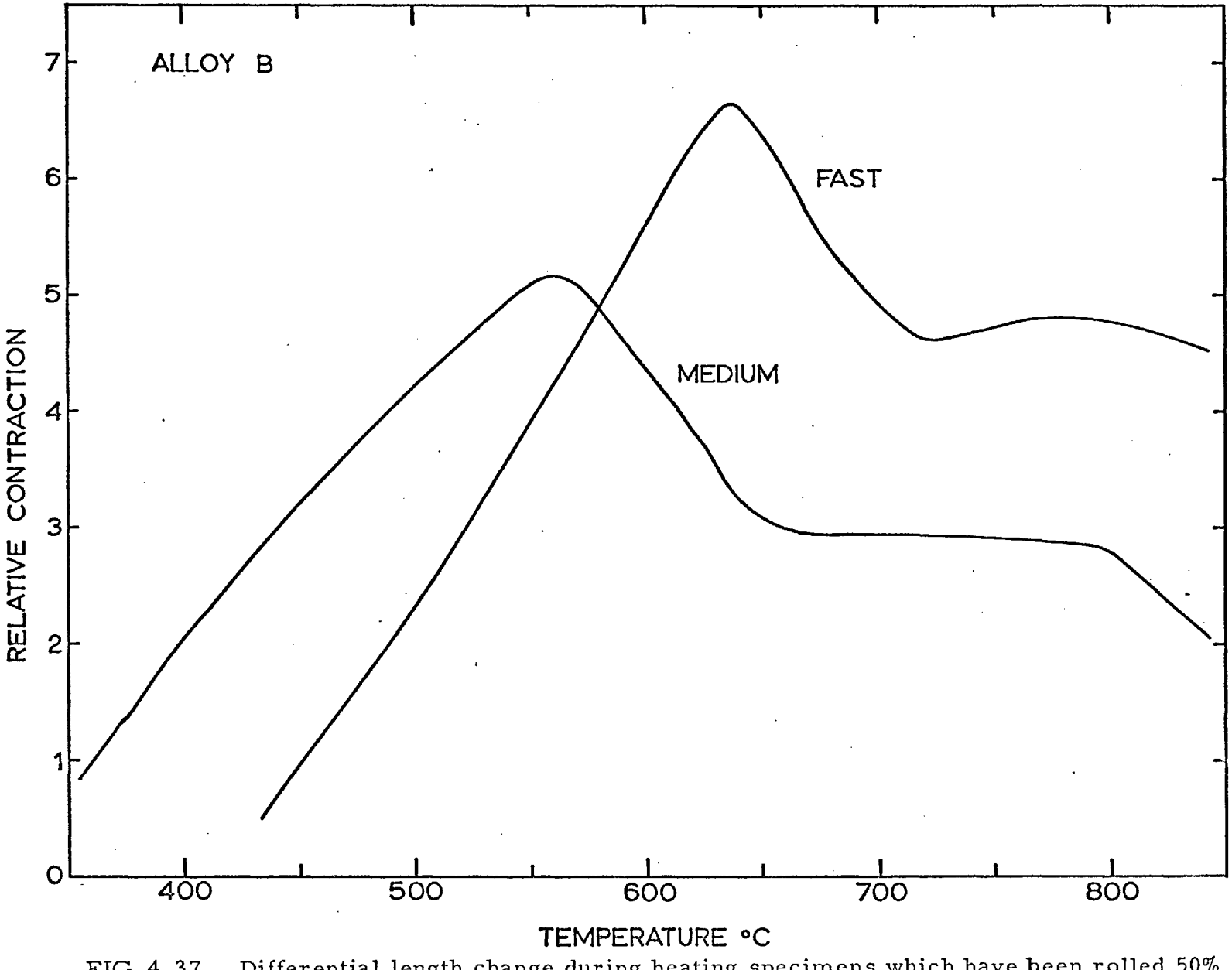

FIG. 4.37. Differential length change during heating specimens which have been rolled 50% at room temperature: 1 unit = 10 microns, arbitrary zero in each case.

various times produces hardness changes as shown in FIG. 4.38. After annealing at 700°C for 150 hours the specimen still maintained a hardness level of 125 (not shown on diagram). Treatments at temperatures from 850°C to 920°C produced a progressive fall in hardness to that of the original annealed austenite; in all such cases this value was reached in times under 10 hours.

An apparent activation energy, E_a, for the annealing process has been obtained by assuming that the time, t, to reach a given fraction of 'recovery' is given by $1/t = A.\exp.(-E_a/RT)$. E_a is then found from plots of log (1/t) against 1/T. Such plots, corresponding to various degrees of completion of the process, are shown in FIG. 4.39. and the values of E_a obtained from these are given in Table II.

TABLE II

Hardness	110	120	to 50% level	Average
E_a	93	78	69	80 Kcal/mole

The annealing behaviour in FIG. 4.38. refers to reversed austenite structures formed during the heating of the partially martensitic specimens to the different annealing temperatures involved. The 'starting' structures may not, therefore, be the same in each case. Consequently, the annealing behaviour of a 'standard' reversed austenite structure was investigated by firstly treating the partially martensitic structure for 2 minutes at 600°C and quenching to room temperature before annealing at the selected temperatures. The results are shown in FIG. 4.40. and comparison with FIG. 4.38. shows that, although general shapes of the hardness curves are the same, the times involved to regain the hardness of the annealed austenite are longer. The corresponding plots for the apparent

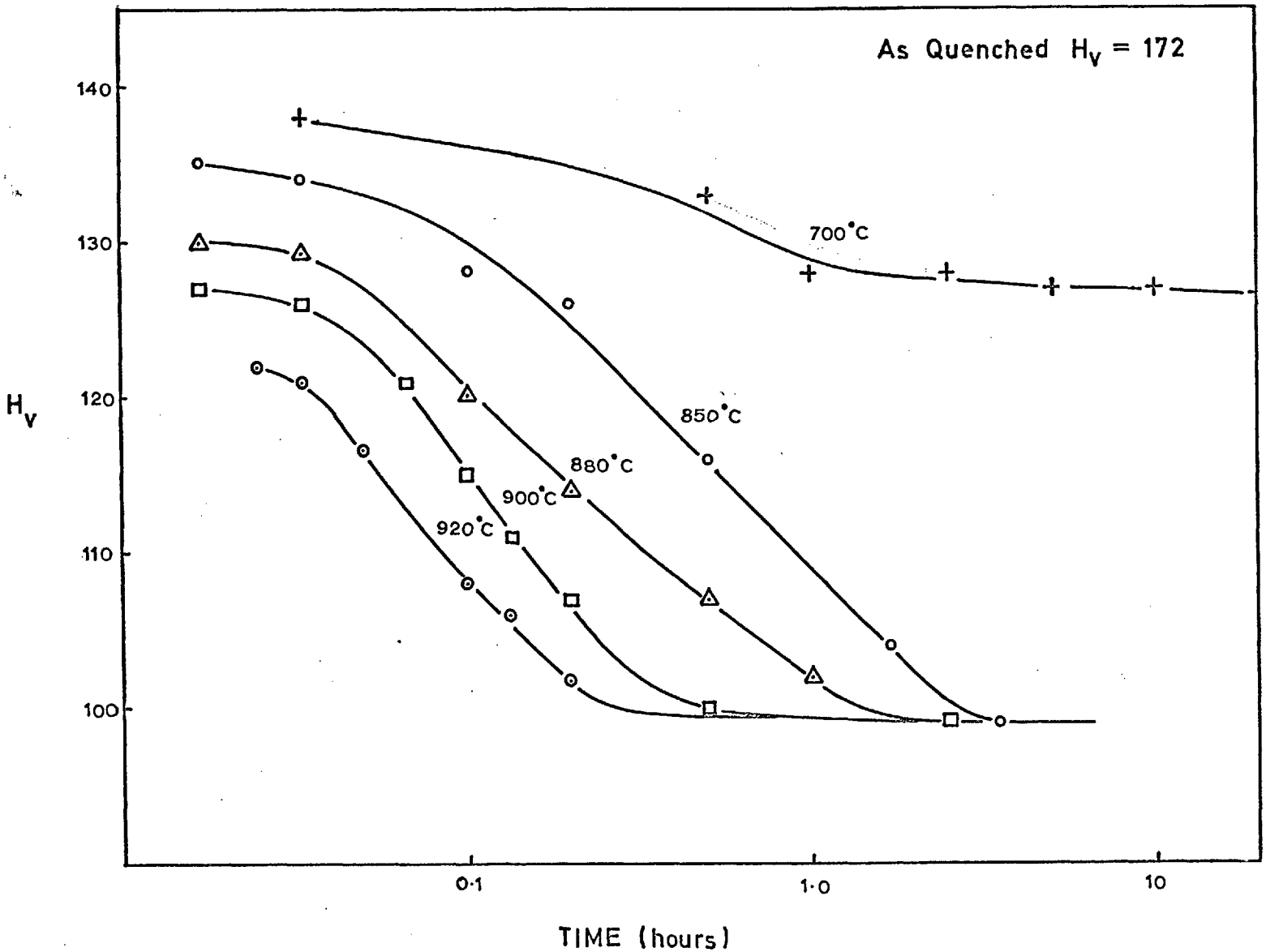

FIG. 4.38. Alloy A: Annealing of 'reversed austenite' formed during heating the partially martensitic structure to the annealing temperature.

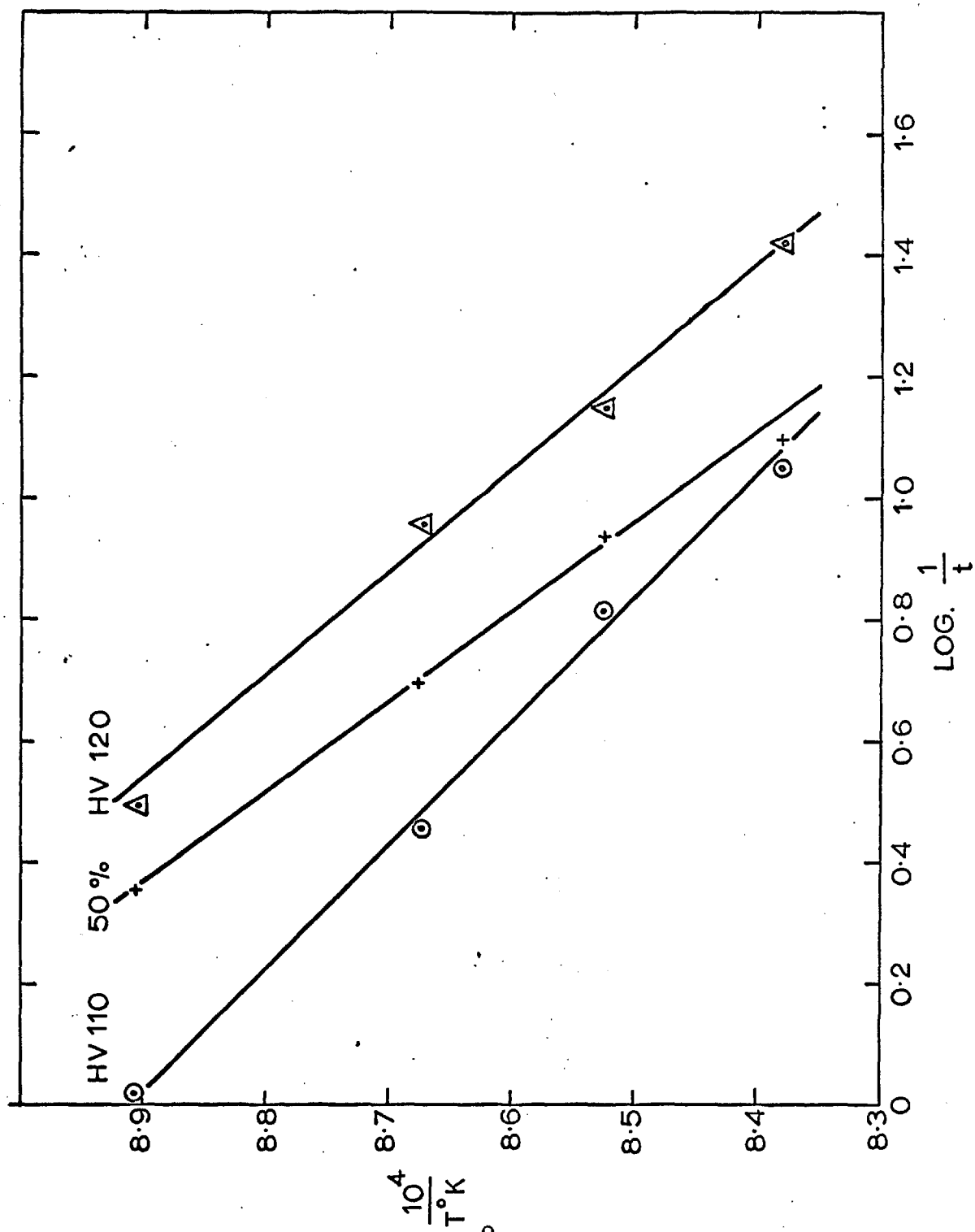

FIG. 4.39. Alloy A: Plots of $1/T\,^{\circ}K$ against $\log(1/t)$ for various stages of completion of the annealing of 'reversed austenite' as in FIG. 4.38.

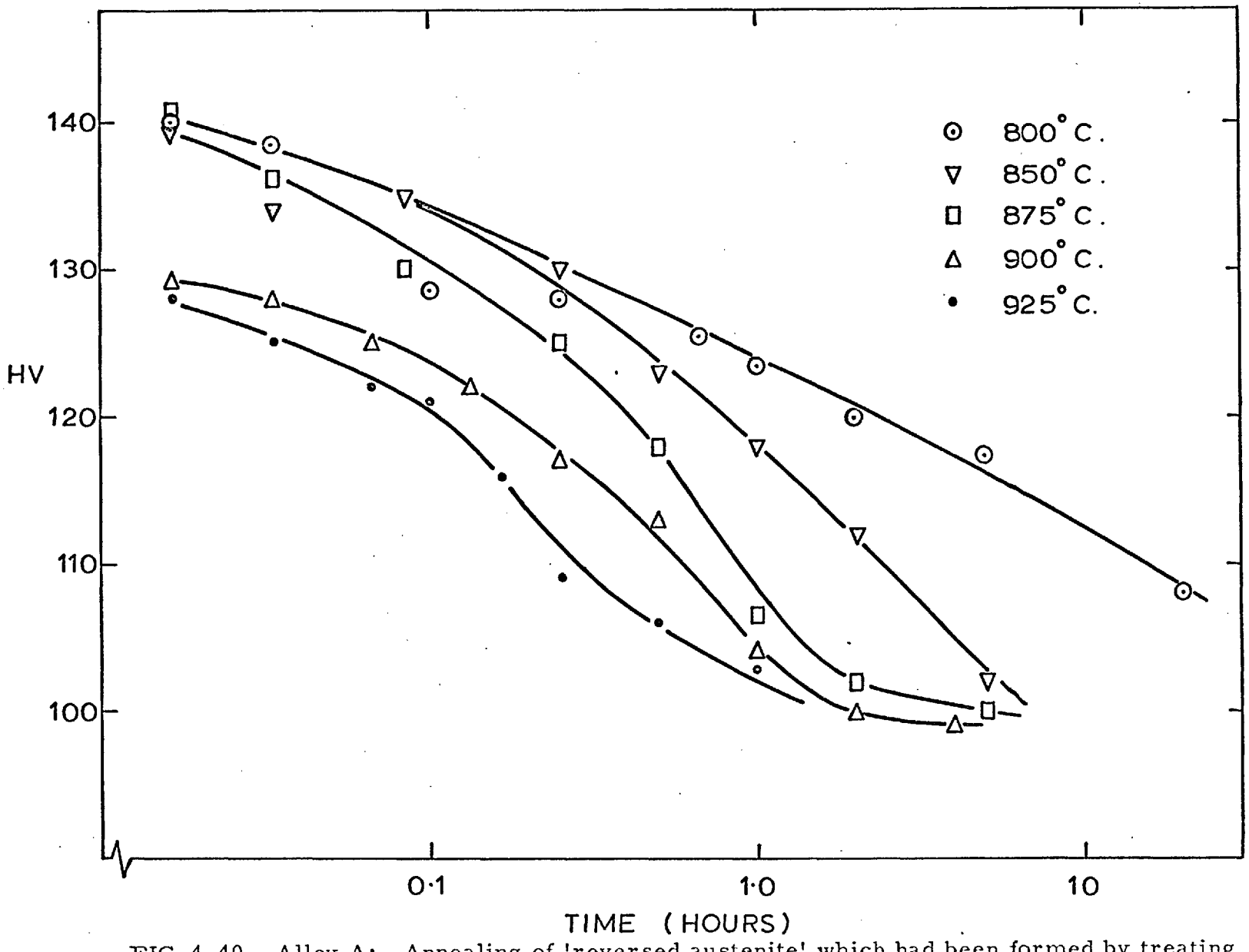

FIG. 4.40. Alloy A: Annealing of 'reversed austenite' which had been formed by treating at -196°C for 15 minutes and then at 600°C for 2 minutes.

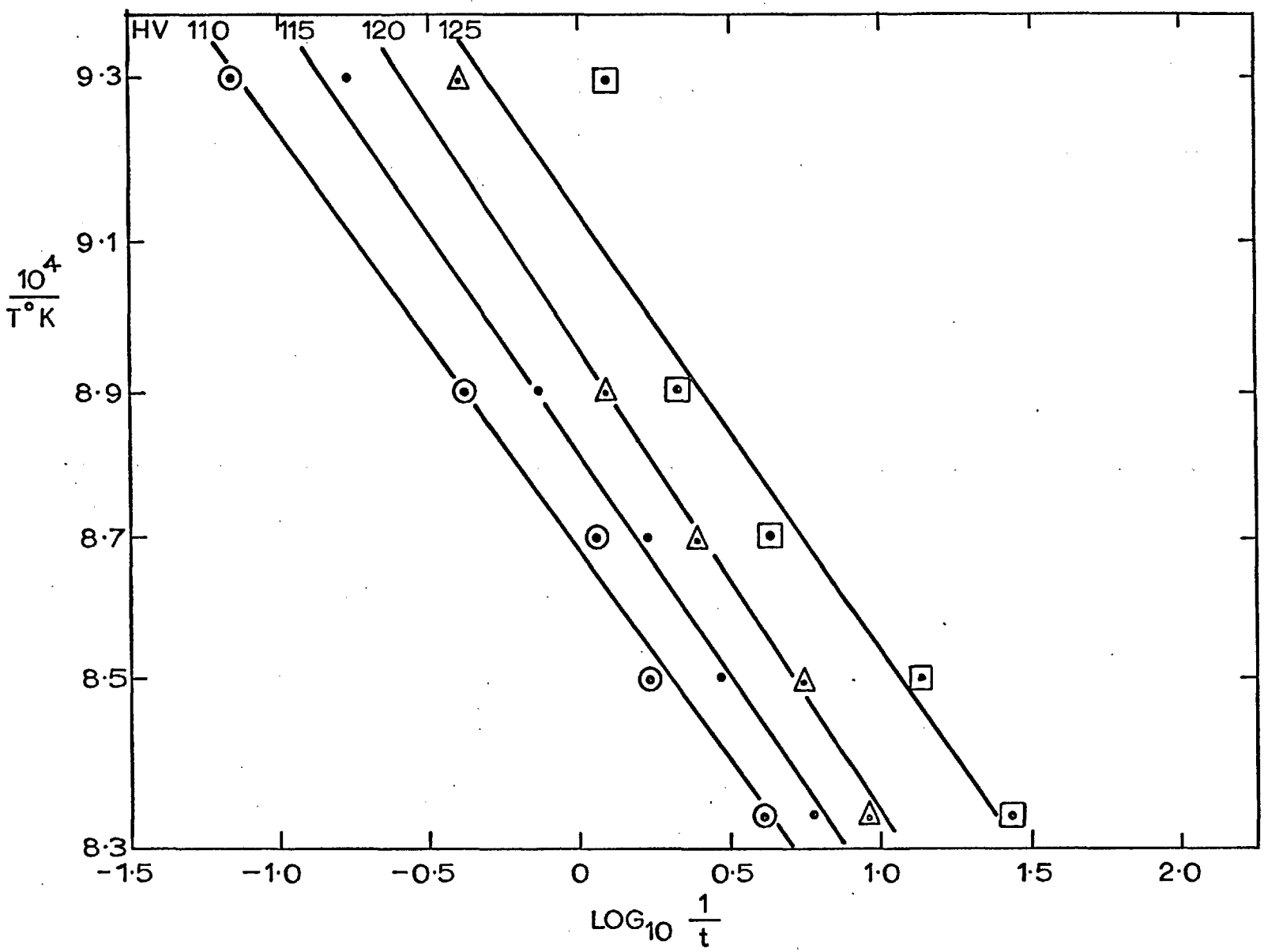

FIG. 4.41. Alloy A: Plots of $1/T^{\circ}K$ against $\log(1/t)$ for various stages of completion of the annealing of 'reversed austenite' produced by the standard treatment, as in FIG. 4.40.

activation energy are given in FIG. 4. 41. and results are summarized in Table III.

TABLE III

Hardness	110	115	120	125	Average
E_a	83	74	75	80	78 Kcal/mole.

(ii) Structural Changes.

The structural changes accompanying the return of the hardness to that of fully annealed specimens during the annealing of reversed austenite were studied by an electron microscopical examination of specimens which had been held for various times at 850°C after a prior reversion treatment. The structure after reversion has already been described (Section 4.2.2.) as consisting of grains of retained austenite, with a low dislocation density typical of a fully annealed structure, within which are laths of 'reversed austenite' which have a much higher density of tangled dislocations and contain small twins (FIG. 4. 9.). The retained austenite remains unaltered throughout the annealing sequence and the following observations refer to changes within the 'laths'.

FIGS. 4. 42. to 4. 46. show the changes which occur during holding for increasing times at 850°C. After 2 minutes the formation of distinct sub-grain boundaries is apparent (FIG. 4. 42.) and none of the twins which existed in the reversed austenite are now visible. The overall dislocation density is noticeably lower after $\frac{1}{2}$ hour at 850°C and more regular arrays of dislocations are observed; FIG. 4. 43. This process of dislocation interaction and annihilation continues (FIG. 4. 44., 2 hours at 850°C) until, after annealing for 5 hours, relatively few isolated networks of dislocations are all that remain; examples are shown in FIGS. 4. 45. and 4. 46. Reference to

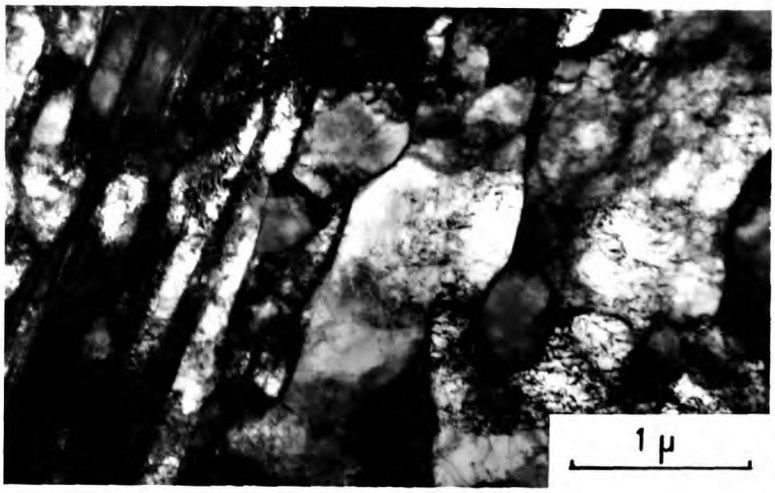

FIG. 4.42.

Alloy A. Reversed austenite annealed for 2 minutes at 850°C.

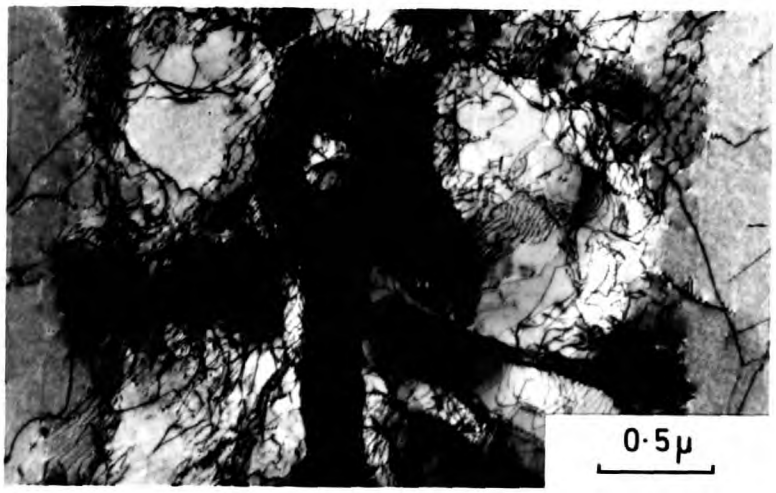

FIG. 4.43.

Alloy A. Reversed austenite annealed for $\frac{1}{2}$ hour at 850°C.

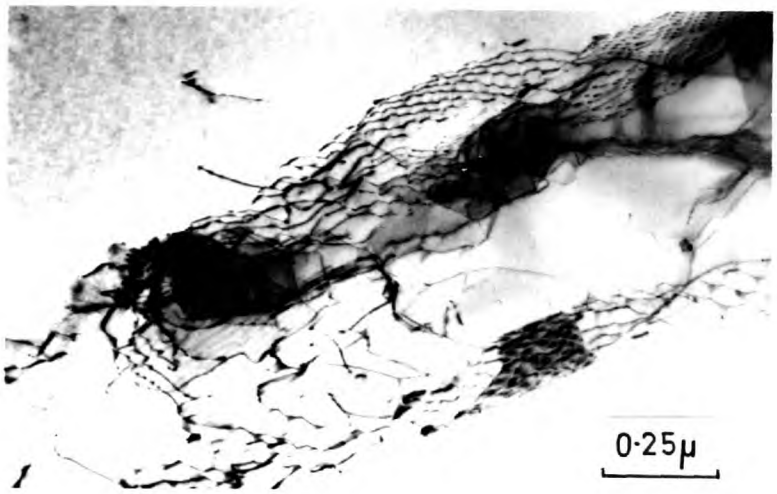

FIG. 4.44.

Alloy A. Reversed austenite annealed for 2 hours at 850°C.

FIG. 4.40. shows that the alloy is almost completely softened again in this condition.

(iii) Comparison with Deformed Austenite.

The sub-structure of reversed austenite has been shown to contain dislocation tangles; these may resemble those of plastically deformed austenite. An attempt was made, therefore, to compare the annealing behaviour of the two structures.

Austenite deformed at room temperature transforms to martensite and would thus add further complication to the problem. The deformation was performed in compression (for practical convenience) in an oil bath at a temperature of 168°C; this was found to be above the M_d temperature for the alloy. It was intended to deform the austenite by an amount which would produce a hardness equal to that of the reversed austenite specimens; the estimated 8% plastic strain was in fact rather too large, FIG. 4.47.

It is difficult to draw meaningful conclusions from the results in FIG. 4.47. although there is some suggestion that the hardness of the reversed austenite falls gradually during the annealing period, whereas that of the deformed austenite decreases first to a value of about 150 and later falls quite rapidly to the hardness value of the original austenite.

The merits of a comparison between one structure containing small areas which are highly deformed, and another containing a more uniform but smaller deformation producing the same overall hardness, are somewhat doubtful. No further work along these lines was performed, therefore.

FIG. 4.45. Alloy A. Reversed austenite annealed for 5 hours at 850°C.

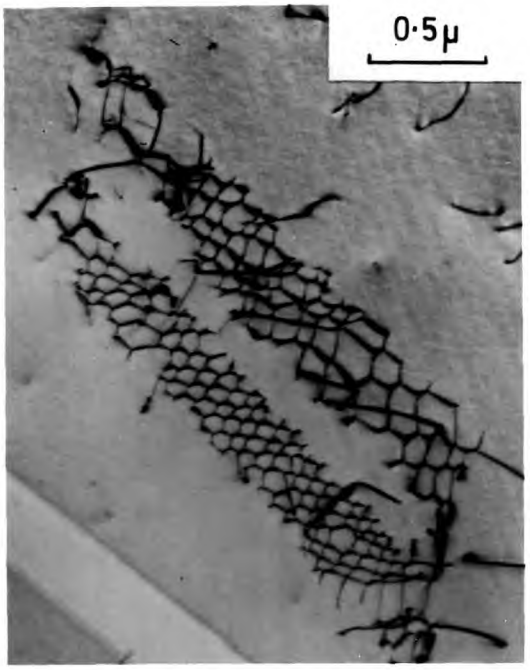

FIG. 4.46. Alloy A. Reversed austenite annealed for 5 hours at 850°C

FIG. 4.49. Alloy A. Cold worked, reversed at 600°C for 2 minutes and annealed for 2 minutes at 850°C.

FIG. 4.50. Treatment as for FIG. 4.49; dislocations at the grain boundaries.

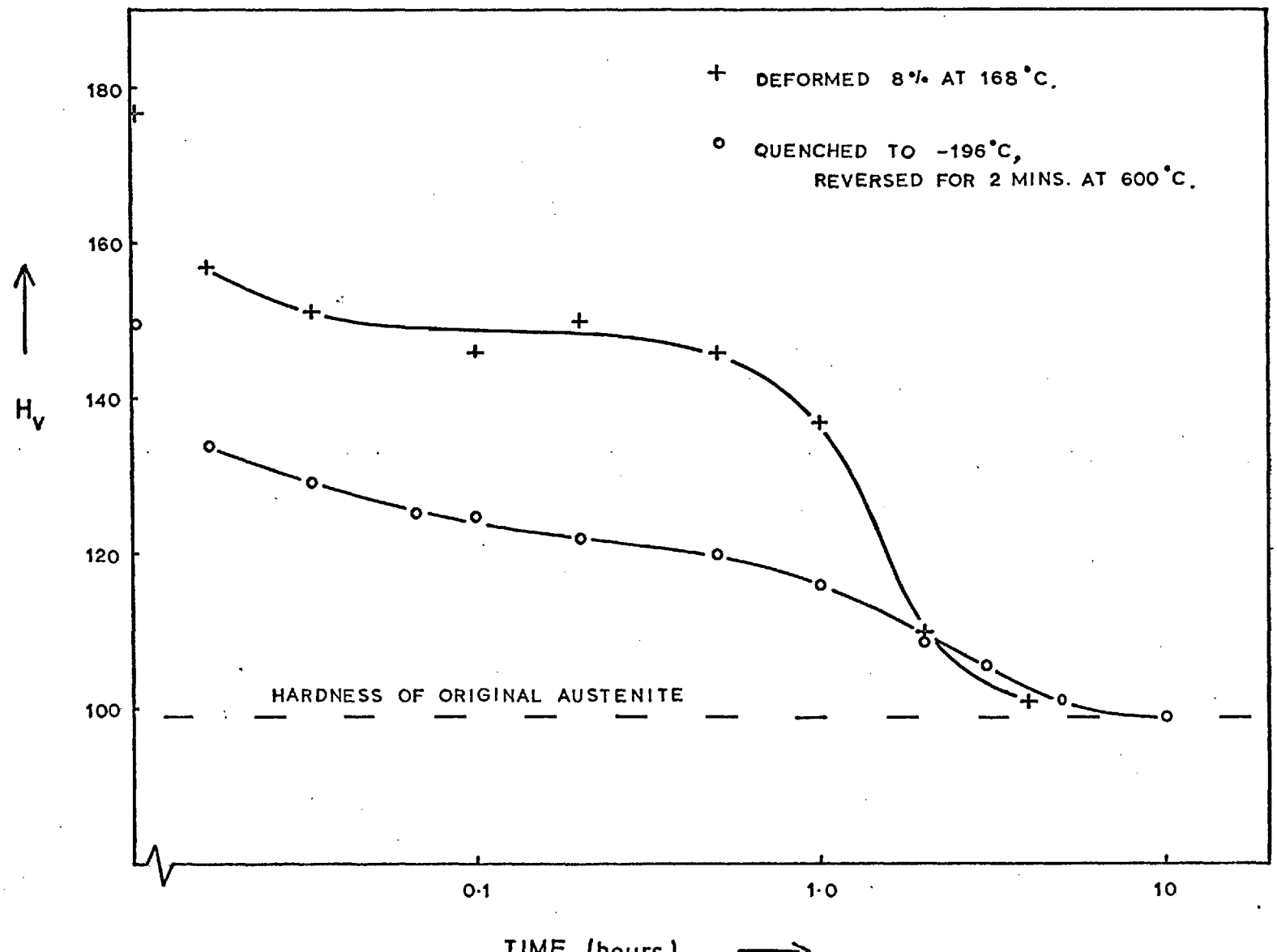

FIG. 4.47. Alloy A: Comparison of the annealing behaviour at 850°C of deformed and reversed austenite.

4.4.2. Reversed Austenite Obtained from Martensite Produced by Deformation:

(i) Hardness Changes.

After rolling 50% at room temperature, resulting in the formation of about 10% martensite, specimens were reversed for 2 minutes at 600°C and water quenched to room temperature. The resulting structure, containing deformed austenite and reversed austenite, was then annealed at 850°C for various times. The results are plotted on FIG. 4.48. together with those representing the annealing of 'standard' reversed austenite at 850°C for comparison purposes.

Only 1 minute at 850°C produces a decrease in hardness from the initial condition of HV = 300 to a value of 126. Further annealing resulted in additional decreases in hardness which were almost linear with the log of the annealing time.

(ii) Structural Changes.

Even after the shortest time investigated, 2 minutes at 850°C, the structure was observed to be fully recrystallised, though having a very small grain size (FIG. 4.49.). A common feature was the frequent observation of annealing twins. With longer annealing times the austenite grain size increased and there appeared to be a decrease in the number of non-coherent twin boundaries although the observation of annealing twins remained very common.

FIG. 4.50. shows dislocations at the austenite grain boundaries after annealing for 2 minutes at 850°C.

4.5. AGEING BEHAVIOUR:

Alloy B:

The ageing behaviour of Alloy B, containing molybdenum and carbon,

HV values at zero time; (a) = 300, (b) = 155.

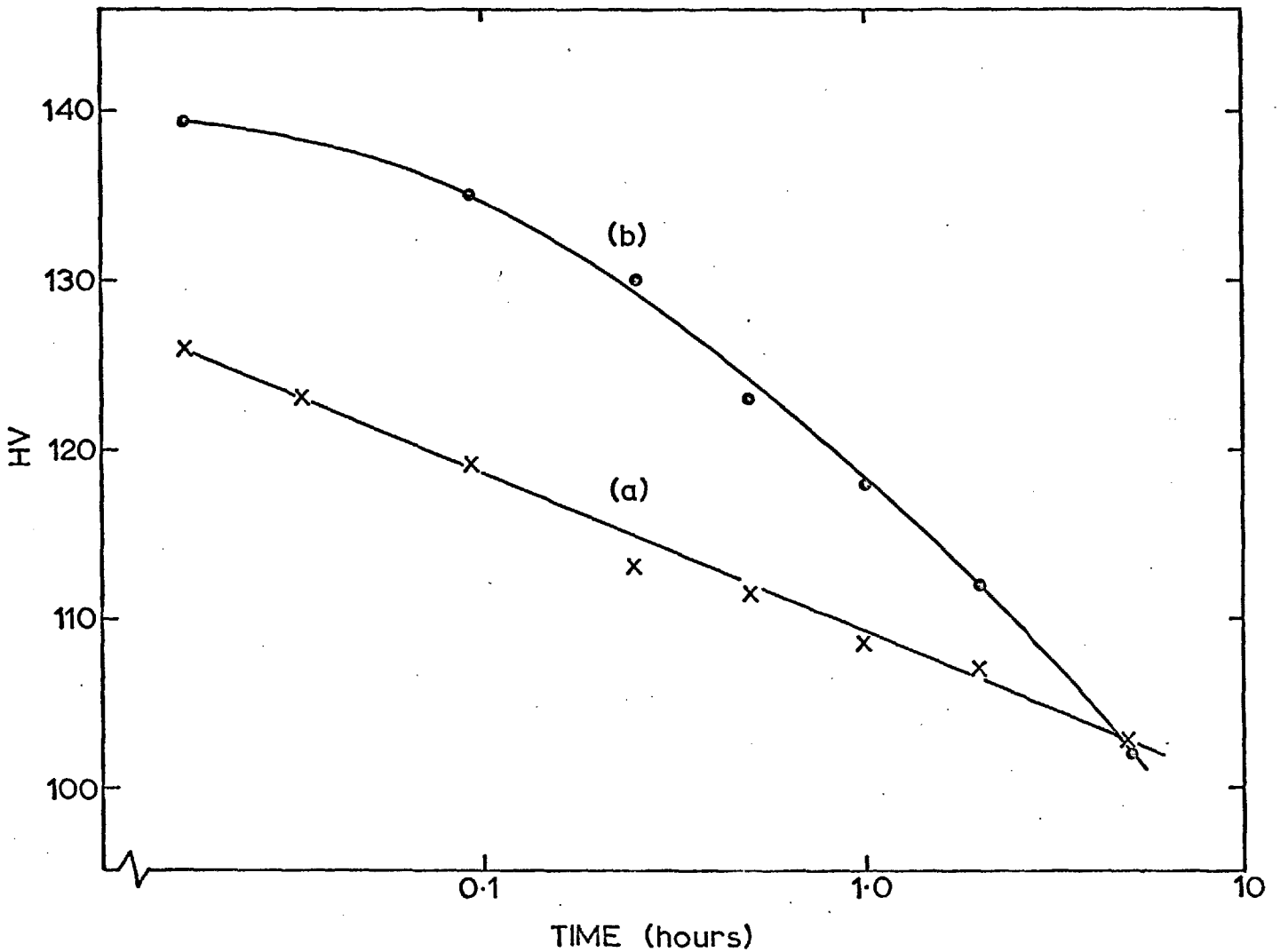

FIG. 4.48. Alloy A: Annealing behaviour at 850°C of 'reversed austenite' produced from martensite which had formed as a result of (a) 50% deformation at room temperature, and (b) quenching to -196°C.

after solution treatment was studied by isothermal treatments at two temperatures; 650°C and 700°C. The influence of the structure of the matrix on the ageing behaviour was also investigated by isothermal treatments at 700°C after, (i) partial transformation to martensite by quenching to -196°C for one hour and then reversion for 1 minute at 775°C, and (ii) partial transformation to martensite by cold working at room temperature and reversion for 1 minute at 775°C.

The development of the precipitation processes during the isothermal ageing of these three matrix conditions was followed at room temperature by measurements of specimen hardness, saturation magnetic intensity and by transmission electron microscopy.

4.5.1. Solution Treated:

The results obtained after ageing the solution treated alloy at 650°C and 700°C are given in FIG. 4.51. A treatment of 1 hour at 650°C produced no measurable increase in hardness but a small magnetic response was obtained from the specimen, equivalent to an approximate content of ½% of ferromagnetic phase. Electron microscopy showed that carbide precipitation had occurred at austenite grain boundaries; indeed, this was indicated by the preferential attack at such regions during electro-polishing the specimens. Carbides were observed to have formed also within certain austenite grains, as shown in FIG. 4.53., whereas many grains contained no precipitates.

Longer ageing at 650°C produced an increase in hardness accompanied by an increase in the magnetic response; occasional small regions of martensite were seen next to grain boundaries. Such regions were commonly observed after ageing treatments and a typical structure is shown later. Little further change is found after ageing for between 10 hours and 100 hours. After 120 hours an additional precipitate morphology to that already shown is observed, and can be seen in FIG. 4.54. As well as grain boundary precipitation, small carbides are

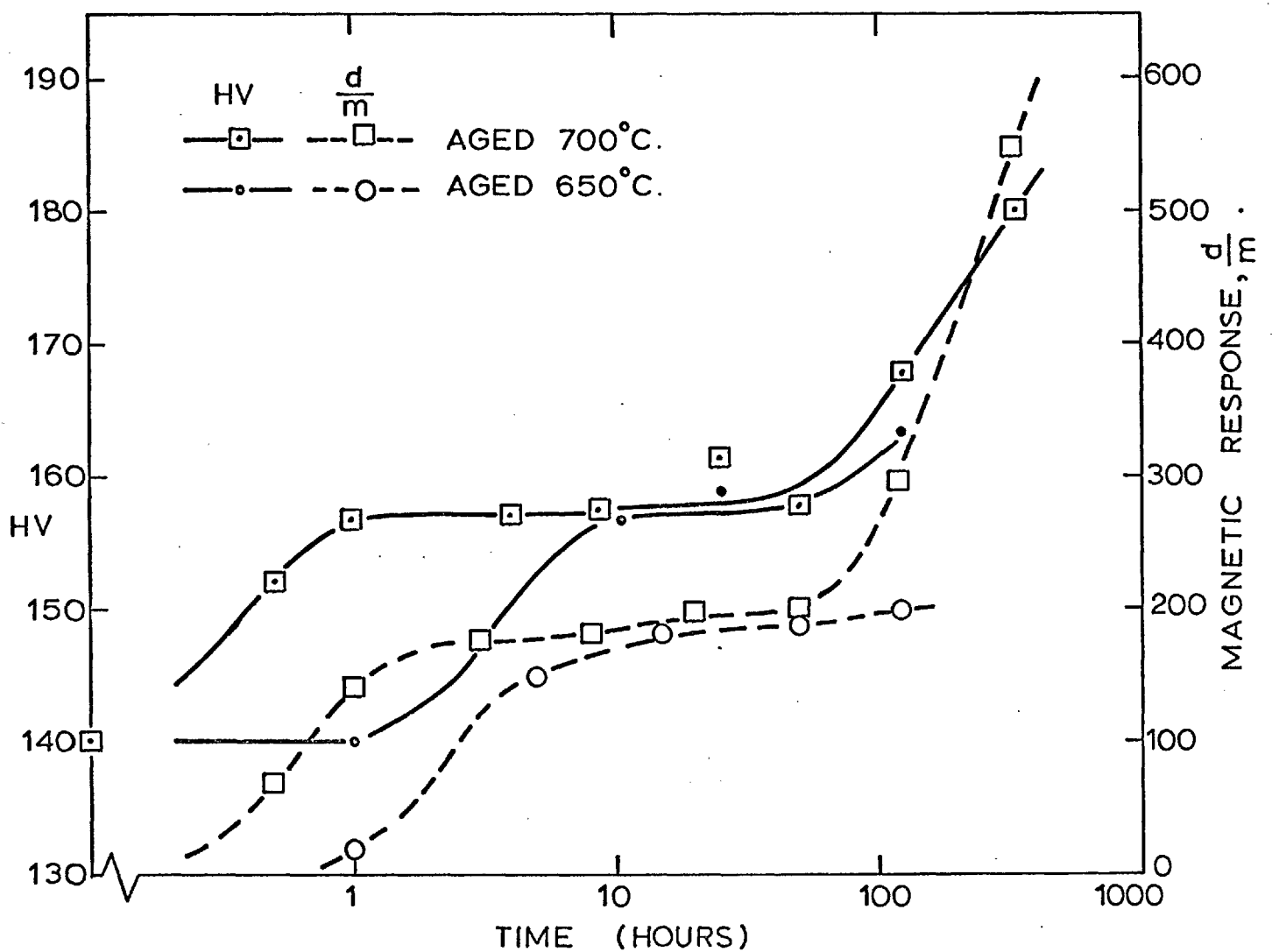

FIG. 4.51. Alloy B: Changes in hardness and magnetic response after ageing the solution treated alloy at 650°C and 700°C.

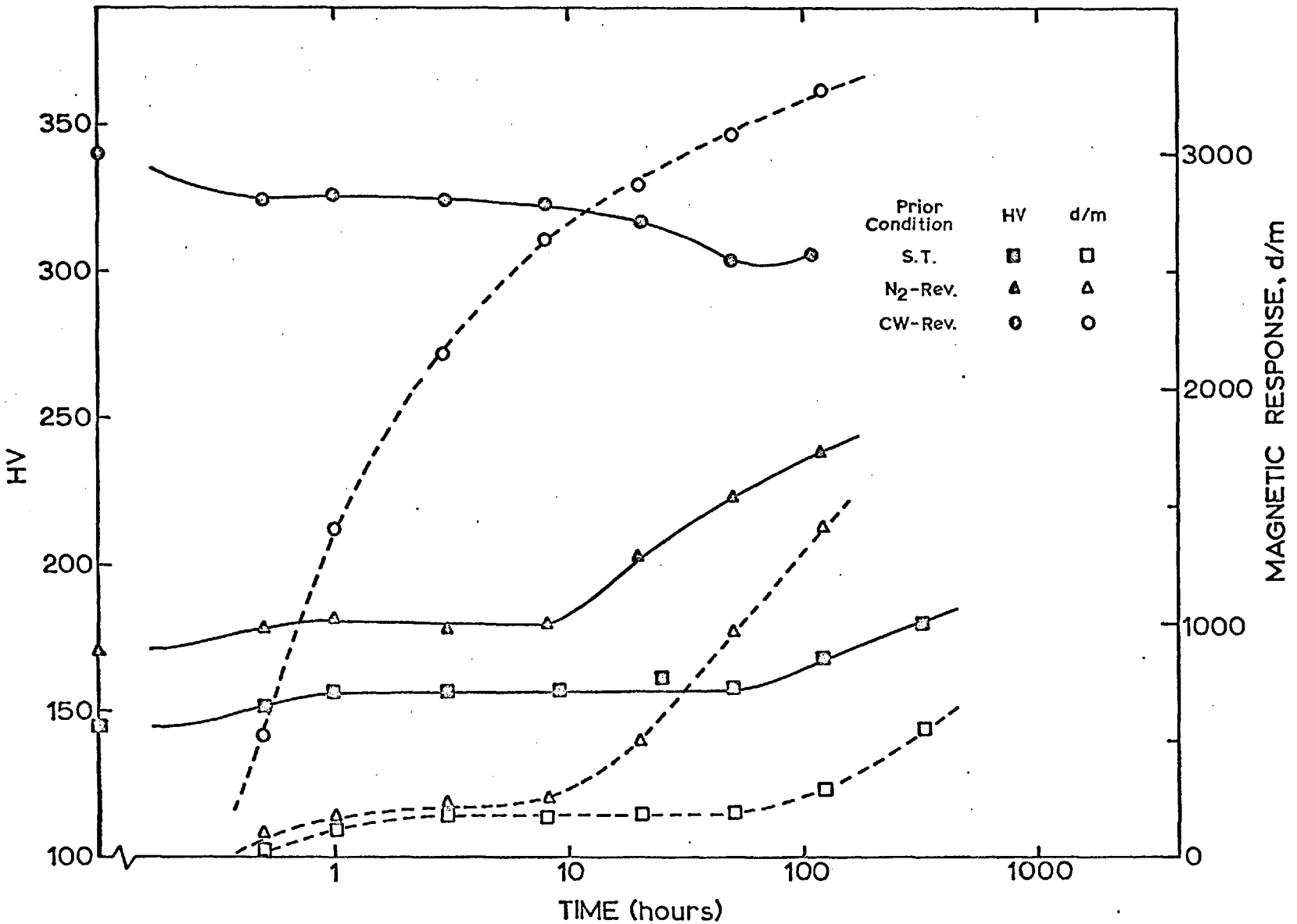

FIG. 4.52. Alloy B: Changes in hardness and magnetic response produced by ageing austenitic specimens at 700°C: solution treated and both varieties of 'reversed austenite'.

FIG. 4.53. Alloy B. Solution treated and aged at 650°C for 1 hour.

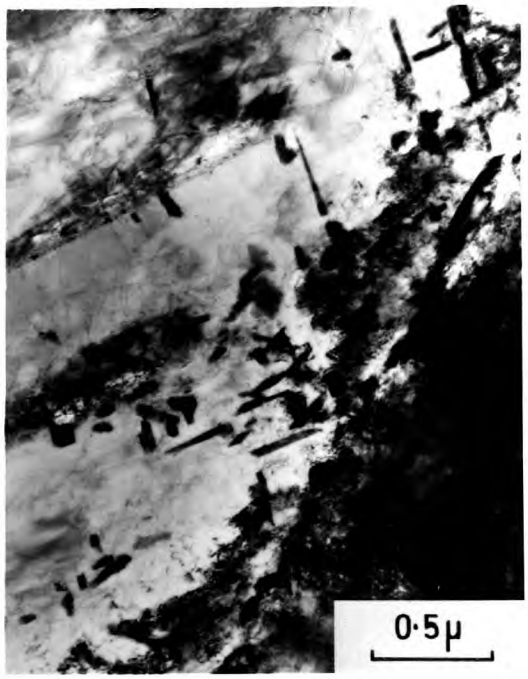

FIG. 4.54. Alloy B. Solution treated and aged at 650°C for 120 hours.

FIG. 4.55. Alloy B. Solution treated and aged at 700°C for 310 hours.

FIG. 4.56. Alloy B. Solution treated and aged at 700°C for 310 hours.

present in the austenite matrix and several of these are of angular shape, sometimes almost cubic. They were established, by electron diffraction, as being $M_{23}C_6$. After this treatment the specimen contains only about 4% ferromagnetic phase; a few austenite grains containing no precipitates and a low dislocation density are still observed.

Ageing the solution treated alloys at 700°C produced an increase in hardness after only a $\frac{1}{2}$ hour treatment, together with a rise in the ferromagnetic content. Between 1 hour and 50 hours the hardness and magnetic response are almost constant and examination of the structure after 25 hours at 700°C showed the presence of grain boundary precipitates together with 'laths' of carbides within the grains. Small martensitic regions and areas of austenite which were precipitate-free and contained few dislocations were also observed. No angular precipitate particles were seen after this treatment.

Heating at 700°C for longer than 100 hours produced a considerable increase in hardness and magnetic response. About 10% ferromagnetic phase was found after 310 hours and electron microscopy did not reveal any austenite grains which were still in the solution treated condition. FIG. 4.55. shows 'laths' of carbide in an f.c.c. matrix adjacent to a region having b.c.c. structure (top of micrograph); both areas contain a high dislocation density. It was not found possible to identify positively the precipitate particles by electron diffraction in this case. Similar carbides were also observed in a b.c.c. matrix.

Some particles formed as 'stringers', as shown in FIG. 4.56., where they are situated along XX, the boundary between two b.c.c. regions. Dark field microscopy has shown that the stringer is made up of $M_{23}C_6$ carbides.

Further examples of carbide precipitates after 310 hours at 700°C which have been positively identified as $M_{23}C_6$ are shown in FIGS. 4.57. (a) and 4.58. (a); in both cases they have an angular

morphology. In the first example the electron diffraction pattern, FIG. 4. 57. (b), which has been rotated by the appropriate amount to correct for the image rotation in the electron microscope, shows that the precipitate has an f. c. c. structure corresponding to $M_{23}C_6$ and that the matrix is b. c. c. The electron beam is parallel to $[110]_{b.c.c.}$ and $[100]_c$ and the carbide diffraction pattern shows that $\langle 110 \rangle_c$ are perpendicular to the sides of many of the carbide particles. In the second case, the electron beam is parallel to $[123]_c$; the matrix reflections do not allow positive identification of its structure although several spots suggested d-spacings consistent with a b. c. c. structure. The diffraction pattern, FIG. 4. 58. (b), shows that $[\bar{1}11]_c$ is perpendicular to one set of sides of the carbide particles in (a).

Several regions were observed which had a martensitic appearance, as shown later in FIG. 4. 63., and which produced b. c. c. diffraction patterns. These areas are quite different in appearance to other b. c. c. regions such as the matrix of FIG. 4. 57. (a).

4. 5. 2. Quenched and Reversed:

The results obtained after ageing at, 700°C, specimens of Alloy B which had previously been given a standard quenching and reversion treatment are shown in FIG. 4. 52. For comparison the results obtained by ageing the solution treated alloy at the same temperature are also plotted on the same graph. In the present case, the initial hardness is slightly higher because of the presence of reversed austenite in the structure. With ageing times of up to 10 hours, however, the changes in hardness and magnetic response of the two specimen conditions are very similar.

After 1 hour, precipitation at the grain boundaries and at certain places in the austenite grains (similar to FIG. 4. 53.) was seen. The reversed austenite regions were clearly visible but no precipitates were identified in these areas. Once again, small areas of martensite were occasionally

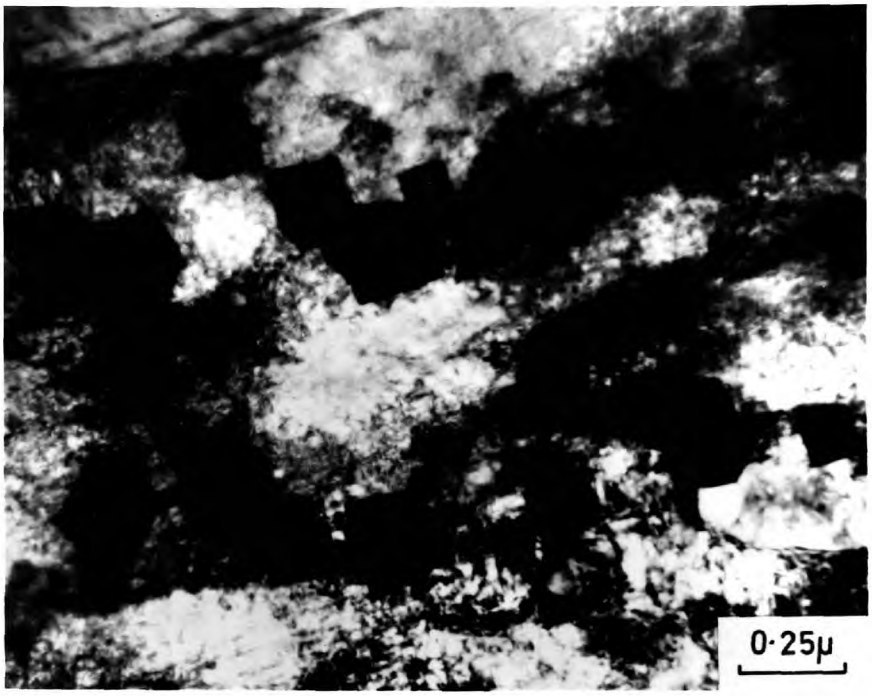

(a)

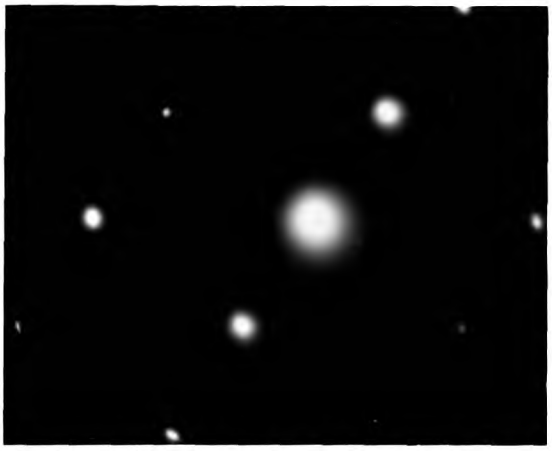

(b)

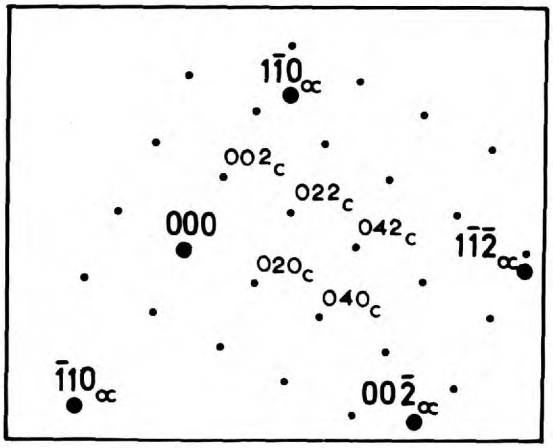

(c)

FIG. 4.57. Alloy B. Solution treated and aged at 700°C for 310 hours.

(a) angular particles of $M_{23}C_6$.
(b) electron diffraction pattern from (a).
(c) interpretation of (b); (not to scale).

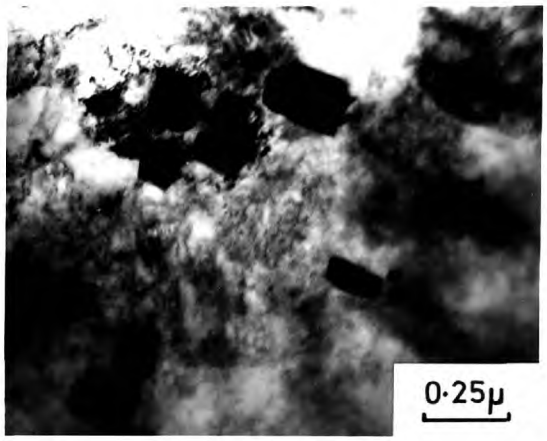

(a)

(b)

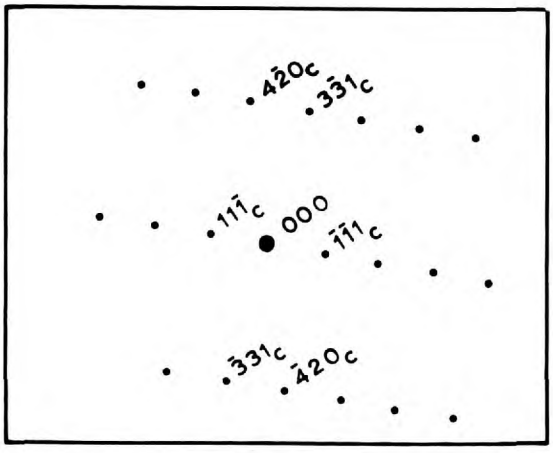

(c)

FIG. 4. 58. Alloy B. Solution treated and aged at 700°C for 310 hours.

(a) angular particles of $M_{23}C_6$.
(b) electron diffraction pattern from (a).
(c) interpretation of (b)

observed. No significant differences in structure were apparent after ageing for 8 hours at 700°C.

With ageing times longer than 10 hours a progressive increase in hardness and magnetic response occurred; in the case of the solution treated alloy the corresponding increase in these properties did not occur until after 50 hours at the same temperature. The magnetic response after ageing the 'reversed' structure for 121 hours at 700°C corresponds to an approximate ferromagnetic content of 30%. In addition to the 'lath' carbides already mentioned as being observed at shorter ageing times, precipitates were now quite clearly visible within the 'reversed austenite' regions, FIG. 4.59. The precipitates again gave rise to diffraction patterns consistent with their being $M_{23}C_6$ and the dark field micrograph shown in FIG. 4.60. was obtained using a carbide reflection. The elongated $M_{23}C_6$ carbides in FIG. 4.61. had also formed in an area which was originally reversed austenite but was now a b.c.c. structure. The matrix structures in FIGS. 4.59. and 4.60. were not identified. None of the original areas of retained austenite were found to have remained in the solution-treated condition.

4.5.3. Cold-Worked and Reversed:

Ageing at 700°C of specimens of Alloy B which had previously been reduced 50% by rolling at room temperature and then reversed for 1 minute at 775°C, resulted in the hardness and magnetic response changes shown in FIG. 4.52. The initial structure consists of approximately 60% deformed austenite and 40% reversed austenite and has a correspondingly high hardness value (HV = 340). After $\frac{1}{2}$ hour at 700°C this value drops to 325 and then remains almost constant for ageing times of up to 10 hours. A small decrease in hardness is produced by further ageing up to 50 hours but this is followed by an apparent upward trend after 120 hours although this was not definitely established. The continuous increase in magnetic response with ageing time, as shown in FIG. 4.52., leads to a ferromagnetic phase content

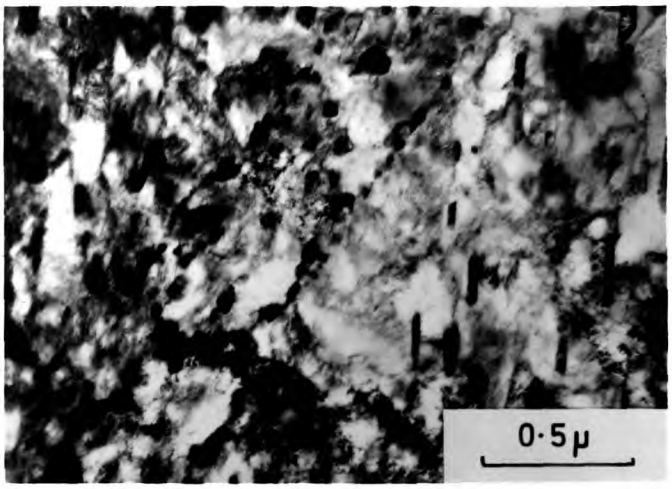

FIG. 4. 59.

Alloy B. Reversed austenite aged at 700°C for 121 hours, showing carbide precipitation.

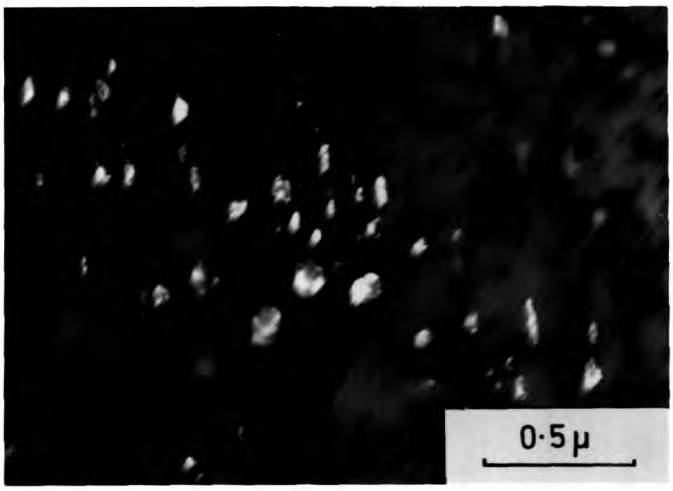

FIG. 4. 60.

Similar area to FIG. 4. 59; dark field micrograph using carbide reflection.

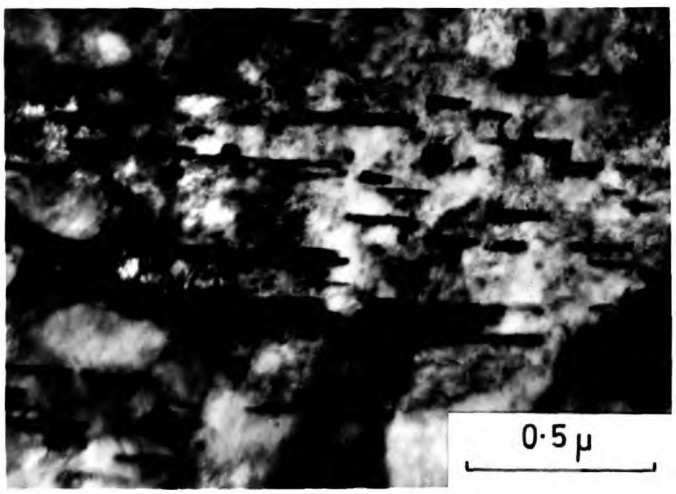

FIG. 4. 61.

Alloy B. Treated as in FIG. 4. 59, showing elongated carbide precipitates.

of the order of 60% after a 120 hour treatment.

After ageing for only 1 hour substantial precipitation has occurred throughout the specimen, as shown in FIG. 4.62.; the small carbide size and its even distribution throughout the matrix are apparent from the micrograph. Occasional areas of martensite were observed and an example is given in FIG. 4.63.

After 8 hours the structure was very similar, but after ageing for 120 hours the precipitates were noticeably larger. The increase in martensitic regions was small but many matrix regions produced b.c.c. diffraction patterns although they were otherwise indistinguishable from the f.c.c. matrix associated with the shorter ageing times. No recrystallised austenite regions were observed after ageing even though such areas are known to be present in the initial reversed structure (FIG. 4.34.); a high dislocation density exists throughout.

4.6. TRANSFORMATION CYCLING:

Transformation cycling, $\gamma \longrightarrow \alpha' \longrightarrow \gamma$, was performed on both alloys by repeatedly transforming them to martensite at liquid nitrogen temperature and retransforming them at their appropriate reversion temperatures. This is shown diagrammatically in FIG. 4.64.

4.6.1. Alloy A:

With five cycles the hardness of the austenite was doubled but the main effect was associated with the first two cycles. The hardness after the martensitic transformation part of the cycle increased with the first cycle but remained unaltered thereafter. The results are shown in FIG. 4.65. and confirm the findings of an earlier investigation in this Department by Miss J. Lakin. Also shown are measurements of the martensite content after cycling. No martensite could be detected following treatments at 600°C and that after holding for 15 minutes at -196°C was found to decrease progressively with increasing number of cycles.

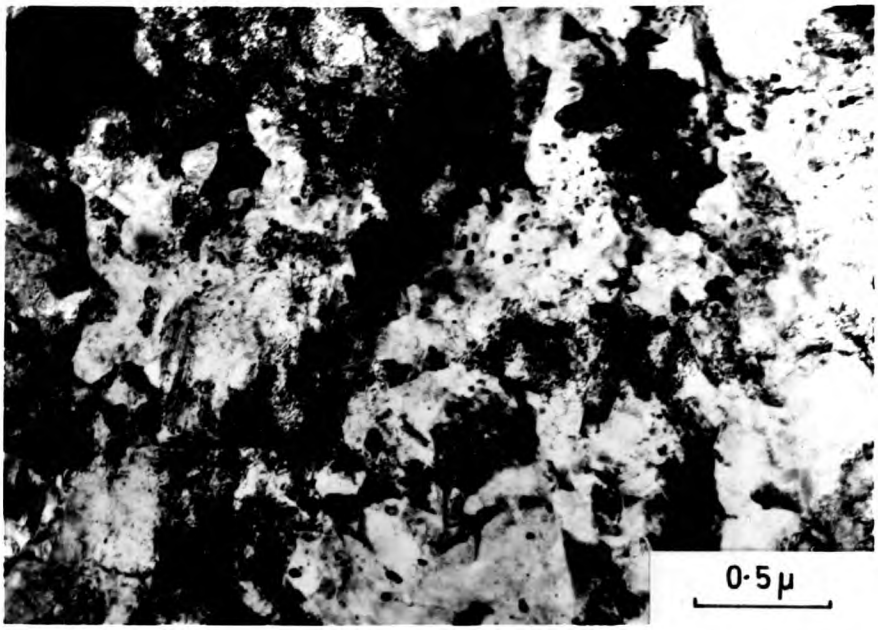

FIG. 4.62. Alloy B. Cold worked, reversed at 775°C for 1 minute and aged at 700°C for 1 hour; carbide precipitation in an austenite matrix.

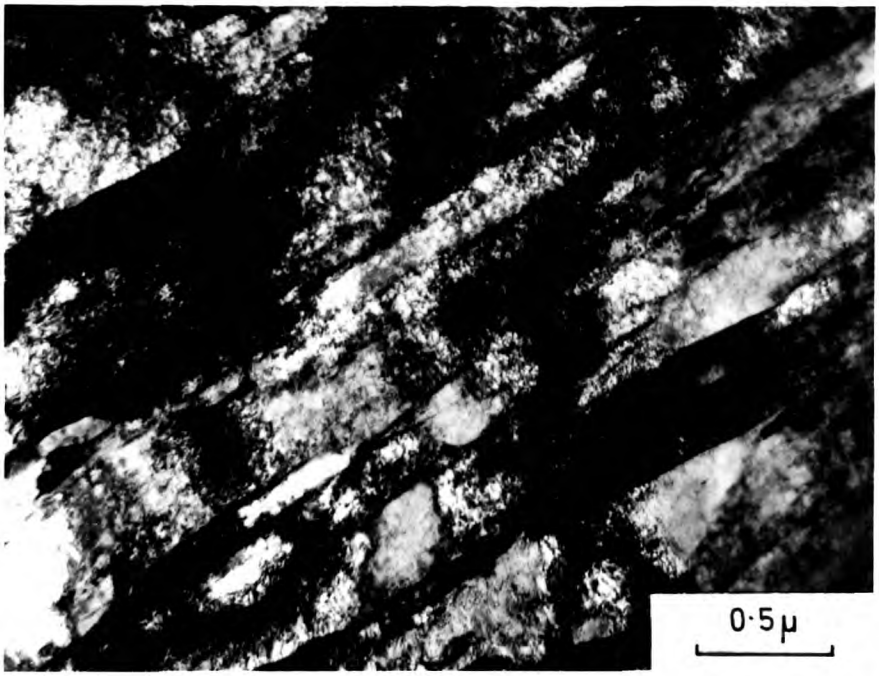

FIG. 4.63. Alloy B. Treated as for FIG. 4.62; martensitic region.

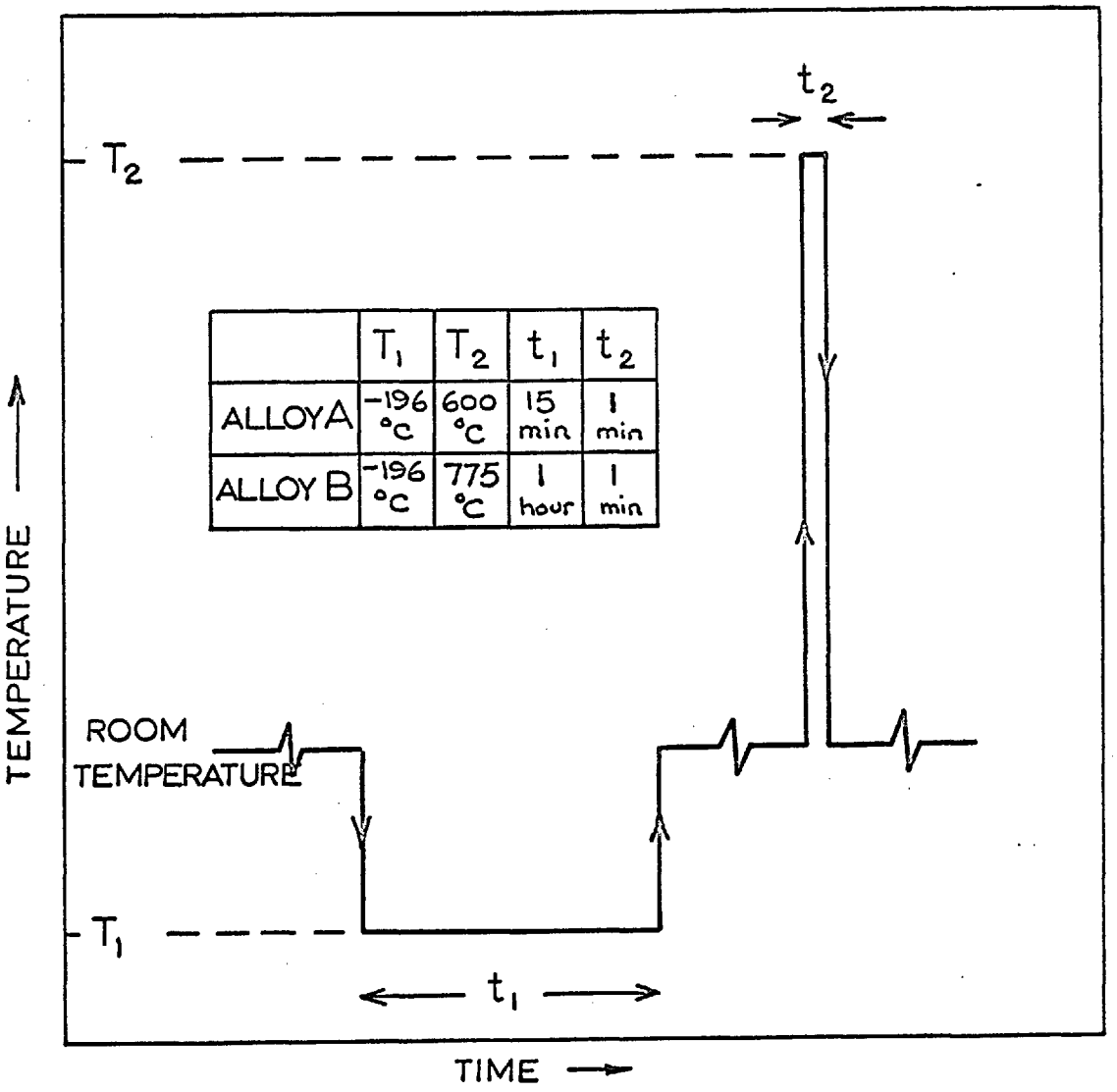

	T_1	T_2	t_1	t_2
ALLOY A	−196 °C	600 °C	15 min	1 min
ALLOY B	−196 °C	775 °C	1 hour	1 min

FIG. 4.64. Diagrammatic representation of one transformation cycle.

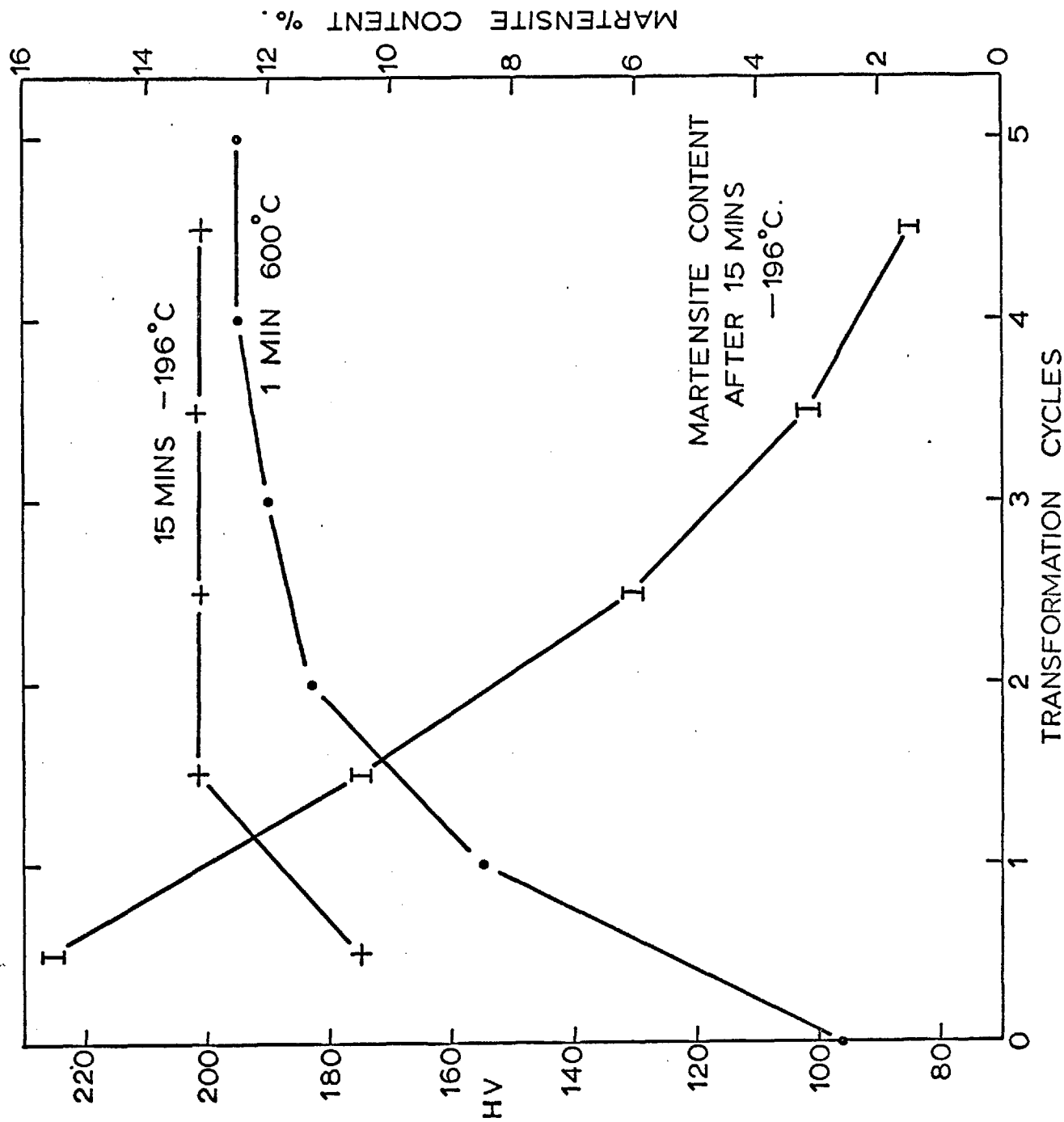

FIG. 4.65. Alloy A: Changes in hardness and martensite content during transformation cycling.

No structural observations of the transformation cycling have been made.

4.6.2. Alloy B:

The hardness was found to increase progressively after both the direct and reverse transformations with increased number of cycles; this can be seen in FIG. 4.66. The % martensite produced during the direct transformation again decreases with increased number of cycles and no martensite was detected at room temperature after the reversion treatments.

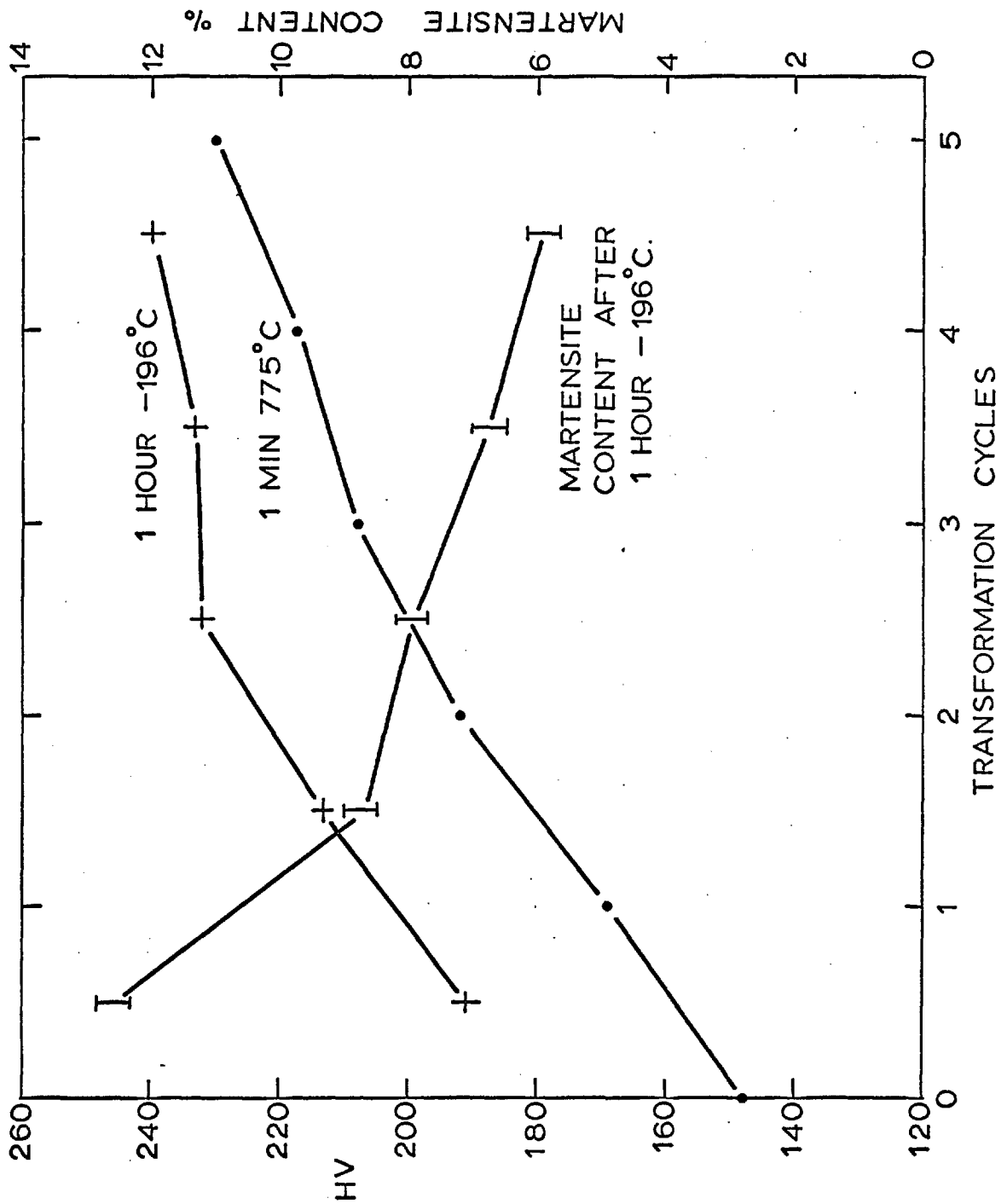

FIG. 4.66. Alloy B: Changes in hardness and martensite content during transformation cycling.

CHAPTER 5

DISCUSSION OF RESULTS

5.1. THE DIRECT TRANSFORMATION:

5.1.1. General:

The experimentally determined M_s temperature for Alloy A and the extent of transformation to martensite at -196°C are close to the values reported by Breedis [8] for a similar alloy; the slightly higher M_s value for the present alloy can be attributed largely to its lower nickel content. In the case of Alloy B, the M_s value is in very good agreement with the predictions of published data [10, 11] on the effect of alloying elements on the M_s temperature in such steels. The martensite content produced by holding at -196°C is of the order expected; the isothermal aspects of transformation will be discussed in the next section.

No significant differences were observed in the morphology of the partially martensitic structure in the two alloys, with the possible exception that details within transformed laths were more clearly visible by light microscopy in the case of Alloy B than Alloy A. The fine structure of the partially martensitic specimens, as revealed by transmission electron microscopy, confirmed the presence of a high internal dislocation density in the α' and the undeformed nature of the retained austenite.

Very little work was done on the crystallography of the transformation products; the observation that the martensite laths are bounded by $\{111\}_\gamma$ planes is in agreement with previous work [14, 15].

The observations suggest that the martensitic decomposition of austenite involves self-accommodation, within each lath, of the shears and volume changes associated with the transformation, leaving the retained austenite relatively unaffected.

5.1.2. Isothermal Aspects:

The isothermal aspects of the direct transformation of austenite to martensite have not been investigated in the case of Alloy A, but are almost certainly present. In the case of Alloy B, this is shown to be so beyond doubt by the results in FIG. 4.3. General features of isothermal martensite transformation in stainless steels have already been discussed in Section 2.2.2.

The transformation is unlikely to proceed by a completely isothermal mechanism but rather by an initial athermal reaction followed by some isothermal transformation. This may be either by the nucleation of new martensite grains or by the growth of existing ones, possibly by the relaxation of opposing stresses. The unusual lath morphology of martensite in stainless steels, compared to the plates found in many other ferrous alloys, makes analysis of this phenomenon more difficult. The $\{111\}_\gamma$ lath faces are observed to be almost completely planar and, as the many α' grains within a lath are unlikely to grow together to maintain a plane lath interface, it is improbable that isothermal transformation proceeds by the thickening of existing laths. Although laths generally terminate either at an austenite grain boundary, an austenite twin boundary or at the intersection with a lath on another $\{111\}_\gamma$ plane, it can be seen from FIG. 4.1. that this is not always the case and that they sometimes stop within the austenite grains. In this case isothermal transformation could occur by the lengthening of such laths. Another possibility is that small regions of γ, ε and/or SFs within a lath transform to α'. The most likely mechanism, however, is that the transformation proceeds at constant temperature by the formation of new laths.

The relative extent of transformation at -196°C and -80°C will depend on the relative contributions of the athermal and isothermal components of the reaction. The results for Alloy B (FIG. 4.3.) suggest that the usual situation exists where the isothermal aspects are of lesser

importance, rather than vice versa [63].

Repeated cycling between room temperature and -196°C is, presumably, expected to produce additional transformation via some sort of relaxation mechanism. In the case of Alloy B, the fact that three one hour treatments at -196°C produced less transformation than one single three hour treatment suggests, perhaps, that returning the specimen to room temperature may have produced a slight stabilising effect. It must be emphasised, however, that the results do not show beyond doubt that the measured difference in martensite contents is significant and that this apparent stabilisation effect is, in fact, real.

5.1.3. Effect of Cold Work:

The partial transformation to martensite, in both alloys, during rolling at room temperature is in agreement with the observations discussed in Section 2.2.1., where the deformation is performed below the M_d temperature. The considerably greater extent of transformation in Alloy B may be due to the fact that the deformation temperature is closer to the M_s temperature in this alloy than in the case of Alloy A.

The failure to observe martensite in the cold-worked specimens by electron microscopy may be connected with Lagneborg's findings [19] that, in the same specimen, some grains contain much martensite while others contain hardly any. Furthermore, the very highly deformed nature of the structure would tend to make identification of small areas of a second phase more difficult, although these should be detectable by electron diffraction and dark field techniques. The limited investigation by electron diffraction which was made showed the presence of only f.c.c. regions; in all cases the diffraction spots were broadened as a result of the deformation of the lattice.

The presence of α' was, however, confirmed beyond doubt by magnetic measurements.

5.2. INTERPRETATION OF DILATOMETRY RESULTS:

5.2.1. General:

The results of the differential dilatometry experiments are not easily interpreted at first sight. It has been pointed out in Appendix C that the curves may exhibit a relative specimen length change with temperature prior to and after the reverse transformation because of small differences in the lengths of the specimen and the 'control' which produces different thermal expansions. These indicated changes in relative length would not be expected to be the same for different experiments. Furthermore, the linear change with temperature should indicate less of a relative contraction after reversion than before because of the disappearance of the martensitic structure which has a lower coefficient of thermal expansion. That is to say, if the two specimen lengths are such that almost no relative length change is indicated during heating before reversion, then one would expect an apparent linear specimen expansion to appear during continued heating of the fully austenitic structure after reversion.

The retransformation of b. c. c. α' to f. c. c. γ will produce a specimen contraction. For reasons explained in Appendix C, results obtained during the early stages of heating have been ignored. Hexagonal martensite, ε , has been shown to begin to retransform to γ on heating at about 140°C [14] and to be completely absent after heating to 400°C [23]. Thus, it was not found possible to follow the $\varepsilon \longrightarrow \gamma$ transformation by this technique. However, the fact that this transformation in an Fe - Mn - C alloy [91] is known to be accompanied by a small volume expansion may provide some information for the shape of the early part of the curves.

5.2.2. Quenched Specimens:

In the case of the results relating to specimens quenched to -196°C (FIGS. 4.17. and 4.24.), the relative slopes of the initial parts of the

various curves are not significant. As already mentioned, the relative position (with regard to length) of each curve on a diagram is also without significance because of the arbitrary choice of a zero value in each case.

The greater overall contraction in the case of specimens of Alloy A is in approximate proportion to the higher martensite content of this alloy, relative to Alloy B, and cannot be regarded as indicating a difference in the specific volume change of the $\alpha' \rightarrow \gamma$ transformation in the two alloys, particularly as expansion will accompany any precipitation of $M_{23}C_6$ in Alloy B.

In both alloys, the temperature at which reversion appears to be completed is found to be independent of the heating rate employed. It is possible that there might be a small contraction effect due to some recovery of the reversed austenite structure (see next section) superimposed on that due to the reverse transformation.

The start of transformation is less easily explained; the experimental observations for Alloy A are summarised below:

heating rate	observation
slow	gradual contraction beginning at about 450°C.
medium	gradual change at 520°C, abrupt at 540°C.
fast	abrupt contraction at 540°C.

A possible explanation of these observations could be that a diffusion controlled reversion process is able to operate with the slowest rate of heating; a diffusionless transformation may be superimposed as the temperature is increased but the dilatometry curves do not show a clear distinction between the two processes. With the 'medium' heating rate the diffusional reversion process operates to a lesser extent and is soon replaced by the diffusionless mechanism, beginning at 540°C:

it is, of course, possible that the two processes operate simultaneously and that one dominates the other at different temperatures. The abrupt change indicating the diffusionless mechanism beginning at 540°C is the only transformation feature observed during 'fast' heating, suggesting complete suppression of the diffusionless reversion process.

It is interesting to note that the temperature of the abrupt contractions, 540°C, for the medium and fast heating rates, agrees closely with the abrupt change in modulus (FIG. 4.16.) which was found to occur at 545°C when using a heating rate which lies between these two. However, it is not easy to account for the much lower value for A_s which was indicated by magnetic measurements after plunging specimens into salt-baths; in this case the heating rate can be termed 'rapid', and is probably of the order of 5000°C/min. It is probably coincidental that the value of 450°C obtained for the A_s with 'rapid' heating corresponds to the temperature at which the gradual contraction was first observed with a 'slow' heating rate.

This apparent anomaly obtained by 'rapid' heating might possibly be explained on a qualitative basis if it can be assumed that a stabilisation effect is involved with the slower rates. This would suggest that the reverse transformation might thus be subjected to the effects of both stabilisation of the diffusionless mechanism and a tendency towards a diffusion-controlled process as the heating rate is lowered. The 'rapid' heating rate could then be considered to suppress both of these effects whereas the 'fast' heating rate permits some stabilisation to develop, yet avoids the diffusional processes. This latter process develops progressively as the 'medium' and 'slow' heating rates are employed.

An alternative interpretation of the lower A_s value obtained from magnetic measurements following 'rapid' heat treatment may be suggested when it is remembered that this 'rapid' technique involves holding for 2 minutes at the various reversion temperatures.

This may allow some isothermal transformation to occur and the correlation of the observed decrease in martensite content in the 'rapid' case with the change in slope of the 'slow' dilatometry curve, both at 450°C, may then be explained in terms of the occurrence of a diffusion-controlled reversion process. The marked drop in martensite content at about 540°C with 'rapid' heating, and the pronounced contraction in the dilatometry curves at the same temperature may be attributed to a diffusionless reversion process. On this basis the diffusionless (shear) mechanism can be regarded as requiring a greater driving force than the diffusion-controlled process for which a longer time is needed.

The progress of the reverse martensitic transformation in Alloy A, during isothermal holding between the A_s and A_f temperatures is currently being studied in this Department by Miss J. Lakin.

In Alloy B, the situation is further complicated by the presence of 0.09% carbon in this alloy which could lead to carbide precipitation during the continuous heating treatments and, possibly, to a greater stabilisation effect.

Irvine et al [10] have shown that carbide precipitation can occur in similar steels after heating for about 5 minutes at 700°C and they emphasise the fact that the carbide, $M_{23}C_6$, precipitates from austenite. Thomas and Krauss [9], however, have observed the formation of $M_{23}C_6$ in martensite during a short reversion treatment although this was not found in the present investigation (Section 4.2.). The results of ageing treatments on a reversed austenite structure (Section 4.5.) suggest that precipitation is confined largely to grain boundaries and twin interfaces with short ageing times. An investigation of the ageing of the martensitic structure prior to reversion was not performed but it is possible that precipitation could develop in this structure, especially as carbon is known to diffuse more easily in a b.c.c. matrix.

The formation of $M_{23}C_6$ from austenite is accompanied by a specimen expansion [92, 93] and will thus influence the shape of the curves in FIG. 4.2/4. The apparently smaller overall contraction indicated on heating Alloy B at the 'slow' rate, as compared to faster heating rates, can be attributed to an expansion contribution due to carbide formation which is more extensive at slower heating rates.

After cooling to room temperature the 'slow' and 'medium' specimens of Alloy B gave weak responses when tested with a small magnet; this is taken as an indication of the occurrence of precipitation, which has resulted in the formation of martensite on cooling as explained in Section 5.5.2. Although there is a possibility of some transformation to ferrite during heating (Section 5.5.2.) the times and temperatures involved suggest that this is unlikely to occur in the present case.

5.2.3. Cold-Worked Specimens:

The results for both alloys (FIGS. 4.30., 4.37.) are characterised by an initial specimen contraction, which had already begun at the lowest recorded temperatures (about 200°C), followed by a pronounced specimen expansion; the change in sign of the relative length change occurred at higher temperatures in the case of the faster heating rate. At still higher temperatures a relative contraction, or a reduction in the rate of expansion, is observed and it is suggested that it is this superimposed contraction which represents the reverse transformation. This point will be developed later.

The initial contraction is believed to be associated with recovery processes which occur during heating of the deformed structure since an increase in density is a feature commonly observed during the early stages of recovery processes [94]. Approximate calculations show that the magnitude of the observed contraction can be accounted for in this way. Garofalo and Wreidt [95] have shown that stainless steel experiences a density decrease as a result of deformation; this may be

attributable to the dilational strain field associated with edge dislocations and to the presence of an excess of vacancies produced by the cold work, provided that these are retained in the lattice at room temperature. Recovery processes are discussed in Section 5.4.

The relative expansion which follows this contraction due to recovery is not easily explained. The volume change accompanying the formation of $M_{23}C_6$ may contribute to the observed expansion in Alloy B but cannot be the sole cause since the same features are exhibited by the carbon-free Alloy A. There is some similarity between the present results and those of Seldovich et al [48] who found that the volume change on the martensitic-type $\alpha \longrightarrow \gamma$ transformation in a textured ferro-nickel alloy was ~~non-isotopic~~ anisotropic; in particular, it was accompanied by elongation of the alloy in the direction of the texture axis, although the specific volume of the γ phase is less than that of the α phase. The results of the present investigation suggest (Section 4.3.) that the reversion of martensite produced by cold working in Alloys A and B occurs at similar temperatures to that in quenched specimens, at least in the case of 'rapid' heating. It is possible, therefore, that the observed specimen expansions are connected with the reverse transformation. However, even if this is the case, other factors must also be involved since relative expansion continues after the transformation appears to have reached completion and, indeed, becomes more pronounced once the estimated A_f temperature has been reached.

It is suggested, therefore, that the observed relative expansions might be connected with anisotropic aspects of a recrystallisation process in these cold-worked materials. In all cases, the length of the dilatometry specimens was parallel to the rolling direction. There is evidence to suggest [96] that the retained austenite in stainless steel rolled at room temperature develops a 'brass texture', namely (110) [T12].

Recrystallisation of this structure produces an annealing texture [97]; although the actual texture found was not reported it was unlike the 'cube texture' which forms from stainless steel rolled at higher temperatures to produce a 'copper-type' deformation texture.

It has been shown (Section 4.3.) that small recrystallised grains were found in Alloy A after a 'rapid' reversion treatment of 2 minutes at 555°C, and in Alloy B after only 1 minute at 655°C. It seems quite likely, therefore, that recrystallisation could begin at the temperatures at which a relative expansion is first observed; being lower as the time available for the initiation of the recrystallisation process increases (i.e. slower heating rate).

If any of the observed expansion is attributable to an anisotropic aspect of the actual reverse transformation it must be associated with the early stages of reversion since the later superimposition of a contraction is almost certainly due to the reverse transformation. In the case of Alloy A, this contraction effect is quite small, presumably because of the low martensite content in these specimens (about 10%). With a 'medium' heating rate the contraction balances the expansion due to recrystallisation to produce almost no relative length change between about 555 and 600°C. A 'fast' heating rate permits only a reduction in the rate of expansion until the transformation is completed at 600°C; above this temperature the expansion continues more rapidly with rise in temperature.

Alloy B contains appreciably more martensite (about 40%) and the superimposed contraction is correspondingly more pronounced. With a 'medium' heating rate the two effects balance to give no relative contraction over the range 660 to 790°C: with a 'fast' heating rate, the rate of expansion is reduced at about 680°C and a change to a relative contraction occurs at 720°C (presumably due to the high rate of reverse transformation) before giving way to a relative expansion once more at 780°C.

The complex nature of the results for these cold-worked specimens prevents an estimation of values of the A_s temperatures although there is some suggestion that these values might be lower in the case of the slower heating rate. Furthermore, it is not possible to postulate the interactions between such effects as stabilisation, diffusion-controlled reversion and carbide precipitation nor, indeed, to say whether or not these effects are actually present.

Testing with a small magnet after the specimens had cooled to room temperature produced a weak response in the case of the 'medium' heating rate specimen of Alloy B, yet none for the 'fast' specimen. This suggests, at least in the former case, that carbide precipitation and possibly transformation to ferrite occur during heating.

5.3. THE REVERSE TRANSFORMATION:

Many of the comments in this section are applicable to both alloys but where differences are thought to arise, these are specifically mentioned.

5.3.1. Reversion of Specimens Transformed to Martensite at -196°C:

(i) The reversion mechanism. Christian [98] has pointed out that there is no satisfactory theory to explain the formation of martensite in stainless steels. Kelly and Nutting [15] suggested that this is because these theories are aimed at producing an invariant plane between the two phases, while the governing condition seems to be the production of an invariant line, which is in fact the long axis of the martensite needles, namely $\langle 1\ 1\ \bar{1} \rangle_{\alpha}$ which is parallel to $\langle 1\ \bar{1}\ 0 \rangle_{\gamma}$. They have proposed a mechanism, which is a modification of Kurdjumov - Sachs double shear mechanism, consistent with an invariant line. However, there are several reports of the existence of an invariant plane (habit plane) for this system; this is often the $\{225\}_{\gamma}$ plane as, for example, found by Reed [14]. In view of the lack of understanding of the direct transformation, it is not surprising that there is considerable difficulty in proposing a mechanism for the reverse transformation.

Evidence for the shear nature of at least part of the reverse transformation is provided by the observation that the reversed austenite regions regain the orientation of the original (retained) austenite, as shown in FIG. 4.12. This is in agreement with the findings of Breedis [8] for a steel of the same composition of Alloy A and it suggests not only that a shear mechanism is involved, but that the same variants of the shears must operate in both the direct and reverse transformations. In the case of Alloy A, it appears that one grain of α' will retransform completely to a single 'grain' of reversed austenite and it is possible that all the grains of α' within a martensite lath will retransform at the same time. This would assist in the accommodation of the transformation shears in a similar manner to the direct transformation to martensite.

In Alloy B, no evidence has been found for the complete transformation of a grain of α' to a single region of reversed austenite and the structure shown in FIG. 4.21. suggests that the martensite grains break up during reversion. Crystallographic studies were not made on this structure, however, and so it is not possible to say with certainty that a shear mechanism has operated and that the structure in FIG. 4.21. has not been produced by a diffusion process. Further support for the suggested break up of the martensite crystals comes from the impression of a greater 'fragmentation' of the reversed austenite structure observed in Alloy B as compared to that in Alloy A.

This may result from the greater opportunity for solute movement in this carbon-containing alloy which tends to hinder the shear processes of the diffusionless reverse transformation and thus prevents entire grains of α' from executing the reverse shears of the direct transformation. Comparison of FIGS. 4.21. and 4.22., from the same specimen, does support the idea that individual laths retransform at different stages in the A_s to A_f temperature range.

The possibility of a diffusion-controlled reversion mechanism has already been mentioned in the previous section (5.2.), the suggestion being that, when there is insufficient driving force to compensate for the large strain energy which is produced by a martensitic reversion mechanism, retransformation may occur by a thermally activated nucleation and growth process. Previous observations of both diffusion-controlled and diffusionless reversion process have already been discussed in Chapter 2 (Section 2.4.).

The dilatometry curves for Alloy A (FIG. 4.17.), which are more easily interpreted than those of the carbon-containing Alloy B, suggest that with the slower heating rates a diffusion-controlled reversion process may operate. It is possible that this mechanism may also be involved in the retransformation which occurs on holding for short times (1 or 2

minutes) at the reversion temperatures after 'rapid' heating in a salt bath. The formation of austenite, isothermally, has been demonstrated by work presently in progress in this Department.

The diffusion-controlled process suggested to explain the present results would seem to be inconsistent with the work of Breedis [8] who found that the martensite content (also measured magnetically) was the same in specimens which had been held for either 2 minutes or 2 hours within the A_s to A_f temperature range. No explanation for this apparent difference in results can be suggested; however, some contribution by a diffusion-controlled process to the transformation of α to γ may provide one explanation of the observation by Breedis of areas in the reversed austenite which differed in orientation to the parent austenite grain and to the majority of the reversed austenite areas.

Further comparison of the present results with Breedis's work shows very close agreement on the progress of the reverse transformation after 2 minute treatments of the partially martensitic structure at various reversion temperatures. However, his observation that, compared with the as-quenched condition, the density of faults and twins between martensite crystals comprising a lath are diminished after a short anneal at 500°C is not borne out by the present results (FIG. 4.10.) where these features are found to have increased after heating for 2 minutes at 525°C. The significance of this and, indeed, the part played by these faults and twins in the reverse transformation are not easily understood.

(ii) Fine structure of reversed austenite. The reversed austenite produced by 'rapid' heating of partially martensitic samples has been shown to contain a high density of tangled dislocations, together with small twins and stacking faults, although the latter have largely disappeared once the reverse transformation is completed.

It seems probable that the high dislocation density in the reversed austenite is, to a large extent, inherited from the martensite crystals from which it forms since these are also known to possess a highly imperfect sub-structure resulting from the direct transformation. A further contribution to the dislocation density will be produced by the various shears, deformations and volume changes associated with the reverse transformation itself, particularly as these have to take place in an already imperfect structure.

It is not clear whether the stacking faults (for example, see FIG. 4.11.) actually participate in the actual mechanism of the reverse transformation or are formed by recovery processes during the short reversion treatment. It is interesting to note that the stacking faults shown in FIG. 4.11. following a short treatment at 550°C (Alloy A) were not observed after treatment below this temperature (e.g. at 525°C) although they were observed after treating specimens for 2 minutes at 575°C. It has already been suggested (Section 5.2.1.) that the diffusionless reversion mechanism for Alloy A begins at about 540°C and this correlates well with the observation of the stacking faults in this alloy.

Stacking faults are observed less frequently in Alloy B and, again, only after reversion treatments close to the A_f temperature. The faults were considerably shorter in length than for Alloy A; this may be due, either to a higher stacking fault energy (SFE) in Alloy B or to the shorter distances over which the leading partial dislocation can move before meeting an obstruction. The latter possibility would be consistent with the apparently greater fragmentation of the reversed austenite in Alloy B.

It is difficult to assess the relative values of the stacking fault energies of Alloys A and B but a qualitative indication of the effects of the compositional differences between the two alloys can be made. The

lower nickel content of Alloy B would be expected to lower the SFE of this alloy relative to Alloy A [7, 99] whereas its lower chromium content should have almost no effect at this composition level [99]. The influence of molybdenum and carbon are not well established but the indications are that both elements cause a small increase in the SFE [99]. On balance there is no clear evidence for the existence of a significant difference between the stacking fault energies of the two alloys.

The small twins which have been observed in the reversed austenite in both alloys, and by Breedis [8] in his material which is almost identical to Alloy A, are considered to be an early stage in the recovery of the reversed austenite. A twin fault has roughly one half of the energy of a stacking fault because only half as many next-nearest neighbour bond violations are involved; thus the formation of a twin from stacking faults would reduce the stored energy of the reversed austenite sub-structure.

These twins are, therefore, analogous to the 'reversal twins' observed by Krauss and Cohen [3] and Krauss [37] during the recovery of reversed austenite in Fe - Ni alloys. In the present case the twins may form below the A_f temperatures, by the recovery of regions which have already retransformed to austenite, because of the higher temperature necessary for the reversion of stainless steels. Furthermore, the lower SFE (and consequently greater tendency to form stacking faults) in the present alloys would increase the probability of the formation of these reversal twins since a deformation twin can be created by the motion of partial dislocations [100]. For example, if a Shockley dislocation of burgers vector $\frac{a}{6}[11\bar{2}]$ moves across each (111) plane in an f.c.c. crystal the stacking sequence would change from ABCABC to CBACBA. Thus it is possible to imagine the formation of reversal twins from stacking faults on adjacent planes and the great similarity in the appearance of the two structures is in agreement with this

suggested mechanism. The contrast effects produced by the twins in the electron microscope suggest that they are extremely thin and the considerable length of the twins shown in FIG. 4.13. is thought to arise because of the extremely small differences in orientation between adjacent reversed austenite regions.

Nakayama et al [101] have reported the formation of small twins (microtwins) in tungsten after annealing the cold-worked structure at temperatures as low as 400°C; they became more frequent and more pronounced at 700°C. The twinning plane was found to be $\{112\}$ and, although the structure is b.c.c., stacking faults were observed in this material after heating above 2000°C. These were also on the (112) planes and a value for the SFE of 14.5 ergs/cm^2 was estimated from extended partial dislocation measurements. Thus there seems to be some similarity with the present case even though the crystal structures are different.

The smaller size of the twins in reversed austenite in Alloy B is, again, thought to be connected with the greater deformation of the reversed regions in this alloy.

Thus, it is suggested that the observed reversal twins result from recovery processes in the reversed austenite and are not formed by shears involved in the reverse transformation.

5.3.2. Reversion of Specimens Transformed to Martensite by Deformation

(i) Transformation temperatures. The results of the isochronal reversion treatments on the deformed specimens, as shown in FIGS. 4.25. and 4.31., suggest that the A_s and A_f temperatures are not influenced to an appreciable extent by the nature of the martensite (i.e. whether produced by quenching or by deformation). However, the results have been replotted in FIG. 5.1. to show more clearly the influence of prior deformation on the reverse transformation. The progress of the

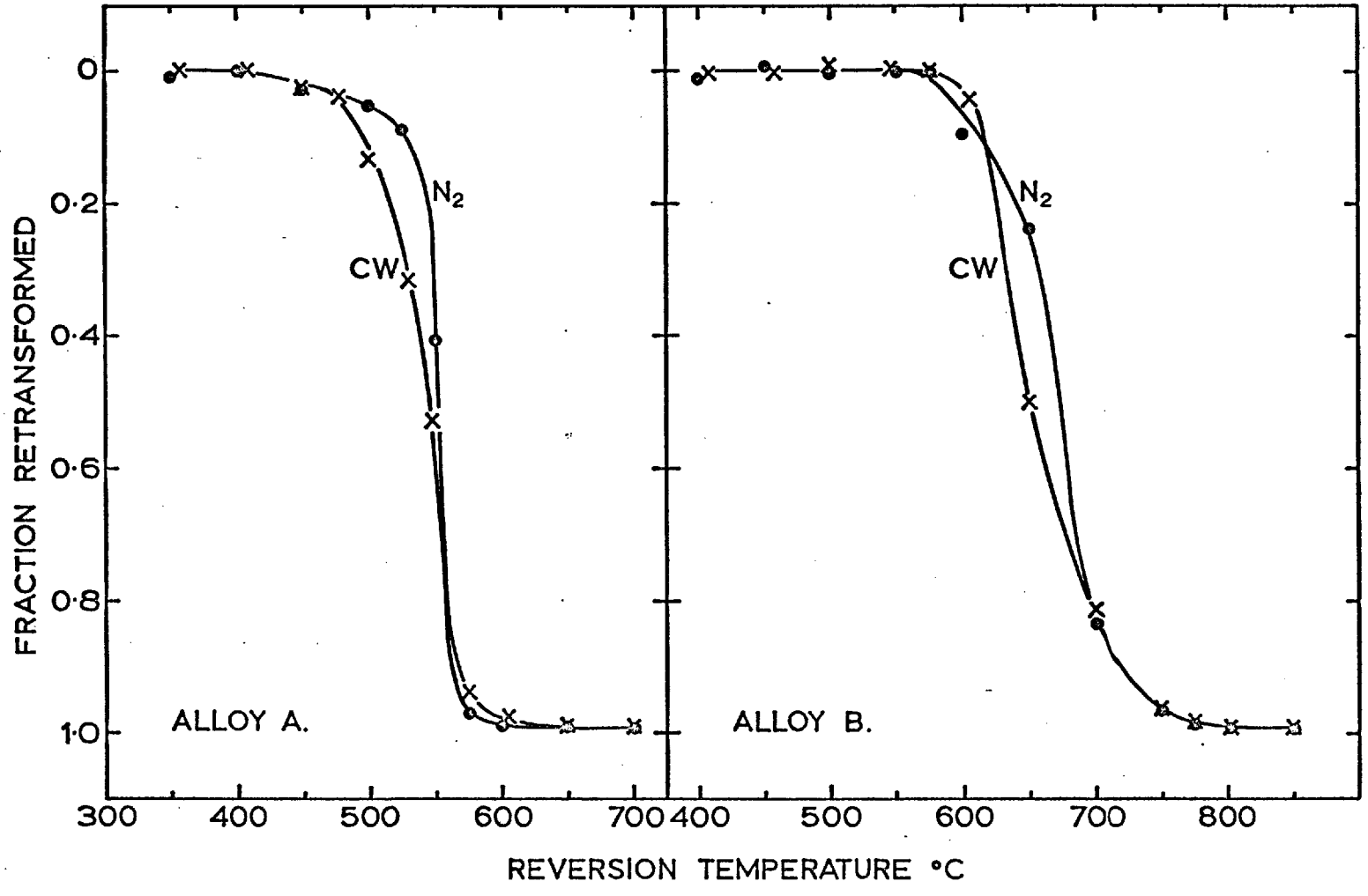

FIG. 5.1. Alloys A and B: Comparisons of the progress of transformation to austenite of martensite produced either by quenching to -196°C or by deformation at room temperature.

reverse transformation is indicated by the fraction of martensite retransformed to austenite as a function of the reversion temperature so as to eliminate the difficulties involved in comparing transformations in which different volume fractions of martensite are participating.

It is difficult to draw conclusions from the results but there is some suggestion that, in Alloy A, the initial slight reversion which takes place below about 475°C is the same in both cases although the retransformation then develops more quickly in the deformed specimens up to 555°C. Above this temperature there is almost no difference between the two sets of specimens. The reverse transformation in deformed specimens of Alloy B, appears to be slightly retarded relative to quenched specimens in the initial stages but then proceeds more rapidly up to about 675°C, above which the curves are indistinguishable.

Previous investigations (Section 2.6.) suggest that the initiation of retransformation is delayed in deformed specimens when this occurs by a diffusionless transformation. In the case of Alloy A the greater retransformation in the cold-worked specimens between 500 and 550°C may be due to an increased contribution from diffusion-controlled processes which may be enhanced in the cold-worked structure. At higher temperatures, where a diffusionless mechanism is thought to dominate the reversion process, the almost negligible difference between the two curves suggests that this mechanism has been unaffected by the deformation processes.

The slight suggestion of the stabilisation of the reverse transformation in Alloy B cannot be regarded as definitely established in view of the small number of experimental points in the region of the A_s temperature. Furthermore, the deformed specimens contain almost four times the martensite content of the quenched specimens and, as the distribution and morphology of the martensite will be different, a direct comparison between the two may not be justified.

(ii) Structural changes. Two main features are observed on heating the deformed alloys into the temperature range of the reverse transformation, namely twins and small recrystallised grains.

Twins were not observed in the as-cold-worked structure and so they must be considered to arise during the reversion treatments. This view is supported by the fact that the twins themselves (FIGS. 4.27., 4.28., 4.33. and 4.35.) do not appear to be deformed as would be likely if they were present during the actual cold-working process. The relative misalignment of the twins on the $(1\bar{1}\bar{1})_\gamma$ planes in FIG. 4.35. can be explained in terms of the 'bending' of these planes within the deformed austenite grain.

However, it is not possible to say whether these twins have been produced by the reverse martensite transformation from regions which were originally martensitic or whether they have formed merely in the deformed austenite regions. In the latter case they may represent an early stage of recovery in an analogous way to the reversal twins observed in the reversed austenite formed in the 'quenched martensite' alloys.

It would, presumably, be quite straightforward to resolve this problem by examination of specimens which had been heavily cold-worked above the M_d temperature and subjected to similar 'reversion' treatments (i.e. by identical treatments of deformed austenite specimens containing no martensite).

The appearance of small recrystallised grains in the reversed samples is to be expected in these heavily deformed specimens. The higher temperature at which the recrystallised grains were first observed in Alloy B may be due merely to the shorter time of the reversion treatments in this alloy (1 minute compared to 2 minutes for Alloy A) or it may be connected with the difference in composition of the alloys, the temperatures of the reverse transformation, or actual differences

in the deformed austenite sub-structure arising from any difference in SFE. It is not clear whether recrystallisation begins in regions of reversed austenite or deformed austenite (i.e. regions which were, and were not, originally martensitic). The former might be expected to possess a more highly imperfect structure than the latter, because of the action of the reverse martensite transformation, and thus provide regions of higher stored energy to act as the driving force for the recrystallisation process.

5.4. ANNEALING BEHAVIOUR:

5.4.1. Annealing Mechanism:

The driving force for the annealing processes, recovery and recrystallisation, is provided by the stored energy of the cold-worked structure and is equal to the difference in free energy between the deformed and annealed states. It is difficult to make a sharp distinction between the processes of recovery and recrystallisation but it is suggested [102] that the former constitutes all those annealing phenomena which occur before the appearance of new strain-free recrystallised grains whereas recrystallisation involves the nucleation and growth of these new strain-free grains and the gradual consumption of the cold-worked matrix by the movement of large angle grain boundaries.

In the case of the annealing of the reversed austenite structure in Alloy A, it is suggested that the attainment of the original annealed structure occurs largely via a recovery mechanism and involves the process of recrystallisation to a small extent only. Evidence for this suggestion comes both from structural observations and kinetic studies. FIGS. 4.42. to 4.46. show that there is no indication of the movement into the reversed austenite of large angle grain boundaries which might have formed between strain-free and deformed regions. On the contrary, it appears that there is a continuous development of dislocation interactions and annihilations within the reversed austenite laths. Consequently, the final structure consists of annealed austenite grains which are essentially unchanged in size, shape and orientation relative to the solution treated material.

The 'recovery' of a property increment due to cold work during annealing shows a different time dependence according to whether a recovery or recrystallisation mechanism is involved [102]. The decay during recovery is most rapid at short times, with no incubation period, and at longer annealing times the rate of decay decreases; i.e. an

exponential decay curve. An incubation period is, however, exhibited by a recrystallisation process during which time the property increment remains appreciably constant but then falls very rapidly. Interpretation of the hardness changes during the annealing of the reversed austenite structures (FIGS. 4.38. and 4.40.) suggests, therefore, that there is a very significant contribution from recovery mechanisms. The overall impression is that recovery and recrystallisation may be simultaneously competing mechanisms in the annealing process rather than recovery being completed before the beginning of recrystallisation. The indications of recrystallisation are clearest at the higher annealing temperatures and for the 'direct' treatment (FIG. 4.38.) rather than the 'standard' reversion (FIG. 4.40.).

These facts can be explained on the basis of competition between the two mechanisms; when recovery and recrystallisation occur together the driving force for recrystallisation is not a constant [103] but continuously decreases and produces a retardation of the recrystallisation. This effect is greatest at lower annealing temperatures because, in general, recovery processes proceed with lower activation energies than those for recrystallisation and low temperature anneals therefore favour recovery and hence retard recrystallisation. The standard reversion treatment has permitted some recovery prior to the annealing treatment, thus lowering the stored energy of the defect structure and hence the likelihood of recrystallisation in these 'standard' specimens. The time for complete 'recovery' at a given annealing temperature is, therefore, longer for the 'standard' than for the 'direct' samples.

The greater separation between the two mechanisms in the case of the deformed austenite (FIG. 4.47.) is commonly found for lightly deformed materials [103].

The apparent difficulty involved in the initiation of the recrystallisation processes is probably connected, to a large extent, with the release of the stored energy of the reversed austenite laths by recovery process but may also be connected with the observation [104] that a material where all the grains or sub-grains are misoriented only a little from one another has more difficulty in recrystallising than one that does not. The reverse martensite transformation has been shown to produce reversed austenite regions which have very similar orientations both to each other and to the retained austenite.

The question remains of how the 'recrystallisation' process actually occurs, especially as no high angle boundary movement is observed. One possibility which appears to satisfy the known facts is that of 'recrystallisation in situ' [104] which is basically a process of sub-grain coalescence. When dislocations leaving a disappearing boundary between coalescing sub-grains annihilate dislocations of opposite sign in the surrounding boundary, the misfit angles of these surrounding boundaries are reduced. No high angle boundary segment would then be formed and no reorientation would occur on recrystallisation.

Thus, there is no clear distinction between the recovery and recrystallisation processes; indeed, according to the 'high angle boundary' definition of the latter, no true 'recrystallisation' process actually takes place.

Summarising the structural changes occurring during annealing, it seems probable that recovery begins with a removal of point defects (mainly vacancies); dislocations may participate in the early processes by acting as sinks and executing small-scale re-arrangements. Micro-twins and stacking faults disappear and dislocations tend to re-arrange themselves on a large scale, eventually forming distinct sub-grain boundaries. Further annealing produces dislocation interactions and annihilations, presumably involving glide and climb processes, and a reduction in the dislocation density. Although some sub-grain boundaries

contain dense dislocation tangles, there is a progressive tendency towards a more regular structure and distinct networks are formed. The boundaries become less pronounced and ultimately fade away, in agreement with the proposed coalescence mechanism [105].

In the case of the 'cold-worked and reversed' specimens which were annealed at 850°C the decrease in hardness with annealing time (FIG. 4.48.) is almost certainly due entirely to a grain size effect since it has been shown (FIG. 4.49.) that the structure is fully recrystallised after only a 2 minute annealing treatment. The extremely rapid rate of recrystallisation in these specimens can be attributed to the much greater stored energy per unit volume of the structure; although it contains 10% 'reversed' austenite compared to 15% in the 'standard' structure (even this may itself be more highly imperfect in the present case) the remaining regions are of austenite which has been deformed by 50% as opposed to a fully annealed retained austenite matrix in the 'standard' structure.

The zig-zag boundary, displaying fringe contrast, in FIG. 4.49. may be a twin boundary partly parallel to (111) and partly parallel to (110) as described by Whelan et al [106].

5.4.2. Activation Energies:

The apparent activation energy for the annealing out of 'reversed austenite' produced both during heating to the annealing temperature and by a standard treatment before annealing was found to be approximately the same in each case, namely about 80 Kcal/mole. This figure cannot be identified with a single thermally activated process, especially as recovery and 'recrystallisation' processes have been shown to be operating simultaneously. However, a value of 80 Kcal/mole is only **slightly** higher than the activation energy [107] for diffusion of nickel in f. c. c. iron-chromium alloys. No values have been found for the diffusion of chromium in austenitic ferrous alloys but it seems likely that the rate determining process during 'recovery' is atomic diffusion.

5.5. AGEING BEHAVIOUR:

5.5.1. Morphology and Structure of Precipitate:

Examination of specimens of Alloy B by transmission electron microscopy after ageing at 650°C and 700°C has revealed the presence of precipitate particles of several different morphologies. These include grain boundary precipitates, 'laths' (FIGS. 4.53. and 4.55.), more angular particles (FIG. 4.54.), stringers (FIG. 4.56.), 'cubes' (FIGS. 4.57. and 4.58.), and elongated particles (FIG. 4.61.). In many cases the precipitates were positively identified as $M_{23}C_6$ by selected area electron diffraction, but this was not possible with the grain boundary carbides formed at early ageing times nor with the 'lath' precipitates. However, both of these morphologies are commonly observed for $M_{23}C_6$ in austenitic steels [108, 109]. Furthermore, many studies of steels of similar composition identified only $M_{23}C_6$ [92, 109 - 114] with the one exception of Moore and Griffiths [115] who also reported the presence of Cr_7C_3; the morphology, however, was different to the present case.

In steels with higher alloy content (e.g. 20% Cr and 25% Ni) precipitates of M_6C, either Cr_3Nb_3C or $(FeNb)_3C$, have been reported [116, 117] but these steels also contained niobium and it appeared that the M_6C formed from NbC precipitates. Hence, it seems most likely that $M_{23}C_6$ is the only precipitating phase in Alloy B.

The mechanism of formation of $M_{23}C_6$ particles of various morphologies has been discussed by several authors [92, 93, 108] and it is well established that nucleation of the carbide occurs preferentially at grain boundaries, coherent and non-coherent twin interfaces, and on dislocations within the matrix. It has been suggested [108] that nucleation on grain boundaries and dislocations may occur by the segregation of the constituent atoms of $M_{23}C_6$ to boundaries and dislocations and/or by a reduction in the strain energy for nucleation

in regions of localised dilation; it was further suggested that growth may be assisted by enhanced diffusion rates of solute along grain boundaries and of carbon along dislocations.

The formation of $M_{23}C_6$ as stringers (FIG. 4.56.) has been explained [92] as the growth, on matrix dislocations, of carbide particles which, initially, have no well-defined shape but later develop as 'cubic' particles which have parallel sides and join up along the dislocation line. It can be seen that the carbides in FIG. 4.56. have sides which are almost parallel to and perpendicular to the length of the stringer, XX; the adjacent b.c.c. regions probably formed on cooling to room temperature.

Even when the matrix has retained an f.c.c. structure it is seen to contain many dislocations. This can be attributed to stresses produced by differences in both elastic modulus and atomic volume between $M_{23}C_6$ and austenite [92, 93]. A further contribution may arise from differential thermal contraction on cooling, and by deformation of the austenite adjacent to regions of martensite.

The martensite present after ageing (FIG. 4.63.) does not have the lath morphology characteristic of the solution-treated and quenched specimens but is similar in appearance to the martensites in the low carbon iron-chromium-nickel alloys [118], of slightly lower alloy content than the present alloy, which were termed 'massive'.

The carbide particles which had developed a well-defined 'cubic' shape, shown in FIGS. 4.57. and 4.58., were found to have interfaces which were perpendicular to the $\langle 110 \rangle_c$ and $\langle 111 \rangle_c$ directions respectively. This might suggest that the interfaces were of the $\{110\}$ and $\{111\}$ type. However, in the former case where the carbide particles have a $[100]_c$ zone axis, both $\{110\}$ and $\{111\}$ carbide planes intersect the (100) surface along $\langle 0\bar{1}1 \rangle_c$ directions. Thus, it is not clear from FIG. 4.57. whether the faces of the 'cube' particles consist of $\{111\}_c$ or $\{110\}_c$ planes.

The probable indices of the interfacial planes, together with the failure to observe triangular carbide precipitates, are more consistent with the almost cubic particle shape, with $\{111\}$ and $\{110\}$ interfaces, suggested for $M_{23}C_6$ particles by Beckitt and Clark [92] than the polyhedral particle shape comprised solely of $\{111\}$ interfaces which has also been reported [108, 119, 120].

$M_{23}C_6$ has a complex cubic crystal structure containing 92 metal atoms and 24 carbon atoms per unit cell. An analysis of planar atomic configurations of the carbide and austenite structures [92] suggests that $\{111\}$ are the most likely interface planes and that $\{110\}$ are more probable than $\{100\}$. The parallel orientation relationship of the two structures [92, 108], $\{100\}_\gamma$ // $\{100\}_c$ and $\langle 100\rangle_\gamma$ // $\langle 100\rangle_c$ could not be confirmed in the present case because of the subsequent transformation of the matrix to a b.c.c. structure (see next section).

5.5.2. Increase in Ferromagnetic Response:

Carbides of the type $M_{23}C_6$ are ferromagnetic, their Curie temperatures increasing as chromium atoms in the structure are replaced by those of iron [121]; thus the presence of these carbides in an austenitic matrix would give rise to a small magnetic response. Another possibility is that the formation of $M_{23}C_6$ raises the M_s of the matrix, by the removal of carbon and chromium, sufficiently to cause partial transformation to martensite on cooling to room temperature after the ageing treatment.

After ageing the solution treated alloy at 650°C for 1 hour, the small magnetic response obtained (FIG. 4.51.) is almost certainly attributable to the presence of the $M_{23}C_6$ carbides, largely at grain boundaries. The possibility of its being due to the formation of martensite is considered unlikely in this case because of the failure to observe this phase in the electron microscope and because of the unchanged specimen

hardness; the carbides are unlikely to strengthen the steel because even those in the matrix exist as a relatively small number of large particles, widely spaced. Although the M_s temperature will have been raised by the carbide precipitation, it is suggested that its value is still below room temperature.

With longer ageing times at 650°C, and after all treatments at 700°C, the solution treated alloy shows an increase in hardness as well as magnetic response; the latter being due to the presence of martensite in addition to the small contribution from the ferromagnetic carbide particles. The magnetic response reaches an almost constant value, after approximately 3 hours at 700°C and 15 hours at 650°C, which is about the same in each case and corresponds to about 4% ferromagnetic phase. The morphology and amount of carbide precipitation is known to be dependent on the matrix structure [122] and, as this is the same in both cases, it is not surprising that the same value is reached (slower kinetics being associated with the lower ageing temperature).

The work of Bendure et al [113] has shown that ageing similar steels at 700°C removes about 0.05% carbon as $M_{23}C_6$. With the accompanying removal of chromium, an increase in M_s of roughly 110°C would be expected; i.e. from -40°C to about +70°C. It has already been shown (Section 4.1.) that, with an M_s of -40°C, cooling Alloy B to -196°C produces only about 12% martensite; therefore, raising the M_s by the amount suggested because of matrix depletion of carbon and chromium can account for the observed content of about 4% martensite on cooling to room temperature, say 20°C.

The abrupt increase in magnetic response found after prolonged ageing of the 'solution treated' alloy at 700°C, and at shorter times in the 'reversed' alloy at the same temperature, (FIG. 4.52.) is not so easily explained on the basis of matrix depletion. In particular, it is difficult to account for the fact that the magnetic response remains appreciably

constant for some time before this pronounced increase occurs, as the development of precipitation processes would be expected to produce a steady increase in response with ageing time.

It is suggested that the observed increase in magnetic response with longer ageing times in these structures is due to the transformation of austenite to ferrite by a nucleation and growth process. The removal of carbon and chromium from the matrix has not only raised its M_s temperature but may also have changed its equilibrium structure from austenite alone to (austenite + ferrite). In the solution treated condition, the composition of Alloy B (FIG. 1.1.) lies very close to the $\gamma / (\gamma + \alpha)$ phase boundary. While $M_{23}C_6$ almost certainly contains some molybdenum, as $(Cr\ Fe\ Mo)_{23}C_6$, a substantial amount of this ferrite-promoting element will undoubtedly remain in the matrix and, together with the removal of the austenite-forming carbon, cause the equilibrium matrix structure to become $(\gamma + \alpha)$.

Supporting evidence for a transformation to an austenite/ferrite structure comes from the electron microscopy observations of b.c.c. matrix structures (e.g. FIG. 4.57.) which do not have the appearance of martensitic regions, and the apparently unchanged content of the latter with increased ageing times. A possible consequence of this transformation may be the formation of additional carbide particles since it is well-known that the presence of (delta) ferrite in an austenitic matrix causes an acceleration of carbide precipitation [113] and that a ferrite-austenite interface is a preferred site for precipitation [10]. Furthermore, the formation of such carbides would further reduce the stability of the austenite ahead of the interface. This may account for the frequent observation of relatively small 'cubic' carbide particles in a b.c.c. matrix after the longer ageing treatments. Alternatively, the formation of the 'cubic' carbides in austenite in the solution treated alloy after long ageing times may provide the additional motivation

required for transformation to ferrite. These carbides might be nucleated on dislocations produced in the austenite around growing precipitates (at grain boundaries and twin interfaces) because of the difference in atomic volume between the precipitate and matrix lattices.

5.5.3. Influence of the Initial Sub-Structure:

The morphology of the precipitate particles which formed in the solution treated alloys has been found to be consistent with the observations of other workers on similar alloys. The attainment of a plateau in the magnetic response readings is taken as an indication that all the immediately available preferential sites for the nucleation of carbides in the solution treated samples (grain boundaries, twin interfaces and occasional matrix dislocations) have been filled. The fact that the height of the plateau is the same at both ageing temperatures is consistent with there being no difference in the initial matrix conditions. The subsequent increase in magnetic response due to the formation of ferrite after prolonged ageing at 700°C is accompanied by the appearance of 'cubic' $M_{23}C_6$ particles although it is not clear which of these effects is responsible for the other.

Ageing the 'quenched and reversed' structure at 700°C for short ageing times produced carbide precipitation at the same type of sites as in the solution treated samples which had been similarly aged. The structural observations are supported by the close similarity between the two magnetic response curves at short ageing times. With longer ageing times, extensive precipitation occurs on the defect sub-structure of the reversed austenite laths. No twins were observed in the reversed austenite; this may be related to the findings of Mazza [111] who found that $M_{23}C_6$ formed on deformation twins in austenite and that the twins became less numerous as ageing proceeded.

Matrix depletion of carbon and chromium in the reversed regions due to extensive carbide precipitation, together with the possibility of more favourable conditions for diffusion in the deformed structure, produced earlier transformation to ferrite than in the solution treated samples. The ferrite/austenite interfaces may, again, provide preferential sites for further carbide nucleation. The less well pronounced 'cubic' shape of the precipitate particles in FIG. 4.59. may be a result of the highly deformed nature of the reversed austenite structure in which they are growing.

The elongated particles of $M_{23}C_6$ shown in FIG. 4.61. might be considered as a variation of the 'cubic' particles where growth has developed preferentially in one direction.

Carbides are formed at very early ageing times in the 'cold-worked and reversed' structure and are clearly visible after only 1 hour at 700°C (FIG. 4.62.). The extremely high rate of precipitation of $M_{23}C_6$ in cold-worked austenite in a steel containing 17% Cr, 7% Ni and 0.11% C has been reported by Bendure et al [113]. The rate of removal of carbon by carbide precipitation at 675°C was found to be greater by more than a factor of ten in deformed specimens, as compared to solution treated samples.

Hatwell and Berghhezan [119], who employed a Type 316 steel, found precipitation of $M_{23}C_6$ within grains only after 20% plastic strain. The difference between their results and those of Garofalo et al [114], is almost certainly due to the two-stage ageing treatment used by the latter. The initial treatment at 480°C nucleated carbides at dislocations and the subsequent treatment at 705°C allowed these to grow [123]. Hatwell and Berghhezan aged their specimens at 750°C after plastic deformation, a temperature too high for nucleation on dislocations, unless the dislocation density is quite high [123].

Transformation to ferrite is similarly more rapid, probably as a direct result of the enhanced rate of carbide precipitation. The relative merits of regions of deformed austenite and those of reversed austenite as preferential sites for precipitation could not be assessed as it was not possible to differentiate between such regions in these specimens. It would appear, however, that the 'cold-worked and reversed' structure is superior in these respects to the 'quenched and reversed' structure.

The failure of the carbide particles to develop well-defined planar interfaces with the heavily cold-worked matrix is in agreement with the observations of other workers [110, 112].

5.6. STRENGTHENING:

In most cases indications of specimen ~~length~~ strength, following the various heat treatments, were gained solely from measurements of hardness. A hardness test does not measure a well-defined property but represents the resistance of the material to indentation which will be a combination of the yield stress, the rate of work hardening and, to a lesser extent, the elastic modulus (through its influence on elastic recovery).

5.6.1. Solution-Treated Specimens:

The fully austenitic specimens of Alloys A and B had approximately the same grain size after solution treatment and no significant difference in the dislocation density or in the frequency of annealing twins in the two alloys was apparent. The difference in the hardness of Alloys A and B in this condition (HV = 100 and 145, respectively) must, therefore, arise from their different compositions (Section 3.1.).

The lower chromium and nickel contents of Alloy B, relative to Alloy A, would be expected to contribute a smaller solid solution strengthening effect and suggests, therefore, that the higher hardness of the former is derived from the presence of molybdenum and carbon in this alloy. However, the effect of molybdenum in solution is comparable to that of nickel and chromium and would, thus, be expected merely to compensate to some extent for the lower Ni and Cr contents of Alloy B. Hence, it appears that the carbon content of this alloy is the main factor responsible for its higher hardness value, possibly involving the formation of Cottrell 'atmospheres' around dislocations.

A further explanation for the higher hardness value of solution-treated specimens of Alloy B may arise from the greater tendency of this alloy to undergo partial transformation to martensite during deformation (Section 4.3.). It is possible that plastic deformation during hardness testing may induce some local transformation and thus increase the

resistance of the specimen to indentation. Magnetic measurements on small specimens which had received ten hardness indentations did not detect the presence of martensite; but the bulk martensite content of the specimens may have been below that which can be measured by the present technique, namely about 0.1%.

5.6.2. Martensitic Specimens:

The structure of martensite in stainless steels has been shown to consist of many individual 'grains' of α', associated with small regions of ε martensite, within 'laths' bounded by $\{111\}_\gamma$ planes. The α' grains are not internally twinned but contain a high dislocation density.

The strength of the martensite can be divided into two separate contributions; firstly, the strength of the b.c.c. ferrite structure of the same composition (which will include solid solution hardening effects) and, secondly the hardening contributed by the sub-structure produced by the martensitic transformation. The sub-structure strengthening will include the effects of both the small size of the individual α' grains, and their high internal dislocation density.

The structure of individual grains of α' in the present alloys is similar to that of the 'massive' martensites in the low-carbon Fe - Cr - Ni alloys studied by Floreen [118] and in the Fe - Ni alloys studied by Speich and Swann [124]. In both these cases the authors concluded that the major hardening component was solid solution hardening. The relative effects of solid solution hardening in the austenitic specimens of Alloys A and B have already been discussed in the previous section and similar arguments will be valid for the b.c.c. structures. The low transformation temperature in Alloy B will tend to prevent the development of 'auto-tempering' of the martensite in this alloy and carbon is unlikely to cause the formation of precipitates but will rather segregate to dislocation sites, as previously described.

No difference in the sub-structures in the two alloys was obvious (i.e. dislocation densities and α' grain size) and it seems probable that the contribution to strength from this source will be same per % α', in each case.

In the absence of direct indications of the strength of the actual martensite laths by microhardness measurements, this must be estimated from the overall hardness of the partially martensitic samples. A 15% α' content in Alloy A increases the hardness value from 100 to 175, whereas $12\frac{1}{2}$% α' in Alloy B raises the hardness to 190 compared with a solution-treated value of 145. Remembering that the retained austenite is apparently unaltered by the direct transformation to martensite in these alloys, there seems to be no evidence for a substantially higher hardness value of the carbon-containing martensite in Alloy B.

The relatively high hardness of the specimens in which martensite has been produced by deformation is expected because the 'retained austenite' in these specimens is, of course, highly deformed and has been shown to have a banded structure containing a high dislocation density. The martensite itself in such specimens may possess a more complex sub-structure which will contribute additional strengthening and the much higher content of this phase in Alloy B (relative to specimens of Alloy A deformed the same amount) is considered to account for the overall higher hardness value measured for this alloy, namely HV = 465 compared to 320 for Alloy A.

5.6.3. Reversion Treatments:

The increase in specimen hardness which was observed at about 500°C during the reversion treatments on quenched specimens of Alloy A (FIG. 4.6.) is not readily explained. A small decrease in the martensite content was produced by treatment at this temperature and one might expect an accompanying decrease in the hardness value instead of this

(reproducible) increase. Perhaps holding for 2 minutes at around 500°C permits solute diffusion to preferential sites on dislocations, although the very low interstitial content of this alloy suggests that this is not likely to be a large effect. Treatment at higher temperatures produces a drop in hardness which corresponds to the retransformation of martensite to austenite; the hardness remains constant once the reverse transformation is complete. The hardness plateau between 600°C and 700°C suggests that no appreciable recovery of the reversed austenite occurs during holding for 2 minutes at these temperatures. The fall in hardness at higher temperatures is associated with the removal of the defect structure of the reversed austenite by a 'recovery' process previously described (Section 5.4.1.)

During the reversion of deformed specimens of Alloy A (FIG. 4.25.) the small increase in hardness measured after treatment at 450°C may not be significant; alternatively, it may be attributable to causes mentioned above. The hardness decrease between 450°C and 600°C is attributable partly to the reversion of martensite to austenite, and partly to the beginning of recrystallisation of the deformed austenite (for example, see FIG. 4.29.). The rate of hardness drop is reduced, briefly, as the temperature of the isochronal treatment is raised above the A_f but then increases again as the deformed austenite structure becomes increasingly 'unstable' as the temperature is raised further. In these specimens, annealing-out of the deformed structure takes place by the more usual mechanism of the formation of strain-free regions and their growth into the deformed matrix.

The comparable results for quenched specimens of Alloy B (FIG. 4.18.) can be similarly explained; the hardness peak obtained after 2 minutes at 500°C can more easily be attributed to diffusion of solute atoms, particularly carbon. Carbide particles were not visible in specimens treated between the A_s and A_f temperatures (see Section 4.2.7.) and it is probable that this small hardening effect is due to the clustering of

solute atoms around dislocations in the martensite.

The more marked initial hardening effect in the deformed specimens of Alloy B may be attributable to the greater martensite content in which this dislocation pinning effect can take place and, possibly, to the presence of a high density of dislocations in the austenite which can similarly be pinned. Enhanced diffusion rates in the deformed structure may also lead to this more pronounced effect. Softening begins well before the reverse transformation takes place and is associated with recovery and recrystallisation of the deformed austenite. The apparent hardness plateau just above the A_f temperature is not easily explained; a reduction in the rate of decrease of the specimen hardness might be expected once the martensite is fully retransformed but the process of recrystallisation would be thought to develop to a greater extent as the reversion temperature is raised. At still higher temperatures the softening process occurs very rapidly and the hardness value falls to 195 after 1 minute at 905°C from an initial value of 465.

The strength (hardness) of the 'standard' reversed austenite specimens, produced by heating partially martensitic (quenched) samples for 2 minutes at 600°C and 1 minute at 775°C for Alloys A and B respectively, is attributed to the defect sub-structure which is present in these specimens. The high dislocation density, together with the presence of stacking faults and reversal twins, in the laths of reversed austenite will act as barriers to the movement of dislocations. It seems likely that the dislocation density in the reversed austenite is comparable to that in the α' grains, although no actual measurements were made, and the 'block size' of the reversed austenite regions appears to be similar to the α' grain size, at least in Alloy A. The lower hardness of the reversed austenite may, therefore, be associated with the fact that the 'blocks' of reversed austenite have the same crystal structure as the retained austenite and differ in orientation from each other and from the

retained austenite, only to a very small extent. However, factors such as the relative magnitudes of the lattice friction stress and the solid solution hardening effect in the b.c.c. and f.c.c. structures may also be involved.

It is not possible to detect any significant differences in the strengthening of reversed austenite in the two alloys. The results of FIG. 4.15. suggest that the longer reversion treatment used for Alloy A does not affect its hardness which would, thus, have been the same (155) if a 1 minute reversion treatment had been used as for Alloy B. The relatively small overall hardness increase produced in the austenite (Alloy A, 100 to 155 and Alloy B, 145 to 170) is attributed to the relatively small amount of martensite present and to the failure of the direct and reverse martensite transformations to produce substantial deformation in the retained austenite.

5.6.4. Annealing of Reversed Austenite:

Hardness changes during the annealing-out of the defect structure produced by the reverse martensite structure have already been discussed, to some extent, in Section 5.4.1. In quenched and reversed specimens of Alloy A (FIGS. 4.38. and 4.40.) the initial hardness drop after short annealing treatments is due to the removal of stacking faults and reversal twins and to the rearrangement of dislocations to produce sub-grain boundaries. Further annealing causes an additional decrease in the hardness as dislocation rearrangements and annihilations continue, reducing the overall dislocation density and the miscrientation between adjacent regions (blocks) of reversed austenite. The structure will offer progressively less resistance to the movement of dislocations and the hardness returns to that of the original austenite as the reversed austenite laths finally disappear.

In the cold-worked and reversed specimens, the hardness changes observed during annealing at 850°C (FIG. 4.48.) are due merely to an increase in grain size as the annealing time is increased since the structure is fully recrystallised (FIG. 4.49.) after only 2 minutes at this temperature.

5.6.5. Ageing Treatments:

The small increase in hardness (about 15 HV) which is observed after ageing solution-treated specimens of Alloy B at 650°C for between 10 hours and about 100 hours, and at 700°C for between 1 hour and 50 hours (FIG. 4.51.) is attributed almost entirely to the formation of about 4% of martensite in these specimens on cooling. The appearance of small amounts of martensite in these specimens has already been explained (Section 5.5.2.). The contribution to the hardness of these specimens by the carbides which have formed at grain boundaries and as 'laths' within the grains is considered to be very small because of their unfavourable size and distribution. The additional increase in hardness which develops in the solution-treated specimens after ageing for more than 100 hours at 700°C can be attributed partly to the formation of a finer distribution of small angular particles of $M_{23}C_6$ in the matrix, and partly to the partial transformation of the austenite matrix to ferrite. The effective grain size may be reduced by the formation of a two-phase matrix structure; dislocations are also present and may have formed by differential thermal contraction effects on cooling and by the growth of the carbide precipitates in the matrix. Some contribution to the overall hardness will be derived from the small areas of martensite which also exist in these specimens.

The hardness changes observed on ageing the quenched and reversed specimens for up to 8 hours at 700°C (FIG. 4.52.) are due, essentially, to the same causes as the solution-treated specimens which have been similarly aged except that the overall hardness is higher in the former specimens because of the strengthening contribution from the reversed

austenite laths. The increased hardening effect after treatments longer than about 10 hours is attributed to the development of carbide precipitation on the dislocation sub-structure of the reversed austenite accompanied by partial transformation of the matrix to ferrite.

In cold-worked and reversed specimens extensive precipitation of carbides occurs in the highly deformed austenitic matrix at very short ageing times, as also does the formation of ferrite. These contributions to the strengthening of the specimens help to offset the softening effects of the recovery and, perhaps, recrystallisation of the deformed austenite, so that only a small softening effect is produced by ageing for as long as 120 hours at 700°C. There is some evidence to suggest that carbide precipitation retards the development of recrystallisation processes and, hence, softening in these specimens.

5.7. TRANSFORMATION CYCLING:

The results shown in FIGS. 4.65 and 4.66. indicate two distinct features of transformation cycling in both alloys; firstly, there is an increase in strength in both the austenitic (reversed) and partially martensitic (quenched) conditions, and secondly, progressively smaller volume fractions of the specimens are undergoing the direct and reverse transformations as the number of cycles increases, i.e. stabilisation occurs. The strengthening will depend to some extent on whether successive generations of martensite form, on quenching, in regions of reversed austenite or retained austenite. No structural observations have yet been made to resolve this question, although such an investigation is presently in progress in this Department, and so the stabilisation phenomena will be discussed first, including a consideration of the likely sites for the formation of subsequent martensite regions.

5.7.1. Stabilisation:

Stabilisation phenomena appear to be divisible into two categories; mechanical stabilisation and thermal stabilisation. The former is associated with deformation of the austenite prior to transformation while the latter is observed when the transformation to martensite is interrupted in the transformation range and is characterised by the failure of the transformation to begin immediately the cooling is resumed.

Mechanical stabilisation of austenite by deformation of the austenite has been attributed to the hindrance of the propagation of the martensite by the tangled dislocation networks produced by the deformation [15]. The influence of the defect structure of austenite on martensite formation was investigated by Sastri and West [125] who concluded that it had a marked influence on transformation kinetics; the importance of the strength of the austenite has also been emphasised by Friestner and Glover [126] and by Jordan and Borland [47].

Similarly, the defect structure of reversed austenite would appear to be responsible for the widely reported stabilisation of austenite, after the reverse martensite transformation (see Section 2.8.). The only results which do not appear to support this view are those of Krauss and Cohen [3] where no appreciable stabilisation was found in iron-nickel alloys after reversion; the stabilisation reported by other workers in these materials (e.g. Ref.36) was attributed [44] to their slower heating rates which may have produced compositional changes in the martensite; namely, the formation of low nickel ferrite accompanied by nickel enrichment of the austenite.

The present results for Alloy A, which are in complete agreement with the results of Breedis [8] following a single reversion cycle in an almost identical alloy, cannot be attributed to compositional changes since it has been shown (Chapter I) that the equilibrium phase is austenite alone, the heating rate employed is very rapid and is equivalent to that used by Krauss and Cohen [3, 44], and the interstitial solute content is negligible. These observations support Breedis's conclusion that the defect structure in the austenite, and not solute redistribution, is behind the stabilisation of the transformation. Further supporting evidence comes from the very close correlation of the present results on the 'annealing-out' of the defect structure of the reversed austenite (Section 4.4.) and the tendency for a reduction in the magnitude of the stabilisation phenomenon as the temperature of reversion was increased above the A_f and with longer time at a particular temperature. For example, Breedis's results indicate that stabilisation would be completely absent after a reversion treatment of 2 hours at about 850°C and the present work (FIG. 4.38.) shows the almost complete 'recovery' of the austenite after such a treatment.

It must be remembered that, after one cycle, Alloy A contains over 80% of 'retained austenite' which still has a very close resemblance to fully annealed austenite. In the absence of direct structural observations it is impossible to say whether the second generation martensite has formed in the reversed austenite, albeit to a lesser extent, whether entirely in 'fresh' regions of retained austenite or in both. Thus, there is no indication of whether the actual regions of retained austenite have become fully or only partially stabilised with regard to transformation on quenching to -196°C. Furthermore, the results do not indicate the nature of the stabilisation; namely, to what extent it is characterised by a depression of the M_s temperature and/or an alteration in the transformation kinetics. It seems probable that both factors will be affected.

Earlier work by Breedis and Robertson [23] found that after reversion for 15 minutes at 900°C (eliminating stabilisation effects) subsequent transformation occurred at the identical sites of the previous transformation, showing the very pronounced heterogeneous nature of the martensite transformation and, presumably the survival of the martensite 'embryos' after reversion. Hence, there is some slight suggestion that second generation martensite might form in the regions of reversed austenite which can be considered to still contain the martensite embryos which participated in the first direct transformation.

Reversion of the second generation martensite (for 1 minute at 600°C, Alloy A) would produce an intensification of the defect structure of the reversed austenite and a consequently greater stabilisation effect, assuming that the martensite has formed in the reversed austenite. Alternatively, if the martensite had formed in retained austenite, additional areas of 'fully stabilised' reversed austenite will be produced. Thus, in either case, progressive stabilisation would be produced by increasing the number of transformation cycles.

In Alloy B the situation is again more complicated by the presence of carbon; although extensive carbide precipitation can produce transformation to ferrite (see Section 5.5.) in this alloy, it is considered that the short reversion time of 1 minute together with the rapid heating rate employed and the absence of extensive precipitation will make such a possibility extremely unlikely. Magnetic measurements made after the reversion treatments confirmed that, within the limitation of the apparatus, no ferromagnetic phase was present in the samples.

No evidence for precipitation was found by electron microscopy in reversed austenite formed by one transformation cycle in Alloy B (see Section 4.2.); thus, it must be concluded that the mechanism of stabilisation is essentially the same as in the case of Alloy A. Any slight, but undetected, precipitation would be further developed on subsequent cycling and, via a purely chemical effect, may account for the slower progressive increase in stabilisation with increasing transformation cycling than was found for Alloy A. Another possibility is that the higher reversion temperatures used for Alloy B permitted more extensive recovery of the defect structure of the reversed austenite with a corresponding reduction in its capacity for stabilisation.

Any possible stabilisation of the reverse transformation of second and subsequent generation martensite to austenite was not detected by the present investigation. Certainly, the A_f temperatures were not raised above 600°C and 775°C for Alloys A and B respectively, as was shown by magnetic measurements after successive cycles.

5.7.2. Strengthening:

After the first quench to -196°C both alloys contain laths of martensite in a matrix of more than 80% retained austenite which has already been shown to be essentially the same as fully annealed austenite. On second and subsequent quenching to -196°C a smaller amount of

martensite is produced, yet the hardness increases due to the presence of some reversed austenite as well as the retained austenite. The amount of reversed austenite present on quenching for a second time may be equal to the amount of martensite which formed during the first cycle, if the second generation martensite formed in regions of retained austenite, or it may equal the difference in the amounts of martensite formed on the successive quenches, if the martensite forms in regions of reversed austenite. The reversed austenite content may, of course, also lie anywhere within these two extremes.

In the case of Alloy A, after further reversion there will either be an additional amount from that present after the previous cycle but with the same defect sub-structure (ignoring any slight recovery on heating the reversed austenite which had remained untransformed during quenching) or the same amount as previously but with an increasingly complex sub-structure. Either of these two extreme cases could account for the progressive increase in hardness observed after successive reversion cycles. The levelling off in the hardness increase is attributable to the decreasing amounts of martensite participating in the reverse transformation.

The constant value of the hardness of quenched specimens of Alloy A after the first cycle is taken as an indication of a balance produced between contributions from the decreasing amount of martensite present and either progressively increasing amounts of reversed austenite or a progressively increasing strength of the same volume of reversed austenite.

A further complication may arise from the fact that martensite formed from reversed austenite may itself be stronger than that formed from annealed (retained) austenite. This does not alter the qualitative explanation advanced for the observed hardness changes. The larger

proportional increase in the hardness of the 'austenitic' rather than the 'martensitic' condition is in agreement with the observations of Krauss and Cohen [3] for Fe - Ni alloys. However, in the present case, there is less tendency for the hardness of the 'reversed' condition to level off after the second transformation cycle; this may be due to the fact that far greater areas of retained austenite are available for strengthening.

Similar explanations can be used for the results obtained for Alloy B. In this case, however, the less well developed progression of stabilisation with increased cycling permits larger amounts of martensite to participate in the later transformations. This results in a more continuous increase in hardness in both the 'martensitic' and 'austenitic' conditions; in the case of the former, the hardness balance between martensite and reversed austenite which was suggested for Alloy A is now lost. Any contribution to the hardness from carbide precipitation would be exhibited by both conditions and it is not possible to say whether or not the continuous hardness increase is partly attributable to progressive precipitation during cycling or entirely due to the larger amounts of martensite still available for reversion.

The strengthening of austenite by thermal cycling in a steel containing Fe - 9.7 Cr - 13.7 Ni - 0.05 C has been studied by Malyshev et al [2]. The yield stress of the austenite was doubled by one complete cycle; this is a higher proportional increase than has been found for the present alloys but is almost certainly due to the greater martensite content (25%) in the Russian investigation. Further cycling produced only a very small increase in strength and pronounced stabilisation of the direct transformation to martensite was observed; for example, only about 2% martensite was formed during the second quench to -196°C. The magnitude of the stabilisation effect in this alloy may be connected with strengthening of the austenite by carbon diffusion during the

relatively long reversion treatment of 30 minutes at 750°C (A_f = 700°C). After the second cycle the austenite was almost completely stabilised (i.e. negligible transformation to α' at -196°C) and its unchanged strength with further cycles could, possibly, be regarded as a balance between strengthening effects due to carbide precipitation and slight softening effects due to 'recovery' of the reversed austenite structure during the reversion treatments.

CHAPTER 6

CONCLUSIONS

The following conclusions can be drawn from the observations which have been made on the two alloys, Alloy A (Fe - 16 Cr - 12 Ni) and Alloy B (Fe - 15 Cr - $8\frac{1}{2}$ Ni - 2 Mo - 0.1 C):

1. Both alloys are fully austenitic at room temperature, after solution treatment, but quenching to -196°C produces partial transformation to martensite. The martensite has a lath-morphology and the parallel-sided transformed regions (laths) contain both α' and ε phases, as has been widely reported. The retained austenite shows almost no deformation as a result of the martensite transformation. The M_s temperatures of Alloys A and B have been found to be -50°C and -40°C respectively and the transformation in Alloy B has been shown to exhibit isothermal characteristics at -80°C and -196°C. Holding for $\frac{1}{4}$ hour and 1 hour at -196°C produces about 15% α' and $12\frac{1}{2}$% α' in Alloys A and B respectively.

2. Transformation to martensite can also be induced in these alloys by deformation at room temperature. A reduction of 50% by rolling produces about 10% α' in Alloy A and just over 40% α' in Alloy B.

3. The reverse martensite transformation, $\alpha' \longrightarrow \gamma$, under the conditions imposed by the short isothermal (1 or 2 minutes) reversion treatments which involve plunging partially martensitic specimens into molten salt baths at various temperatures, is considered to occur largely by a shear (martensitic) mechanism. The temperatures at which the transformation begins and ends under these conditions (A_s and A_f) have been estimated as 450°C and 600°C for Alloy A, and 560°C and

775°C for Alloy B. Structural observations suggest that, at least in Alloy A, the austenite produced by the reverse transformation has an almost identical crystallographic orientation to the original (retained) austenite. In the same alloy, it appears that individual grains of α' retransform completely to produce regions of reversed austenite of similar size and shape although the indications are that in Alloy B there is a tendency for each α' grain to produce several regions of reversed austenite which are misorientated with respect to each other.

4. The appearance of the reversed austenite is similar in both alloys and its structural imperfections are indicated by the 'ghost areas' which are visible by light (optical) microscopy after etching. Electron microscopy has shown that these areas contain a high density of tangled dislocations, stacking faults and reversal twins. The dislocations are considered to arise largely from an inheritance of the defects which exist in the martensite and to some extent by the inhomogeneous deformation involved in the reverse transformation. It is thought that the reversal twins do not arise by a shear associated with the reversion process but that these represent an early stage in the recovery of the reversed austenite sub-structure. The structure of the retained austenite is not altered to an appreciable extent by the reverse martensite transformation.

5. The nature of the reverse transformation during slower rates of heating has been investigated by a differential dilatometry technique and by measurements of dynamic Young's modulus (Alloy A only). The results are difficult to interpret but there is some suggestion that, in Alloy A, heating at 4.5°C/min. permits the reverse transformation to proceed by a diffusional process before the shear mechanism becomes operative at higher temperatures. The possibility of stabilisation of the

diffusionless (shear) mechanism during the reversion treatments involving slower heating has also been considered. It is thought that holding at the reversion temperature for the short times used in the case of the 'rapid' treatments may permit diffusion-controlled reversion to take place to some extent, particularly at the lower temperatures where there may be insufficient driving force for the diffusionless transformation. In Alloy B the results are further complicated by the tendency for precipitation of carbides to occur.

6. On the basis of the present results, very little difference is thought to exist between the progress of the reverse transformation in deformed specimens and in quenched specimens produced by 'rapid' heat treatments; in particular the values of the A_s and A_f temperatures do not appear to be appreciably altered. Fully retransformed specimens were found to contain twins in the deformed austenitic matrix but it was not possible to say whether these were formed in regions of reversed austenite or of deformed (retained) austenite.

7. The progress of the reverse transformation in the deformed specimens with slower heating rates, as measured by dilatometry, was largely obscured by a superimposed contraction effect at lower temperatures and one of expansion at higher temperatures. The former has been attributed to a density increase produced by recovery processes in the deformed specimens while the latter is thought to be connected with possible anisotropic aspects of the recrystallisation process.

8. The annealing-out of the defect structure of the reversed austenite in Alloy A, produced from specimens which had been partially transformed to martensite by quenching to -196°C, has been investigated at temperatures in the range 700°C to 925°C. The mechanism by which the reversed austenite is removed is thought to be

one of continuous recovery, or recrystallisation 'in situ', but does not involve the movement of high angle boundaries through the structure. The fully-annealed structure thus contains grains of austenite which are not significantly different in size, shape or orientation from those of the original solution-treated specimens. The apparent activation energy for the 'recovery' process is approximately 80 Kcal/mole.

9. Annealing processes in the 'cold-worked and reversed' specimens of Alloy A are much more rapid than in 'quenched and reversed' specimens and the structure is fully recrystallised after only 2 minutes at 850°C. In this case the annealing process is thought to involve the usual formation and growth of strain-free regions in the deformed structure, involving the movement of high angle boundaries.

10. Precipitation processes in austenitic specimens of Alloy B have been studied, at 650°C and 700°C, by measurements of hardness, saturation magnetic intensity and by electron microscopy. Carbides, often identifiable as $M_{23}C_6$, were observed to form in the solution-treated specimens at grain boundaries, as 'laths' within grains (probably associated with twin boundaries), as 'stringers' along dislocations and as angular ('cubic') particles. The latter has been shown to possess interfaces of $\{111\}_c$ and, perhaps, $\{110\}_c$ planes and the observations of the precipitate morphology appear to be consistent with the particle shape suggested for $M_{23}C_6$ by Beckitt and Clark [92].

11. Carbide precipitation in quenched and reversed specimens of Alloy B takes place, initially, at the same sites as in the solution-treated material which had received the same ageing treatment (i.e. mainly at grain boundaries and twin interfaces), but later develops also

in the laths of reversed austenite. Precipitation occurs extensively throughout cold-worked and reversed specimens of Alloy B, even after only half an hour at 700°C.

12. The increase in ferromagnetic response shown by aged specimens has been related to the formation of martensite on cooling, due to an increase in the M_s temperature of the matrix by removal of carbon and other alloying elements during precipitation. It is suggested that the more pronounced increase observed at longer ageing times in the solution-treated and 'quenched and reversed' specimens is due to the partial transformation of the austenite matrix to ferrite by a diffusional process. This transformation to ferrite may occur at very early ageing times in the 'cold-worked and reversed' specimens.

13. Transformation cycling, $\gamma \rightarrow \alpha' \rightarrow \gamma$, causes stabilisation of the austenitic specimens in respect of the direct transformation, $\gamma \rightarrow \alpha'$; the effect on the reverse transformation, $\alpha' \rightarrow \gamma$, was not indicated except that the values of the A_f temperatures did not appear to have been raised. The stabilisation phenomenon becomes more pronounced as the cycling is continued, although this effect is less marked in Alloy B than in Alloy A.

14. The strengthening of both the 'austenitic and martensitic' structures, measured by hardness tests, produced by the transformation cycling, increases in Alloy B as the number of cycles increases (up to 5). In Alloy A there is a tendency for the hardness to level off after two cycles and this is thought to be due largely to the small volume fraction of the material participating in the direct and reverse transformations. The increase in strength in Alloy A is greatest in the austenite, where the hardness is approximately doubled after four cycles, and arises from the defect structure inherited from the martensite and also produced by the reverse transformation. In Alloy B,

there may be some contribution to the strength from the precipitation of carbides during transformation cycling.

15. The somewhat smaller strength increase of austenite produced by the reverse martensite transformation in these alloys as compared to the effect of similar transformation in iron-nickel alloys with comparable M_s temperatures is attributable to the characteristics of the direct martensite transformation in stainless steels. Firstly, cooling below the M_s temperature fails to produce substantial transformation to martensite and the martensite content produced for a given amount of undercooling is therefore small compared to many other ferrous alloys; thus, only small volume fractions of the alloy participate in the direct and reverse transformations. Secondly, the mechanism of the direct (and reverse) transformation is such that substantial deformation of the retained austenite does not occur and thus, unlike iron-nickel alloys, strengthening occurs only in the small volumes which had transformed to martensite and not in the retained austenite.

SOME SUGGESTIONS FOR FUTURE WORK

Some suggestions for further work arise directly from the present investigations. The detailed mechanism of the reverse transformation is still not fully understood, particularly during relatively slow heating, and it would be interesting to gain a deeper knowledge of the diffusion-controlled reversion processes and of the stabilisation of the diffusionless reverse transformation. Thus, dilatometry measurements during heating partially martensitic specimens to various temperatures below A_s and between A_s and A_f, and holding for various times before heating is continued might produce useful results.

The suggested partial transformation of austenite to ferrite during the ageing treatments performed on specimens of Alloy B may be verified, or disproved, by repeating these treatments in the dilatometer. As well as indicating the volume changes which occur during ageing, transformation to martensite during cooling from the ageing temperature to room temperature will also be detected. After ageing treatments at 700°C on solution-treated specimens the magnitude of the expansion indicated on cooling, due to the formation of martensite, would be expected to change little after about the first 3 hours even though the ferromagnetic response at room temperature increases with ageing time after long treatments.

The mechanism of strengthening by transformation cycling would be more clearly understood if structural observations were made to reveal the sites at which successive generations of martensite form and whether the actual structures of the martensite and reversed austenite are changed as the number of cycles is increased. Studies of the contribution of carbide precipitation to the strengthening in Alloy B could also be made; it is possible that longer reversion treatments might produce a greater increase in strength via precipitation processes

(which could outweigh any recovery effects in the reversed austenite) provided that stabilisation of the austenite does not become more pronounced.

Some indication of the origin of the twins in the deformed specimens of both alloys after reversion treatments might be gained from similar experiments on specimens which had been deformed above the M_d temperature (possibly at about 200°C). The observations of twins in such specimens, which have contained no martensite, after 'reversion treatments' would suggest that these twins are not produced by the reverse martensite transformation, and vice versa.

More generally, it appears that the characteristics of the martensitic transformation in semi-austenitic stainless steels are such that strengthening by the reverse transformation in these steels is unlikely to produce very large increases even though the individual regions of reversed austenite might have considerable strength. Other ferrous alloys might benefit to a greater extent from the effects of the direct and reverse martensite transformations which serve to produce internal deformation of the austenitic structure without the need for external shape change. This process might be regarded as being analogous to that of ausforming and might produce similar strengthening effects, particularly if the phase transformations occurred in the presence of a fine distribution of carbide particles. Low alloy steels and martensitic stainless steels are possible materials for study.

The combined phenomena of precipitation hardening and reversion strengthening might be extended to include the precipitation of inter-metallic phases, as well as carbides. A study of maraging steels could be made to investigate these combined effects.

ACKNOWLEDGEMENTS

I would like to express my gratitude to Dr. D.R.F. West for his interest, guidance and advice throughout the course of this work, and to Professor J.G. Ball for the provision of laboratory facilities. Thanks are also due to many colleagues and friends in the Department, especially Mr. F.A. Thompson and Drs. V. Ramaswamy, N.K. Nagpaul and B.A. Parker, for their assistance with various parts of the experimental work.

The support for this project provided by the Science Research Council and the Ministry of Technology is greatly appreciated and I am indebted to International Nickel Ltd. for supplying the two experimental alloys, to Firth-Vickers Stainless Steels Ltd. for samples of two commercial steels which were used in preliminary experiments and to Murex Ltd. for a quantity of pure chromium.

I would also like to thank my wife for her encouragement, assistance and tolerance, particularly during the final stages of this project.

REFERENCES

1. Chukleb and Martynov, Phys. M.M. 1960 10 (2) 80.
2. Malyshev et al, Trudy Inst. Fiz. Met. 1958 20 339.
3. Krauss and Cohen, A.I.M.E. 1962 224 1212.
4. Zatsev and Gorbach, Phys. M.M. 1965 20 (4) 135.
5. Zatsev and Gorbach, Phys. M.M. 1964 17 (5) 68.
6. Ctte, Acta Met. 1957 5 614.
7. Goldman and Wagner, Acta Met. 1963 11 405.
8. Breedis, A.I.M.E. 1966 236 218.
9. Thomas and Krauss, A.I.M.E. 1967 239 1136.
10. Irvine, Llewellyn and Pickering, J.I.S.I. 1959 192 218.
11. Truman, I.S.I. Sp.Rp. 86, p.84.
12. Rees, Burns and Cook, J.I.S.I. 1949 162 325.
13. Breedis, A.I.M.E. 1964 230 1583.
14. Reed, Acta Met. 1962 10 865.
15. Kelly and Nutting, J.I.S.I. 1961 197 199.
16. Kelly, Acta Met. 1965 13 635.
17. Dash and Ctte, Acta Met. 1963 11 1169.
18. Koepke, Jewett and Chandler, Nature 1966 210 1252.
19. Lagneborg, Acta Met. 1964 12 823.
20. Breedis and Robertson, Acta Met. 1963 11 547.
21. Cina, J.I.S.I. 1954 177 406.
22. Cina, J.I.S.I. 1955 179 230.
23. Breedis and Robertson, Acta Met. 1962 10 1077.
24. Fielder, Averbach and Cohen, A.S.M. 1955 47 267.
25. Venables, Phil. Mag. 1962 7 35.
26. Reed and Gunter, A.I.M.E. 1964 230 1583.
27. Cina, Acta Met. 1958 6 748.

28. Watson and Christian, A.I.M.E. 1962 224 998.
29. Gunter and Reed, A.S.M. 1962 55 399.
30. Breedis, Acta Met. 1965 13 239.
31. Bressanelli and Moskowitz, A.S.M. 1966 59 223.
32. Llewellyn and Murray, I.S.I. Sp.Rp. No.86 p.197.
33. Binder, Metal Prog. 1950 58 201.
34. Reed and Mikesell, Adv. Cry. Eng. 1960 4 84.
35. Kishkin and Klypin, Metal i Obra. Met. 1959 5 15.
36. Edmondson and Ko, Acta Met. 1954 2 235.
37. Krauss, Acta Met. 1963 11 499.
38. Zakharova, Ignatov and Khatanova, Phys. M.M. 1958 6(3) 89.
39. Izmailov, Gorbach and Yakhontov, Phys. M.M. 1963 16(3) 349.
40. Izmailov and Gorbach, Phys. M.M. 1965 20(1) 101.
41. Melnikov, Sokolov and Stregullin, Phys. M.M. 1964 17(2) 151.
42. Kessler and Pitsch, Acta Met. 1967 15 401.
43. Gorbach and Butakova, Phys. M.M. 1963 16 112.
44. Krauss and Cohen, A.I.M.E. 1963 227 278.
45. Shapiro and Krauss, A.I.M.E. 1967 239 1408.
46. Jana and Wayman, A.I.M.E. 1967 239 1187.
47. Jordan and Borland, J.Aust.Inst.Met. 1964 9 171.
48. Seldovich et al, Phys. M.M. 1966 22(6) 890.
49. Kessler and Pitsch, Archiv/Eisen 1967 June p.469.
50. Kessler and Pitsch, Archiv/Eisen 1967 April 321.
51. Sokolov et al, Phys. M.M. 1964 17 153.
52. Eichelman and Hull, A.S.M. 1953 45 77.
53. Monkman, Cuff and Grant, Metal Prog. 1957 71 94.
54. Imai, Izumiyama and Sasaki, Sci.Rep.Ritu. 1966, A, 18(1) 39.
55. Troiana and McGuire, A.I.M.E. 1942 32 340.
56. Gordon Parr, J.I.S.I. 1952 171 137.
57. Gordon Parr, J.I.S.I. 1952 171 214.

58. Gordon Parr, Acta Crys. 1952 5 842.

59. Sanderson and Honeycombe, J.I.S.I. 1962 200 934.

60. Mizagi and Wayman, A.I.M.E. 1966 236 806.

61. Goldman, Robertson and Koss, A.I.M.E. 1964 230 240.

62. Gunter and Reed, Adv. Cry. Eng. 1961 7 500.

63. Kulin and Speich, A.I.M.E. 1952 194 258.

64. Uhlig, A.S.M. 1942 30 947.

65. Gorbach and Malyshev, Phys. M.M. 1964 17(2) 65.

66. Shapiro and Krauss, A.I.M.E. 1966 236 1371.

67. Sokolov and Gorbach, Trudy Inst. Fiz. Met. 1959 p.123.

68. Golovchiner, Phys. M.M. 1963 15(4) 54.

69. Wasserman, Mitt. K.-W. Inst. 1935 17 149.

70. Hyatt and Krauss, A.S.M. 1968 61 168.

71. Habrovec et al, J.I.S.I. 1967 205 861.

72. Yakhontov, Phys. M.M. 1966 21(1) 41.

73. Kessler and Pitsch, Acta Met. 1965 13 871.

74. Golovchiner and Tyapkin, Prob. Metal i Fiz. Met. (Moscow 1955) Aec-tr-2924, 1957, 141.

75. Zwell, Gorman and Weisserman, A.S.M. 1966 59 491.

76. Haworth and Gordon Parr, A.S.M. 1965 58 476.

77. Zerwekh and Wayman, Acta Met. 1965 13 99.

78. Lacoude and Goux, Comp. Rend. 1964 259 1858.

79. Shklyar et al, Phys. M.M. 1966 21(2) 75.

80. Lysak and Nikolin, Phys. M.M. 1967 23(1) 93.

81. Yershova and Bogachev, Phys. M.M. 1962 13 133.

82. Gorbach, Izmailov and Malyshev, Phys. M.M. 1965 20(5) 101.

83. Sorokin, Phys. M.M. 1966 22(2) 239.

84. Gridnev et al, Metal i Obra. Met. 1957 5 7.

85. Goldberg, A.S.M. 1968 61 26.

86. Goldberg and O'Conner, Nature 1967 Jan. p.170.

87. Yegolayev et al, Phys. M.M. 1967 23(1) 78.

88. Satyanarayan, Eliasz and Miodownick, Acta Met. 1968, 16 877.

89. Lytton et al, Brit. J. Appl. Phys. 1964 15 1573.

90. Reed and Mikesell: Advances in Cryogenic Engineering, Plenum Press Inc., New York, 1958.

91. Schumann, Acta Cryst. 1967, June, p.275.

92. Beckitt and Clark, Acta Met. 1967 15 113.

93. Singhal and Martin, Acta Met. 1967 15 1603.

94. Clarebrough et al, 'Recovery and Recrys. of Metals', A.I.M.E. Conf. 1962 p.63.

95. Garofalo and Wreidt, Acta Met. 1962 10 1007.

96. Goodman and Hu, A.I.M.E. 1964 230 1413.

97. Hu and Goodman, A.I.M.E. 1963 227 1454.

98. Christian, in 'Theory of Transformations in Metals and Alloys', Pergamon Press, 1965.

99. Dulieu and Nutting, I.S.I., Sp.Rp. 86, 1964, p.140.

100. Weertman and Weertman, 'Elementary Dislocation Theory', Macmillan, New York, 1964.

101. Nakayama et al, in 'Director Observations of Imperfections in Crystals', Interscience Publ., New York, 1962.

102. Byrne, in 'Recovery, Recrystallisation and Grain Growth,' Macmillan, 1965.

103. Vandermeer and Gordon, 'Recovery and Recrystallisation of Metals', Interscience Publ., New York, 1963.

104. Hu, ibid.

105. Hu, A.I.M.E., 1962 224 75.

106. Whelan et al, Proc.Ray.Soc., 1957, A, 240 524.

107. Hancock and Leak, Metal Sci. J., 1968 1 33.

108. Lewis and Hattersley, Acta Met. 1965 13 1159.

109. Banerjee et al, A.S.M. 1968 61 103.

110. Hopkin and Taylor, J.I.S.I., 1967 205 17.

111. Mazza, J.I.S.I., 1966 204 783.

112. Barford and Meyers, J.I.S.I. 1963 201 1025.

113. Bendure et al, A.I.M.E. 1961 221 1032.

114. Garofalo et al, A.S.M. 1961 54 430.

115. Moore and Griffiths, J.I.S.I. 1961 197 29.

116. Dewy et al, J.I.S.I. 1965 203 938.

117. Summerling and Nutting, J.I.S.I. 1965 203 398.

118. Floreen, A.I.M.E. 1966 236 1429.

119. Hatwell and Berghazen, I.S.I. Sp.Rp. 84, 1958 88.

120. Plateau et al, ibid, p.157.

121. Glowacki et al, J.I.S.I. 1968 206 393.

122. Decker and Floreen, in 'Precipitation from Fe-base Alloys', A.I.M.E. 1963 p.69.

123. Keh, Leslie and Speich, A.I.S.I. Contrib. Met. Steels 1963 March p.43.

124. Speich and Swann, J.I.S.I. 1965 203 480.

125. Sastri and West, J.I.S.I. 1965 203 138.

126. Priestner and Glover, I.S.I., Sp.Rp. 93, 1965 p.38.

APPENDIX A

ESTIMATION OF MARTENSITE CONTENT USING A MAGNETIC RING BALANCE

A.1. INTRODUCTION:

Among the methods which have been used for measuring the martensite content of steels are quantitative metallography, X-ray diffraction, electrical resistivity and various magnetic techniques.

Quantitative metallography is inherently slow and tedious, and requires great care in the choice of the areas of the specimen to be examined if they are to be representative of the complete sample. Difficulty may be experienced in distinguishing between the martensite and other phases present, and a false value of the percentage martensite present may result from over-etching; especially at high levels of martensite content when small areas of retained austenite are easily obscured.

A second absolute method for martensite determination is by the measurement of the integrated intensities of X-ray reflections. The accuracy is known to fall off seriously when the specimen contains less than about 70% martensite.

Electrical resistivity and most 'low-field' magnetic properties are influenced by grain-size, internal stresses, cracks and the size and distribution of particles comprising the aggregate. However, the specific saturation magnetic intensity, σ , is insensitive to such factors and is a direct function of the proportional amounts of each phase present in the alloy and their respective σ values. The contribution of austenite can usually be neglected as it is paramagnetic, and so the saturation intensity of the aggregate gives a direct measure of the ferromagnetic, α' , martensite content. The measurement of σ is useful for tempering studies as well as for martensite content determinations. It is a rapid technique capable of a high degree of accuracy and requires only moderate care in specimen preparation.

A.2. THEORY:

The magnetic balance measures the force on a ferro-magnetic specimen placed in a non-uniform magnetic field with constant field gradient produced by an electromagnet.

The specimen is placed in a position of constant field gradient where it experiences a force equal to M dH/dx in the direction of the field gradient (i.e. vertically downwards). The operating conditions are such that the downward movement is sufficiently small to ensure that the specimen remains in the region of constant dH/dx. M, the saturation magnetic moment of the specimen, equals J_s V = σ m where V is the volume, m the mass of the specimen and J_s the saturation magnetization. σ is thus defined as the saturation magnetic moment per unit mass but usually called the specific magnetic intensity.

The force on the specimen is then given by: $F = \sigma\ m\ dH/dx$

If σ is in c.g.s. units, m in grams, H in oersteds and x in centimetres, then F is given in dynes. Thus a specimen of pure iron of mass 0.1 gm in a typical field gradient of 900 oersted/cm will experience a force of approximately 20 grams.

The force F, exerted on the specimen produces a downward displacement, D, which is balanced by the elastic distortion of the ring from which it is suspended. The following relationship is obtained:
$D \propto F \propto m\sigma dH/dx$; therefore $D = Km\sigma$
where K is a constant for the apparatus used under standard conditions. Hence, although an absolute value of σ is not obtained, an accurate comparison can be made between the σ values of two specimens. The apparatus is therefore calibrated by measuring the deflection due to a specimen of known mass prepared from material of known σ. Pure iron is the obvious choice as its σ value is both accurately known and is comparable with that of substantially martensitic steels.

Hence $$\frac{D_s}{D_{Fe}} = \frac{K.m_s.\sigma_s}{K.m_{Fe}.\sigma_{Fe}} = \frac{m_s.\sigma_s}{m_{Fe}.\sigma_{Fe}}$$

If the specimen, s, contains only one ferromagnetic phase, then its magnetic response can be attributed entirely to this phase with little error. The saturation intensity of the specimen as a whole, σ_s, is related to that of the ferromagnetic phase, σ_M, by the relationship:

$$\sigma_s = \sigma_M \frac{\%M}{100}$$

Substitution in the previous equation gives:

$$\frac{D_s}{D_{Fe}} = \frac{m_s\ \sigma_M\ \%M}{m_{Fe}\ \sigma_{Fe}\ 100}$$

$$\text{hence } \%M = \frac{D_s\ m_{Fe}\ \sigma_{Fe}\ 100}{D_{Fe}\ m_s\ \sigma_M} = \frac{D_s}{m_s\ D_{Fe}} \times C \quad \text{(where C = constant)}$$

The displacement of a standard iron specimen, D_{Fe}, is measured each time to check the calibration. Thus when C has been evaluated for a particular composition, the martensite content of a specimen is found merely by measuring its mass and its displacement under the standard conditions.

A.3. CALCULATION OF σ_M:

An evaluation of σ_M for a particular composition can be made by taking into account the effects of the various alloying additions on the value of σ_{Fe}. Chromium and nickel atoms substituted in the iron lattice contribute to the ferromagnetism.

1 mole Ni weighs A_{Ni} gms and contains No molecules (atoms).
$\therefore$ W_{Ni} gm of Ni contain $\frac{W_{Ni}}{A_{Ni}}$. No atoms.

Thus, in 100 gm alloy, nickel contributes $\frac{W_{Ni}}{A_{Ni}}$. No atoms

Similarly for Fe and Cr $\therefore$ in 100 gm of alloy the number of atoms of these three elements is:

$$\text{No} \left\{ \frac{W_{Cr}}{A_{Cr}} + \frac{W_{Ni}}{A_{Ni}} + \frac{W_{Fe}}{A_{Fe}} \right\}$$

Each Cr atom contributes 0.22 Bohr magnetons.
Each Ni atom contributes 0.6 Bohr magnetons.
Each Fe atom contributes 2.2 Bohr magnetons.

$\therefore$ Number of Bohr magnetons in 100 gm alloy is:

$$\text{No} \left\{ 0.22 \frac{W_{Cr}}{A_{Cr}} + 0.6 \frac{W_{Ni}}{A_{Ni}} + 2.2 \frac{W_{Fe}}{A_{Fe}} \right\}$$

Neglecting interactions between Ni, Cr and Fe and assuming other elements have merely a dilution effect, we can continue as follows, taking Alloy B as an example:
Number of Bohr magnetons in 100 gm of alloy is:

$$6.023 \times 10^{23} \left\{ \frac{0.22 \times 14.9}{52.0} + \frac{0.6 \times 8.7}{58.71} + \frac{2.2 \times 74.14}{55.85} \right\}$$

$$= 6.023 \times 10^{23} \times 3.072$$

The Bohr magneton, $\mu_B = \frac{eh}{4 \pi m}$

where $e/m = 1.759 \times 10^{7}$ e.m.u.
and $h = 6.62 \times 10^{-27}$ erg. sec.
$\therefore \mu_B = \frac{6.62 \times 10^{-27} \times 1.759 \times 10^{7}}{4\pi}$
$= 9.266 \times 10^{-21}$ c.g.s. units

Hence, saturation magnetization due to 100 gm of alloy
$= 6.023 \times 10^{23} \times 3.072 \times 9.266 \times 10^{-21}$
$\therefore$ saturation magnetization due to 1 gm alloy, σ_M.
$= 6.023 \times 10^{23} \times 3.072 \times 9.266 \times 10^{-21} \times 10^{-2}$
$\therefore \underline{\sigma_{M(B)} = 171.0 \text{ c.g.s. units}}$

Similarly for Alloy A, $\underline{\sigma_{M(A)} = 168.8 \text{ c.g.s. units}}$

A.4. DESCRIPTION OF APPARATUS AND ITS OPERATION:

The apparatus is comprised of an electromagnet, its power supply and a ring balance, as described below.

A.4.1. Magnet:

The electromagnet used was a 4" Newport Instruments type 'A'. The basic features of the pole tips are shown in Fig. A.1.; they are essentially truncated cones of 55° semi-angle having faces of about 6 cm diameter and an inclined band 2 cm wide running horizontally and making an angle of about 5° with the vertical. The pole gap was nominally 3 cm and the design was such that the position of the maximum field gradient remained appreciably constant in all fields used. An operating current of 14 amps produced a field of about 12,000 gauss.

A.4.2. Power Supply:

The power pack was capable of supplying 15 amps D.C. from a 240 v A.C. mains, according to the circuit shown in Fig. A.2. The operating current, (its values chosen by experiments described later) was indicated on a large scale ammeter and controlled accurately at the chosen value by adjustment of the coarse and fine variable transformers. Current changes due to fluctuations in mains voltage and to changes in the coil resistances of the electromagnet due to heating could thus be reduced to very small values.

A.4.3. Ring Balance:

Although the original design of Sucksmith (Proc. Roy. Soc. 1939 (A), 170, 551) is followed quite closely, modifications have been made to the specimen rod, the shape of the specimens and the method of measuring the specimen displacement, according to suggestions made by Dr. S.G. Glover, Birmingham University.

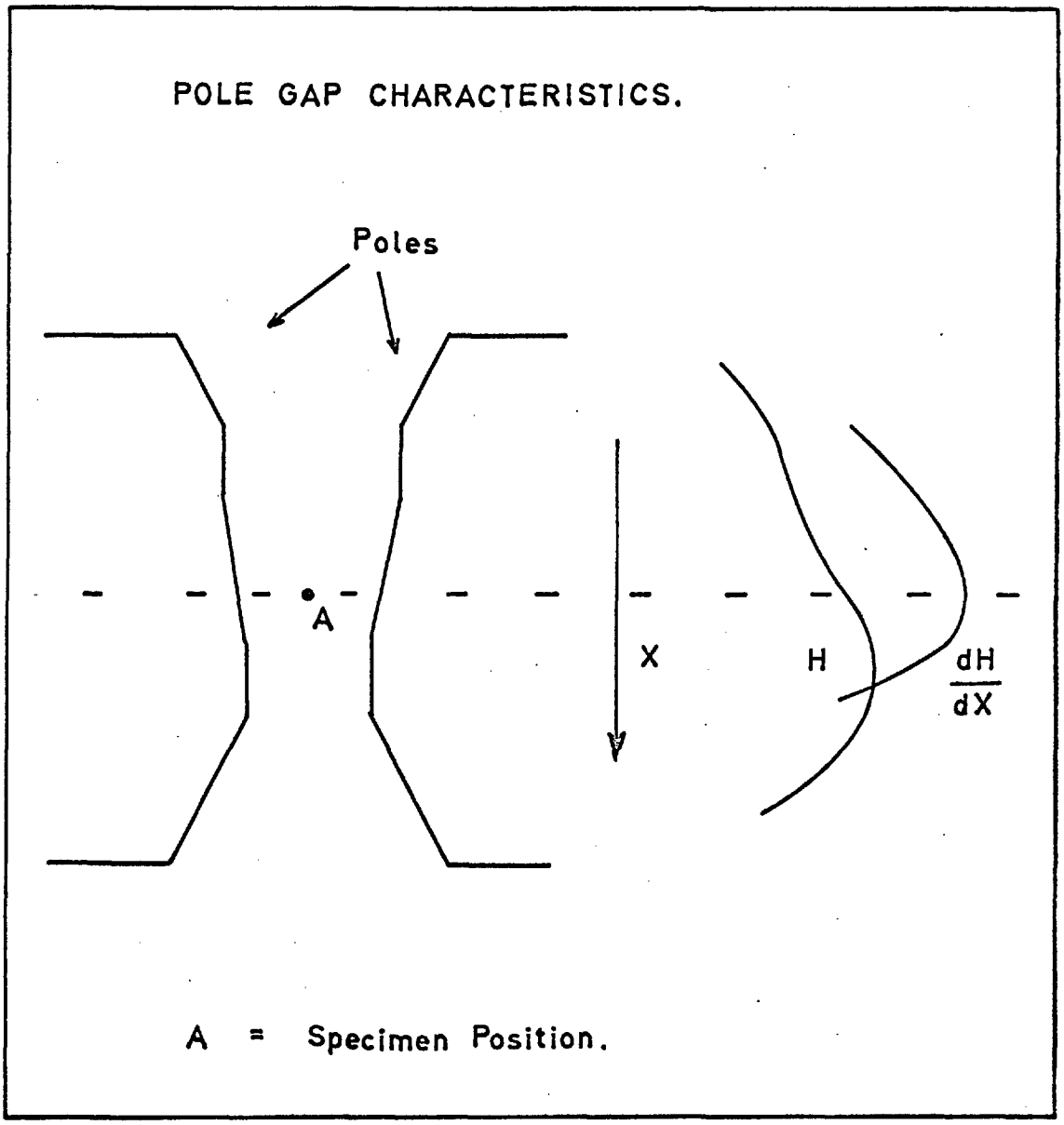

FIG. A. 1. Pole Gap Characteristics

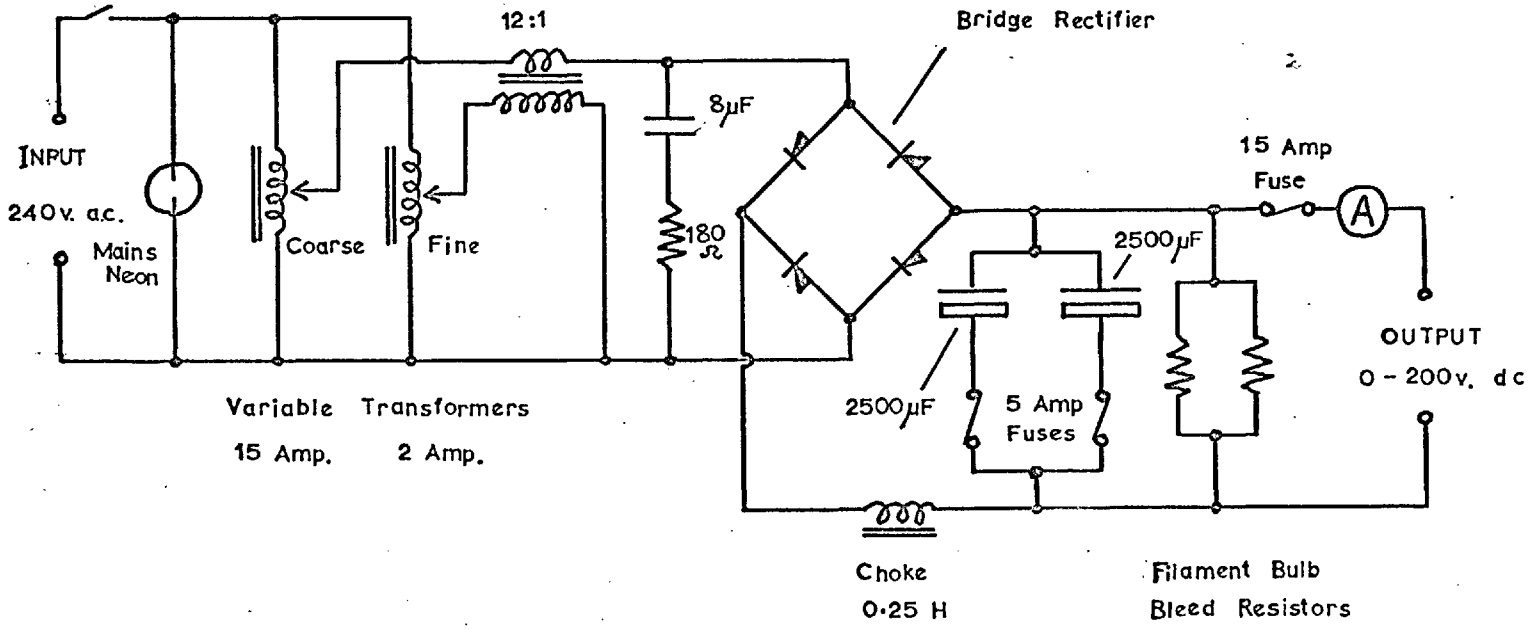

FIG. A. 2. POWER SUPPLY FOR MAGNETIC BALANCE.

The construction of the balance is shown diagramatically in Fig. A.3. A circular ring, diameter about 6 cm, of copper-beryllium strip about 4 x 0.3 mm. is supported in a vertical plane at its highest point. To the lower end of the ring is attached a brass rod, joined to which is the specimen holder at its lower end and the armature of a miniature displacement transducer at its upper end. The downward force due to the attraction of the specimen into the stronger field deforms the ring, thus displacing the armature. Movement of the armature varies the inductances of the two arms of the transducer differentially, thus unbalancing the bridge and giving rise to an output signal at carrier frequency which can be measured to give an accurate indication of the displacement of the specimen.

Lateral constraint of the specimen rod is effected by two flat spiral springs which prevent the specimen being pulled in to one or other of the poles of the magnet. Their influence on the restoring force does not affect the linearity of the relationship between displacement and the applied force. It was not found necessary to use a dash pot to damp out vibrations in the system but a perspex draught excluder was employed.

The specimen rod junction was designed to give the correct vertical positioning of the specimen by locating the end of the upper rod against the bottom of the aperture in the junction. The specimen is attached to the rod by using the 10 BA thread on the end of the rod and the small hole drilled in the specimen prior to heat treatment.

A.5. CALIBRATION AND ACCURACY:

The balance was calibrated and its performance assessed by experiments based on those of Glover (Ph.D. thesis, Birmingham Univ., 1956).

A.5.1. Uniformity of Specimen Displacement with Applied Force:

Weights from 0.3 to 19.3 gm were suspended from a hook attached to the end of the specimen rod and the resulting displacement shown on the transducer meter was recorded. Complete proportionality between the two was observed over this range.

A.5.2. Vertical and Horizontal Distribution of the Field Gradient between the Poles of the Magnet:

Since $F = m\sigma \, dH/dx$, the force on a standard specimen of constant mass and specific magnetic intensity is directly proportional to the value of the field gradient at any point in the pole gap. The gradient was thus measured as a function of vertical position and field coil current by recording the force on a standard pure iron specimen under such conditions. The results are shown in Fig. A.4.

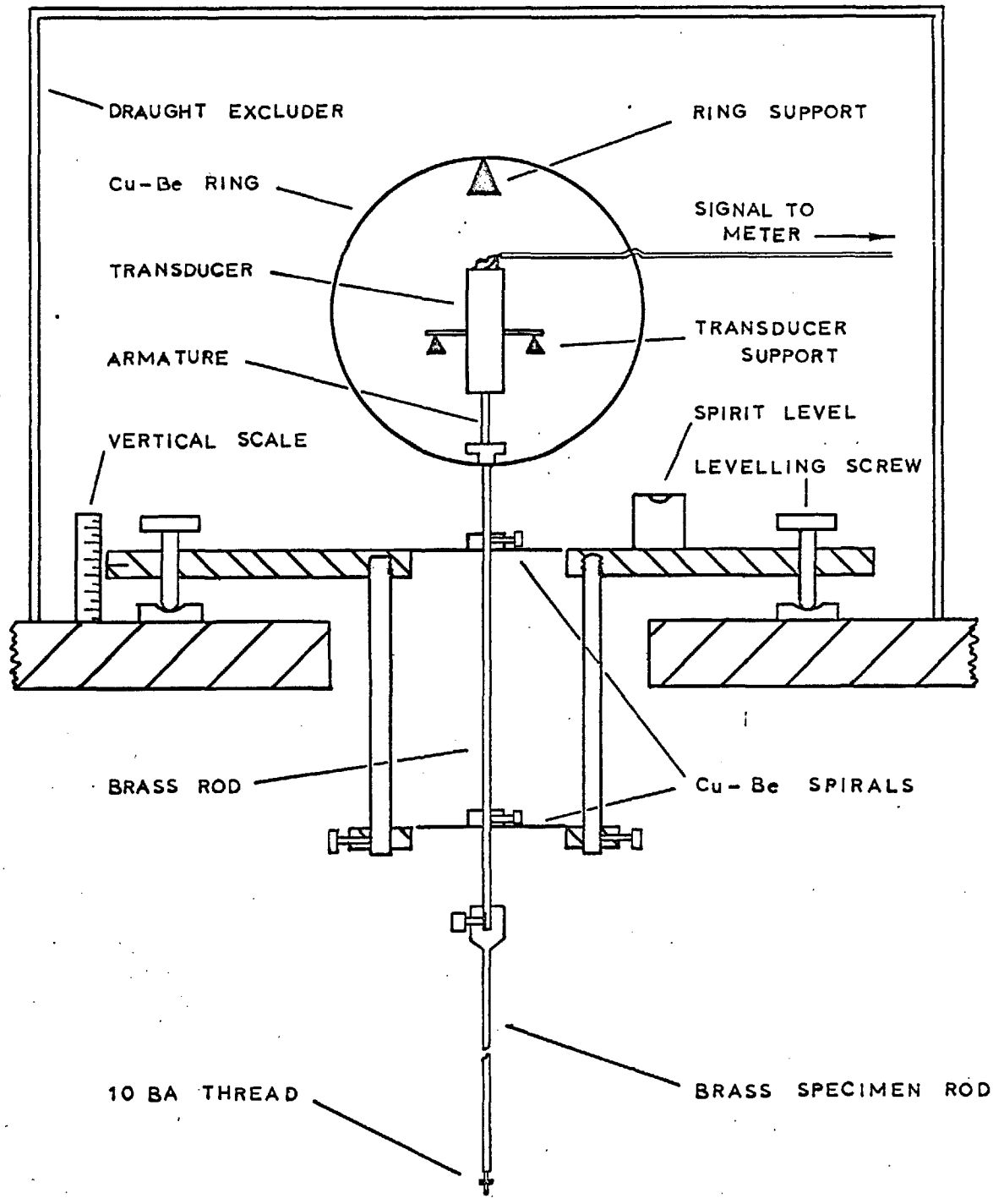

FIG. A. 3. THE RING BALANCE.

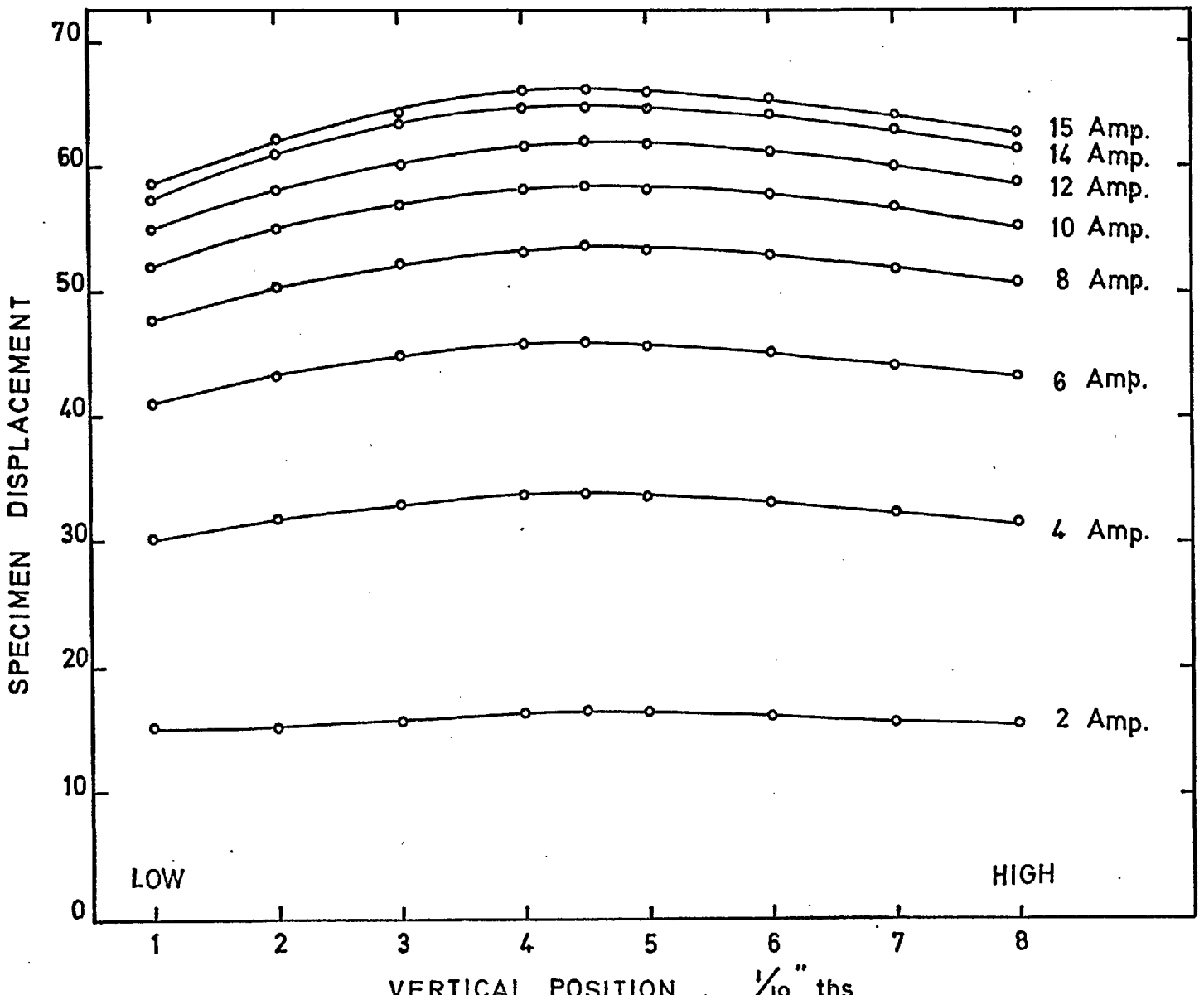

FIG. A. 4. Variation in field gradient, indicated by the displacement of a standard specimen, with specimen position and field coil current.

The optimum position for the specimen is at the point where d^2H/dx^2 is zero since a small change in specimen position will not appreciably alter the value of dH/dx. This will minimise the errors introduced by incorrect positioning of the specimen and by its downwards movement during measurement.

At a current of 14 amps the force is almost at its maximum (hence better sensitivity) and the equipment is being used within the operating limits of the power supply and magnet.

The maximum displacement likely to be encountered was for a pure iron specimen of about 100 mg. weight under the influence of a field gradient produced by a current of 14 amps. In this case the specimen displacement is approximately 0.016". The error introduced, due to a non-constant value of dH/dx at 14 amps, by a specimen moving through a distance of 0.02" does not exceed 0.1 in 64.9, i.e. 0.15% of the measured value. Should the specimen be incorrectly sited vertically in the pole gap by as much as $\pm$0.05" the resulting error would be 0.6%. These values were obtained from the information in Fig. A.4.

As well as incorrect vertical positioning of the specimen, horizontal misplacement can occur but it is unlikely to exceed 0.1" from the central position. The change in displacement of a standard specimen under these conditions did not exceed 0.15% and is thus considered satisfactory.

A.5.3. Equality of Force Ratio with Mass Ratio:

Values of σ were measured for three specimens of pure iron weighing 0.0423 gm., 0.0723 gm. and 0.1039 gm. and agreement was found to be within 0.48%. The specimens had been weighed to $\pm$0.0001 gm. and this weighing error could largely account for the observed differences in the σ values. Thus, within the limits of accuracy of the method, the measured values of σ are independent of m.

A.5.4. Equality of Force Ratio with Intensity Ratio:

Specimens of pure iron and pure nickel having weights of 0.0484 gm. and 0.0743 gm. respectively were found to give a ratio value of their intensities of 3.920. Quoted values are 3.975 (Weiss and Forrer) and 3.946 (Sucksmith) and the error would thus appear to be of the order of 1% which is considered acceptable.

A.5.5. Field Strength Required for Magnetic Saturation of the Specimen:

It has been stated that the specific magnetic intensity value of a specimen is structure insensitive. For advantage to be taken of this fact, it is

essential that the specimen should be magnetically saturated at the field strengths used.

It is generally true that the field required for magnetic saturation of a specimen increases with its mechanical hardness. The minimum field for saturation was thus assessed by comparing the magnetic response of magnetically soft pure iron with a harder high carbon steel which is mainly martensitic. The displacements for the two specimens were compared at different values of the operating current and their ratio was found to be almost constant above 7 amps (corresponding to a field strength of approximately 9000 gauss). A current of 14 amps (approximately 12,000 gauss) was therefore more than satisfactory from the point of view of specimen saturation, as well as desirable from sensitivity considerations.

A.5.6. Estimation of the Sensitivity:

The sensitivity of the apparatus depends on two factors; firstly, on the stability of the field current and secondly, on the accuracy of the measurement of specimen displacement.

The current could be read and held to within 0.02 amps which corresponds to a reading change of 0.045% (from Fig. A.4.). This error in the specimen displacement will be equivalent to smaller errors in the martensite content the lower is the % martensite of the specimen. The specimen displacement could be read to 0.2 divisions on the transducer meter scale (full scale ≡ 100 divisions). The error in martensite content which this represents depends on the meter range being used which, in turn, depends on the martensite content of the specimen. With a typical specimen weight of 100 mg. this error is equivalent to 0.04% M on the '2.5 range' (0 - 20% M) and 0.16% M on the '10 range' (20 - 85% M).

As the scale can be read to 0.2 divisions, a deflection of 0.5 divisions could be taken as a definite indication of the presence of martensite in the specimen. Hence 0.1% martensite can be detected by the apparatus. If larger specimens were used, smaller martensite contents would be detectable for a similar displacement.

The reproducibility was assessed by repeated measurements on a standard iron specimen which was removed from and replaced in the apparatus each time. A total of 50 such measurements produced a scatter of 0.6 in the average measured deflection of 64.9, i.e. less than 1%. This would represent 0.1% M at the 10% martensite content level.

Specimen to specimen variations in martensite content due to the heterogeneous nature of the transformations necessitated assessment of several individual specimens for an average value. Measurements on three separate specimens could vary by as much as 0.4% M at the 15% M level (i.e. variation of $2\frac{1}{2}$%) and hence the capabilities of the apparatus are entirely adequate for the present requirements.

The relative accuracy of the results has thus been shown to be good. In the present case the absolute accuracy cannot be assessed from a direct calibration with X-ray or quantitative metallography techniques and is therefore dependent on the accuracy of the calculated σ_M values. If the error in σ_M were as high as 10 in these values of ~170 (i.e. about 6%), this would correspond to a possible absolute error of 0.6% M at the 10% martensite level which is the sort of content commonly encountered in the steels in this investigation. The error in σ_M is, however, unlikely to be this great.

APPENDIX B

ELEVATED TEMPERATURE MEASUREMENT OF YOUNG'S MODULUS

B.1. INTRODUCTION:

An apparatus constructed in this Department by Mr. B.A. Parker was used for the determination of dynamic Young's modulus in vacuum at temperatures up to 650°C by means of transverse free - free vibration (motion transverse to the specimen's longitudinal axis and both ends of the specimen unrestrained). Under such a mode of vibration the resonant frequency, according to Fine (1952), is given by:

$$f_r = \frac{\pi K}{2 L^2} \cdot \beta^2 \cdot \sqrt{\frac{E}{\rho}}$$

where f_r = resonant frequency.
K = constant for a given specimen geometry, (equal to $\frac{t}{2\sqrt{3}}$ for rectangular cross sections of thickness t in the direction of vibration.)
L = length of specimen.
β = constant depending on type of vibration and is equal to 1.5056 for the present case.
E = Young's modulus.
ρ = specimen density.

Values of Young's modulus can thus be found from measurements of specimen geometry and resonant frequency alone.

B.2. APPARATUS:

The apparatus was similar to that described by Lytton et al (BRIT. J. APPL. PHYS. 1964, 15, 1573) and can be considered in three sections.

B.2.1. Vibration Excitation and Detection Equipment:

The strip specimen was suspended at its nodes by two fine wires which act as the driving and sensing wires and also as the two components of a thermocouple to indicate specimen temperature. A Pt wire was spot-welded to one node point for the fundamental mode of vibration, and a Pt - 13% Rd wire spot-welded to the other. The driving wire was connected to the cone of a 3" moving coil loudspeaker which received a signal from an audio-oscillator. Frequencies in the range 700 - 1200 cycles/sec. were found suitable for the specimen sizes used.

The specimen vibration was transmitted by the sensing support wire to a piezoelectric crystal to which the wire was attached. The output of the detecting crystal was fed into a vacuum tube voltmeter to measure the signal amplitude and hence the amplitude of specimen vibration, which is a maximum at the resonant frequency.

The input and output signals of the specimen were displayed on an oscilloscope to confirm that the maximum amplitude shown on the voltmeter was attributable to a vibration of the required type. The value of the resonant frequency was measured by a digital counting device which was accurate to one part in 10,000.

B.2.2. The Radiation Furnace:

The specimen temperature was raised by means of an elliptical radiation furnace, described by Lytton et al. A line heat source provided by a quartz infra-red heating element at the focus of a polished stainless steel tube of elliptical section radiates energy to the specimen sited at the other focus. The very rapid heating rates obtainable with this furnace were not required for the present series of experiments. The power to the heating element was adjusted so as to maintain a specimen heating rate of about $20^{\circ}C$/min. and the average specimen temperature was measured by the thermocouple support wires, as previously described.

B.2.3. The Vacuum System:

The specimen suspension system and the elliptical furnace were positioned in a large bell jar which was flushed with argon and evacuated to a pressure of 3×10^{-3} mm. Hg.

B.3. OPERATIONAL PROCEDURE:

Strip specimens about 10 cm. in length, 0.02" thick and 0.25" wide were held in liquid nitrogen for the appropriate time and attached to the support wires at their nodes (approximately 2 cm. from the ends of the specimens). The system was evacuated and the resonant frequency measured at room temperature and at higher temperatures as the power supplied to the furnace was increased. The rate of heating was governed by the speed with which simultaneous measurements of resonant frequency and average specimen temperature could be made. In practice this was about $20^{\circ}C$/min.

Although heat shields were employed, a temperature increase in the crystal and loudspeaker occurred and produced deterioration in the signal. Operation of the apparatus at temperatures above 650°C was thus not possible with these slow heating rates. Thus, once this temperature was attained the power to the furnace was reduced and measurements of resonant frequency were made during cooling to room temperature. A new specimen was used for each subsequent run. It can thus be seen that the results of any particular run, showing the relationship between resonant frequency and specimen temperature, avoid many of the possible experimental inaccuracies.

B.4. ACCURACY:

Measurement of Young's modulus by this technique can produce possible inaccuracies from the following sources.

B.4.1. Inexactness of the Equation:

The equation does not take account of rotary inertia and shear and a correction must be made for specimens whose thickness is not small with respect to its length.

B.4.2. Specimen Dimensions and Mass:

Errors can arise from measurements of specimen dimensions and mass at room temperature and from the increase in these dimensions during heating.

B.4.3. Temperature Measurement:

The thermocouple arrangement using the actual specimen as the hot junction was found to indicate the average specimen temperature to within about 2°C. Temperature gradients through the specimen were considered to be insignificant because of the thinness of the specimen and the slow heating rates used and longitudinal temperature variations were estimated as being not greater than 5°C.

B.4.4. Measurement of Frequency at Maximum Amplitude:

Errors from this source can arise in three ways. Firstly there is the difficulty in setting the oscillator frequency output at exactly the maximum amplitude. Setting exactly at the resonant point depends on the damping capacity of the specimen and on its support system. In the present case an error of less than 0.5% in the resonant frequency arises from this source.

Secondly, the measurement of the frequency after adjusting for maximum amplitude will involve some small error. However, the frequency counter can measure to 1 part in 10,000 and contributes very little to the overall error.

Thirdly, the absolute accuracy of the modulus measurements depends on the reproducibility of the resonant frequency with variations in experimental assembly for the same specimen. This does not, however, arise in the present series of experiments where each run is made on one particular specimen without removing it from the apparatus.

The apparatus is used here merely to observe the temperatures at which abrupt changes in resonant frequency occur during heating and cooling, thus indicating the temperature ranges over which certain transformations take place. Hence the exactness of the equation relating the modulus to the measured resonant frequency, the measurements of specimen mass and dimensions and the changes in these dimensions at elevated temperatures do not influence the accuracy of the present experiments. Errors arise, therefore, solely from inaccuracies in temperature measurement and from measurement of the frequency at maximum amplitude, both of which have been shown to be very small.

APPENDIX C

DILATOMETRY MEASUREMENTS

The dilatometry measurements were made on an apparatus constructed in this Department by Mr. F. A. Thompson and described in detail by Barford (J. Sci. INSTRUM., 1963 VOL 40, p. 001). The differential technique, using a control specimen of the same coefficient of thermal expansion as the real specimen, is necessary since the value of the thermal expansion up to the temperature range required is large compared to the dilation on transformation. For example, on heating from room temperature to 700°C a stainless steel specimen 4 cm. long undergoes a thermal expansion of about 450 microns whereas the contraction due to a martensite content of about 15% transforming to austenite in such a specimen is found to be of the order of 40 microns.

Length changes are measured using a variable inductance transducer. Thermal expansion of the control specimen during heating acts to move the body of the transducer; thus although the real specimen also expands on heating and moves the transducer operating pin, only changes in length due to transformations are recorded by the transducer. However, this is not strictly true for the present series of measurements since the control specimen has an f. c. c. austenitic structure whereas the real specimens contain various amounts of b. c. c. martensite (and possibly h. c. p. martensite). The b. c. c. structure has a lower coefficient of thermal expansion than the f. c. c. so an apparent specimen contraction is indicated as the temperature is raised.

Any small difference in length between the real and control specimens will produce a change in the transducer readings with temperature, of a magnitude and direction which will be dependent on the relative lengths of the specimens; it may tend either to reinforce or counteract the effect due to the different crystal structures. The present investigation is concerned more with the temperatures at which non-linear length changes due to phase transformations occur, than with the absolute values of the magnitudes of such changes. These two effects were, therefore, unimportant.

However, of far greater importance is the possibility that the temperature of the two specimens increased at different rates due to differences in their surface condition (i. e. different reflectivities and emissivities). Before each run both specimens were chemically cleaned and then rubbed with fine silicon carbide paper so that their surface conditions were identical. As the surface effects were likely to influence the results during the initial rapid rise in specimen temperatures, results obtained below 300°C were not used.

Specimens were 4 cm. in length by 1 cm. wide and 0.020" in thickness; the length of the furnace constant temperature zone together with the small specimen thickness ensured that both longitudinal and transverse gradients within the specimens were minimised. The specimen temperature is measured by a thermocouple mounted with its end close to the specimen.

The reproducibility of the results was considered to be very good in that repeated runs on similar specimens gave curves of the same form and the temperatures at which abrupt changes occurred agreed to within $5^{\circ}C$ even with the fastest heating rate.